



University  
of Glasgow

<https://theses.gla.ac.uk/>

Theses Digitisation:

<https://www.gla.ac.uk/myglasgow/research/enlighten/theses/digitisation/>

This is a digitised version of the original print thesis.

Copyright and moral rights for this work are retained by the author

A copy can be downloaded for personal non-commercial research or study, without prior permission or charge

This work cannot be reproduced or quoted extensively from without first obtaining permission in writing from the author

The content must not be changed in any way or sold commercially in any format or medium without the formal permission of the author

When referring to this work, full bibliographic details including the author, title, awarding institution and date of the thesis must be given

Enlighten: Theses

<https://theses.gla.ac.uk/>  
[research-enlighten@glasgow.ac.uk](mailto:research-enlighten@glasgow.ac.uk)

# "THE STUDY OF CONTROL SYSTEMS BY CORRELATION METHODS."

## SUMMARY

In the testing of control systems, particularly the smaller types, it has long been the practice to apply to them test signals of a simple mathematical nature, for ease in evaluating test results. The principal signals used for this purpose are the step functions, ramp function, and the sinusoid. As the scale of systems has grown, so the complexity has increased also, and with that the severity of the effect of such disturbances, until the stage is reached when dangerous conditions may be induced thereby. As an alternative, means have been sought to obtain information of the system characteristics from data collected during normal operation; by this means, unduly severe disturbances are avoided.

This work describes one such method of system analysis. In it, certain statistical properties of the data produced by the normal running of a control system are calculated. These statistical features are used to determine in the end the frequency response of the system, both in amplitude and in phase. Since in laboratory tests the scale of the apparatus used is restricted, use is made of an analogue computer to simulate the control systems, and also to assist in the statistical computations. A source of random signals of the type encountered in practical systems is required to drive such a simulator, and an account of the development of such a device is included. A device giving fixed time delay, needed for the statistical work, is also described.

The process is based on the use of the correlation functions of the time/

ProQuest Number: 10656197

All rights reserved

INFORMATION TO ALL USERS

The quality of this reproduction is dependent upon the quality of the copy submitted.

In the unlikely event that the author did not send a complete manuscript and there are missing pages, these will be noted. Also, if material had to be removed, a note will indicate the deletion.



ProQuest 10656197

Published by ProQuest LLC (2017). Copyright of the Dissertation is held by the Author.

All rights reserved.

This work is protected against unauthorized copying under Title 17, United States Code  
Microform Edition © ProQuest LLC.

ProQuest LLC.  
789 East Eisenhower Parkway  
P.O. Box 1346  
Ann Arbor, MI 48106 – 1346



time signals produced by the system; the auto-correlation function of the input or output signal, and the cross-correlation function between these two signals, form Fourier transform pairs with the power spectral densities of input and output signals, and the cross-spectral density between them, respectively. Numerical methods of Fourier transformation are used to obtain these power spectra; once they are known for both input and output of a control system, its frequency transfer function is readily determined. This direct approach to the mathematical manipulations represents a departure from most previous methods used, in that they have frequently involved the preparation and adjustment of a model to have the same performance as the original system, followed by a response analysis of the model.

Results of tests on two types of systems are given, and probable sources of error indicated. It is conceded that the system as applied here is tedious to operate, and has several inherent sources of error. Lines of further development are indicated which could dispose of these, and would produce an attractive and versatile method of system analysis.



"THE STUDY OF CONTROL SYSTEMS BY CORRELATION METHODS"

THESIS

presented for the degree of Master of Science in Electrical  
Engineering, of the University of Glasgow,

by

J. FALCONER, B.S.c.

December, 1961.

### ACKNOWLEDGMENTS.

The author wishes to express his sincere thanks to Professor F.M. Bruce, M.Sc., Ph.D., M.I.E.E., M. Amer, I.E.E., A.Inst.P. for his kindness in granting the laboratory facilities of his department, and to Dr. I. Cochrane, B.Sc., Ph.D and Mr. Z. Jelonek, Dipl.Ing. of the Electrical Engineering Department, for their valuable guidance and helpful criticism throughout the course of this project. Thanks are also due to Mr. J. Brown and his colleagues in the Department workshops for their assistance with the thorny problems involved in putting the theory into practice.

INDEX.

	<u>Page.</u>
<u>Chapter 1.</u> INTRODUCTION.	2.
<u>Chapter 2.</u> PRACTICAL METHODS OF STATISTICAL COMPUTATION.	13.
<u>Chapter 3.</u> FREQUENCY TRANSFER FUNCTION COMPUTATION.	21.
<u>Chapter 4.</u> TESTING AND ASSESSMENT OF SYSTEM.	31.
<u>Chapter 5.</u> THE RANDOM SIGNAL GENERATOR (R.S.G.).	45.
<u>Chapter 6.</u> THE TIME DELAY UNIT.	51.
<u>Chapter 7.</u> CONCLUSIONS.	60.
REFERENCES.	62.
<u>Appendix 1.</u> ANALYTICAL DERIVATION OF CORRELATION FUNCTIONS.	64.
<u>Appendix 2.</u> THE ANALOGUE COMPUTER.	76.
TABLES OF RESULTS.	83.
GRAPHS 1 to 14	following page 84.



## THE STUDY OF CONTROL SYSTEMS BY CORRELATION METHODS

### 1. INTRODUCTION

#### 1.1. Alternatives available in Transfer Function analysis.

The problem of verifying experimentally the response characteristics of electrical networks is one which has exercised the minds of engineers from the earliest days, and many different approaches have been made to it. In general, most methods employed a test signal, of clearly defined and simple mathematical nature, which could readily be generated for application to the input of the network. From the measured response of the network to this input were then derived input - output relations valid for any form of input.<sup>20</sup>

The nature of the test signal used, and of the resulting relation is influenced by the use to which the network is to be put; for example a network to handle continuous signals would be tested by application of a continuous waveform, often sinusoidal, and of varying frequency,<sup>20</sup> while systems whose behaviour under different conditions is of interest would have a step or a ~~ramp~~-type signal applied to them.<sup>5</sup> As a result, several different functions are now in common use to describe the performance of systems, namely their frequency response, step response or impulsive response. For linear systems, whose characteristics are independent of the form of input applied, these functions are quite simply related, so if any one is determined, the others may be obtained, if required, without the need for further tests.

#### 1.2. Limitations of the Test Signal approach.

The application of the above methods of analysis is simple and convenient when the systems to be tested are sufficiently simple for/

for estimation to be made, in advance of the test, of any limits, e.g. of input amplitude, which may be necessary to ensure a stable, bounded response to the desired input, and where the systems may readily be taken out of normal operation to be tested. Many instances occur, particularly when dealing with large closed-loop control systems, where either or both of the above conditions may not apply. Such systems will often involve several feedback paths, and will contain components with limited ranges of linearity; this renders any estimation of permissible input levels very difficult and tedious. The work on which these systems are engaged may well be part of a continuous production flow which cannot readily be interrupted to allow one part to be tested. As a further complication, the response of the system may be influenced by its operating environment, an influence which could be altered by testing it under artificial conditions.

All these difficulties have combined to stimulate investigation of the possibility of devising for such systems test procedures,<sup>2,3</sup> which can be applied without introducing any artificial disturbance into the system, and without interrupting its operation, yet which will produce, from data collected from normal operation of the system, the required characteristic functions.

### 1.3. System analysis based on random signal techniques.

Before proceeding to the examination of detailed techniques of analysis using the signals available during normal operation of a control system, some consideration must be given to the nature of these signals, and their tractability by mathematical manipulation.



The type of control usually effected by the system is that of maintaining some parameter of the controlled process at a preset level, or within preset limits. Since the factors which cause the parameter to deviate from the preset value are likely to be numerous and unpredictable, at least in their combined effect, the error signal generated by the deviation will be a random signal, to which only a statistical description can be assigned.<sup>5</sup> The properties of the signal used in this form of analysis are therefore also statistical, though it will be demonstrated that they are simply related to the absolute properties employed in the classical methods of analysis.

This firm relation between statistical and analytic properties, which is particularly simple in its application to linear systems, allows of the computation of response functions of the classical type from knowledge of the statistical properties of the available data. As it has already been shown, however, that the classical response function may take several forms, it is natural that several different approaches have been made to the statistical form of analysis also, each aimed at deriving a different form of response function. The work described in later stages of this thesis is an attempt to develop a process for computation of the system frequency response; other methods to which reference will be made have been directed towards obtaining the impulsive response.<sup>2,3</sup>

It should perhaps be stressed here that, in the main, the forms of analysis described have been developed on the basis of their application to linear systems, and are in most cases only capable of/



of producing a linear approximation to the response of a system containing any appreciable non-linearity. A considerable amount of work has been done recently, by West<sup>1</sup> and others, to determine the distorting effect of non-linearities of commonly occurring types on the functions used in the statistical analysis; this could lead to the employment of statistical techniques to detect, identify and evaluate the extent of such non-linearities..

The possibilities and limitations of random signal analysis will perhaps become clearer once the fundamental relationships on which it is based have been set out, and its terminology defined, and this will now be done.

#### 1.4. Basis of statistical description of random functions.

The regular analytic signals on which the classical methods of analysis are based have a number of mathematical properties which are capable of absolute definition, such as the amplitude or the frequency of a periodic signal, or the amplitude and time of occurrence of a step function. These forms of description cannot, however, be applied to the randomly occurring signals referred to above. Other features must be used to describe their behaviour; these are the statistical features of the signal, which assess the probability, rather than the certainty, that the signal will possess, for example, a given amplitude at a given time. Such properties are generally based on the average, and not the instantaneous, value of a property of the signal. The most important of these properties now require to be defined.

##### (a) Correlation Functions./

(a) Correlation Functions.

Two types of correlation functions are required;

(i) The autocorrelation function,<sup>5</sup> of a time signal, is a measure of the possibility of predicting a future value of the signal, if its present value is known. It is a function of the time interval,  $T$ , separating the occurrence of the two values of the signal, and is generally defined as<sup>6</sup>

$$A(T) = \lim_{r \rightarrow \infty} \frac{1}{2r} \int_{-r}^r f(t) \cdot f(t+T) dt. \text{-----} (1)$$

$$\text{So } A(-T) = \lim_{r \rightarrow \infty} \frac{1}{2r} \int_{-r}^r f(t) \cdot f(t-T) dt.$$

$$= \lim_{r \rightarrow \infty} \frac{1}{2r} \int_{-r}^r f(s+T) \cdot f(s) ds, \text{ where } s=t-T,$$

$$= A(T).$$

$A(T)$  is evidently an even function of  $T$ , and its maximum value, at  $T=0$ , is equal to the mean square value of  $f(t)$ .

(ii) The cross-correlation function<sup>5</sup> between two time signals measures the possibility of predicting a future value of one time signal,  $f_1(t)$ , if the present value of a different time signal,  $f_2(t)$ , is known. It is defined similarly as<sup>6</sup>

$$C_{12}(T) = \lim_{r \rightarrow \infty} \frac{1}{2r} \int_{-r}^r f_1(t) \cdot f_2(t+T) dt. \text{-----} (2)$$

$$C_{12}(-T) = \lim_{r \rightarrow \infty} \frac{1}{2r} \int_{-r}^r f_1(t) \cdot f_2(t-T) dt$$

$$\neq C_{12}(T)$$

so  $C_{12}(T)$  is not an even function of  $T$ , and in general has no recognisable symmetry.

(b) Power spectra.<sup>6</sup> The power spectrum, or more explicitly the squared-amplitude spectrum, of a time signal is defined on the basis of the power which would be dissipated on applying the signal to a one-ohm/



one-ohm resistance. The amplitude-frequency spectrum of a signal,  $F(w)$ , is defined by the well-known Fourier transform relation

$$F(w) = \int_{-\infty}^{\infty} f(t) \cdot e^{-j\omega t} dt.$$

where  $F(w)$  is a complex function of  $w$ . It thus represents the amplitude distribution of the sinusoidal components contained in  $f(t)$ .

If we now define a function  $P(w) = F(w) \cdot F^*(w) = |F(w)|^2$ , it will represent the distribution of dissipated power among these components when  $f(t)$  is applied to a one-ohm resistance. This is defined to be the power spectral density, or more shortly the power spectrum, of  $f(t)$ . Note that  $P(w)$  has the dimensions of power per unit bandwidth; hence we have an alternative definition,

$$\overline{f(t)^2} = \frac{1}{\pi B} \int_{-B}^B P(w) dw. \quad (\text{from the Parseval Theorem})$$

As with correlation functions, we define also a cross-spectral density<sup>6</sup> between two time signals,  $f_1(t)$  and  $f_2(t)$ , as follows:-

Let the amplitude spectra, defined as in (3) above, of  $f_1$ , and  $f_2$  be  $F_1(w)$  and  $F_2(w)$  respectively. Then the cross-spectral density between the two signals is  $P_{12}(w) = F_1(w) \cdot F_2^*(w)$ .

### 1.5. Fundamental Equations in statistical analysis

A rigorous development of the relationship between the power spectral density and correlation function of a signal or signals will be found in the translation of the work of Solodovnikov<sup>6</sup>, and also in a much earlier work by Wiener, and is another Fourier

transform relation, viz.  $P(w) = \int_{-\infty}^{\infty} A(T) e^{-j\omega T} dT$ . ----- (4)

$$A(T) = \frac{1}{2\pi} \int_{-\infty}^{\infty} P(w) e^{j\omega T} dw.$$

Similarly,  $P_{12}(w) = \int_{-\infty}^{\infty} C_{12}(T) e^{-j\omega T} dT$ . ----- (5)

$$C_{12}(T) = \frac{1}{2\pi} \int_{-\infty}^{\infty} P_{12}(w) e^{j\omega T} dw,$$



Thus there is an evident analogy between the description of a random signal by the statistical functions defined above and the description of a periodic or other analytic signal by its analytic properties. For example, if a network of transfer function  $G(w) = K(w)e^{j\phi(w)}$  has a sinusoidal signal  $f_1(t) = Ae^{j\omega t}$  applied to it, the output signal  $f_o(t)$  will be  $f_o(t) = Ae^{j\omega t} \cdot Ke^{j\phi}$ , where  $K$  is the gain and  $\phi$  the phase shift of the network at that frequency  $w$ . If however the input contains a number of different frequency components, it is conveniently specified by its amplitude spectrum  $F_1(w)$  defined as in (3) above. The output amplitude spectrum is then given by

$$F_o(w) = F_1(w) \cdot G(w) \text{ ----- (6)}$$

Since  $F_1(w)$ ,  $F_o(w)$  and  $G(w)$  are the respective Fourier transforms of  $f_1(t)$ ,  $f_o(t)$  and the network impulse response  $W(t)$ , the time relation corresponding to (6) is the convolution integral (5, p. 54)

$$f_o(t) = \int_0^{\infty} W(x) \cdot f_1(t-x) dx. \text{ ----- (7)}$$

From (6) we can derive the cross-power spectrum between input and output,  $P_{10}(w) = F_1(w) \cdot F_o^*(w)$  by definition

$$\begin{aligned} &= F_1(w) \cdot F_1^*(w) \cdot G^*(w) \\ &= P_1(w) \cdot G^*(w). \text{ where } P_1(w) \text{ is the input power spectrum} \end{aligned} \text{ ----- (8)}$$

This relation (8) is equally applicable to random signals as to analytic signals, so comparison of equations (6) and (8) makes the analogy between the treatment of the two types of signal quite clear.

From the Fourier transform relations in (4) and (5) above, a relation similar to that in (7) may be obtained for use with random signals, thus<sup>2</sup>

$$C_{10}(T) = \int_0^T W(x) \cdot A_{11}(T-x) dx. \text{ -----(9)}$$

where  $A_{11}(T)$  is the autocorrelation function of  $f_1(t)$ .

It will be seen later that equation (8) forms the basis for the method of computation of frequency response described as the main work of this thesis; equation (9) is used to develop other methods for finding the impulse response.<sup>2,3.</sup>

#### 1.6. Effect of internally-generated noise on statistical analysis.

The random signals used in the statistical form of analysis must not be confused with background noise, which may be generated within the control components themselves. Random signal as used here refers to the result of disturbances occurring in the controlled variable due to external causes; these are sensed in the normal way, and the controller attempts to correct them. Noise may be generated additionally within the control network, e.g. hum and shot noise in valve amplifiers,; it is therefore of interest to consider what effect the occurrence of noise of this sort will have on the analysis.

Several attempts have been made by previous authors to discover the solution to this problem by making the assumption either that the noise has a certain definite description ( e.g. Murphy<sup>4</sup>, Ch.9.), or that it occurs at a definite point in the network<sup>2</sup>, or both<sup>3</sup>. Henderson<sup>2</sup> takes the case of noise which occurs in the measurement of the signals in the network, especially of the output signal, as in Fig.1(a), where a 'noise source' is interposed between the output node and the



# OCCURRENCE OF INTERNAL NOISE.

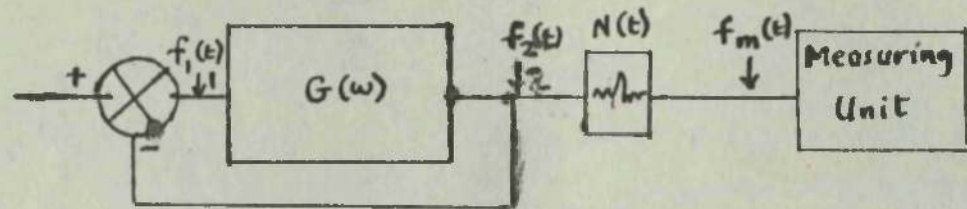


Fig.1(a). Outwith control loop, (Henderson<sup>2</sup>).

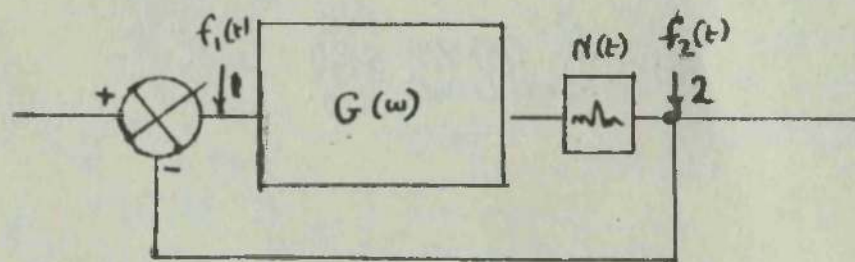


Fig.1(b). Within forward control loop, (Goodman<sup>3</sup>).

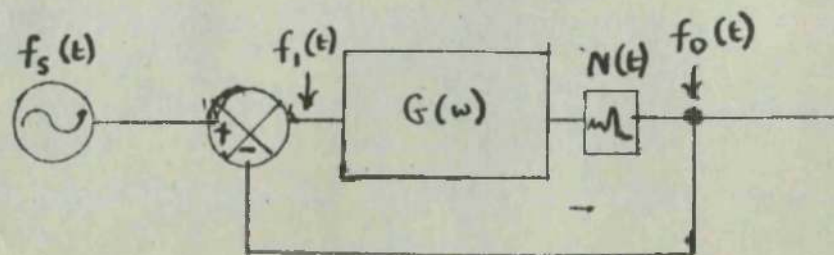


Fig.1(c). Sinusoidal testing of noisy component. (Lee,<sup>7</sup>)



measuring instrument. In this case it is evident that the noise here will not be fed back into the network, so it will appear only in the measured output signal  $f_m(t)$ . If the cross-correlation of  $f_m(t)$  with  $f_1(t)$  is effected, the measurement noise will be eliminated from the result, which will contain only information on the relation of  $f_1(t)$  to  $f_2(t)$ , at the true output. This is of course a rather artificial example. Goodman<sup>3</sup> considers the case of noise occurring as in Fig.1(b), in the forward path, and occurring particularly as short distinct bursts of shot noise. He concludes that, since such a burst will appear first in  $f_2(t)$ , and later after feedback in  $f_1(t)$ , it will affect only that part of the function  $C_{12}(T)$  for which the delay  $T$  is negative.(i.e. for which a value of  $f_2(t)$  is correlated with a later value of  $f_1(t)$  ). This argument seems to neglect the fact that, once it has occurred, the burst will circulate around the loop, so that, after its first appearance in  $f_1(t)$ , it will reappear in  $f_2(t)$  later passing through the forward path. Hence the suggestion that the effect of noise occurring in this way will be minimised in correlation analysis, by confining it to the negative portion of  $C_{12}(T)$ , would appear to be fruitless, as in its repeated circulation round the loop, the burst will evidently affect the function  $C_{12}(T)$  several times.

A closer look at these two examples reveals a more important feature of the effect of noise like this on a correlation study. If we attempt, in the circuit of Fig.1(b), to find the forward transfer

function  $G(w)$ , by finding the correlation functions  $A_{11}(T)$  and  $C_{12}(T)$ , an interesting fact emerges. The input signal  $f_1(t)$  and the output signal  $f_2(t)$  will both be contaminated with noise from the source  $N(t)$ . However, if we regard the network as consisting of a passive part  $G(w)$  and an active source  $N(t)$  as shown, we find that  $f_2(t)$  contains the response of the network  $G(w)$  to the complete input  $f_1(t)$ , (including the noise), plus a fresh contribution from  $N(t)$ . When the processing of the correlation functions is completed, the result will therefore be the response function of the network over the whole bandwidth of  $f_1(t)$ . The noise will simply be treated as an additional component in the signal passing through the network, and the response of the network to it will be included with the response to the control signal in the final result.

Thus it would appear that the handling of internal noise presents much less of a problem to correlation analysis than to conventional analysis. The strength of the correlation method, in the presence of noise, lies in the fact that it takes account of noise, and the response of a network to it, in just the same manner as it takes account of the wanted signal. By contrast, in conventional analysis, efforts must usually be made to eliminate the noise entirely from the measured signals for an accurate result to be obtained. It also seems possible that the response function produced by correlation may contain some separable information about the composition of internal noise.

Correlation techniques have also found application in assisting

in the evaluation of the network response to a sinusoid, when the output is heavily contaminated with noise.<sup>7,8</sup> The technique is illustrated by Fig.1(c). The cross-correlation function between the sine input  $f_s$  and the noisy output  $f_o$  is compared with the autocorrelation function of  $f_s$ . These functions will be sinusoids of the same frequency, and their relative amplitudes and phase shift will give the gain and phase shift of the network at that frequency. This method has been applied with some success to communication networks suffering from severe noise.<sup>7</sup> It will be noted that, since the noisy output  $f_o$  is correlated with the stimulating signal  $f_s$ , instead of with the error signal  $f_1$  (as in Fig.1(b) ), noise occurring anywhere within the network will not contribute to the cross-correlation function.



## 2. PRACTICAL METHODS OF STATISTICAL COMPUTATION.

### 2.1. Sequence of computation required.

The computation of system characteristic functions according to the equations set out in chapter 1 must for practical purposes be broken up into several stages, only some of which are common to the various systems of computation which have been devised. These stages, when dealt with in any practical detail, are thus better treated separately.

The sequence of operations, and the variations which occur in it in the several processes, are set out below:-

- (i) The calculation of autocorrelation functions of input signal and/or output signal, and of the cross-correlation function between input and output,
- (ii) To find the impulse response, applying the convolution process set out in equation (9) to the correlation functions,
- (iii) To find the frequency response, obtaining the Fourier transforms of the correlation functions.

Comparison can now be made of the methods which have been employed to perform these separate steps of the calculation.

### 2.2. Methods of calculating correlation functions.

The calculation involved averaging the product of two values of time functions at instants separated by a variable interval  $T$ . One other fundamental postulate of statistical theory is needed to distinguish two possible ways of taking this average. This is the ergodic hypothesis, a fuller treatment of which is given by Solodovnikov<sup>6</sup>, (pp.87-90). Briefly, it may be stated as follows.

A stationary random process is definable only in terms of the statistical properties of its governing variables; there will thus be a large group, or ensemble, of time functions having the statistical characteristics of the process, any one of which may be taken as representative of it. By the hypothesis, a long series of values of one of these functions will have the same statistical properties as a series consisting of the same number of values, one from each, taken simultaneously from the whole ensemble.

In particular, this implies that the time average of any one function of the ensemble (or any function of that one) is identical to the ensemble average, found by averaging the simultaneous values of all functions in the ensemble (or of the same function of each of them).

The application of this in the topic under discussion is to the calculation of the average of the product  $f(t) \cdot f(t+T)$ , which is the core of a correlation function. The method used by the equipment described later in the thesis requires  $f(t)$  as a continuous function of time; to correlate this, the time average of  $f(t) \cdot f(t+T)$  over a substantial period of time is found. By contrast, the work of Lee<sup>7</sup>, et al., employs an ensemble average of the function  $f(t) \cdot f(t+T)$ : the ensemble consists of portions of a very long record of  $f(t)$ , each long enough to be statistically characteristic of it. The product of two values of  $f(t)$  separated by the same interval  $T$  is taken from each portion, and the average of the products found. Singleton's paper<sup>8</sup> describes a device operating on the same sequence, but using digital techniques of storage, multiplication and averaging.



This method, as was mentioned in chapter 1, was designed for use in overcoming noise problems in communication equipment, and was therefore built for operation in the a.f. band. The records used were quite short, as the total delay required was a few tens of microseconds. It was felt that the units of such a high-speed system would require very extensive redesign for operation at servo frequencies, and were in any event rather too complex to be developed successfully in the time available. The method does have one notable feature in its favour; it is capable of producing a plotted record of the complete correlation function, for a preset range of delay, in one continuous operation.

Several other practical methods have been tried or suggested, based on the time-averaging principle. Henderson<sup>2</sup> makes reference to the possibility of computing the average product of two samples of the signals, for many sample pairs, using a digital computer. In the analogue field, brief notes are to be found in Solodovnikov's work<sup>6</sup> on several systems, both mechanical and optical, while Henderson<sup>2</sup> suggests that the delayed signals could be made available by recording the original on magnetic tape. Two pickoff heads would play back two separate values of the signal, over the whole length of the record, enabling the time average of their product to be evaluated by standard analogue methods.

The method finally used for correlation, described in chapter 3, avoids the use of the modulating equipment needed for tape working. Instead, the incoming signal is delayed in an electro-mechanical delay unit, and the product of the two signals, direct and delayed, is formed and averaged by an analogue computer. This scheme uses the minimum of auxiliary equipment to prepare the signals for computation,



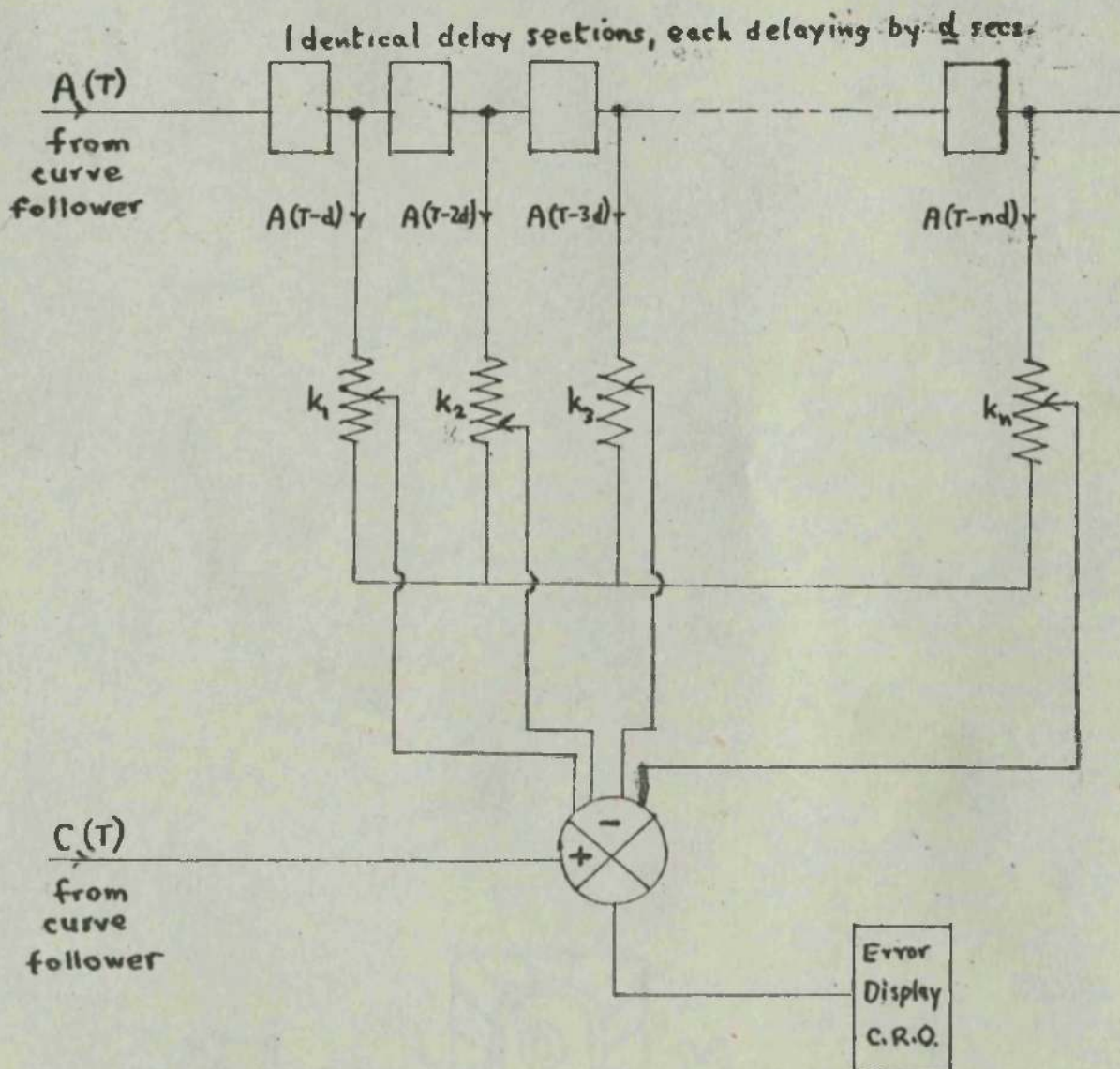


Fig.2. Delay line synthesizer.<sup>3</sup>

and is capable of producing correlation functions over a range of time delay extending to 750 milliseconds, which is about the minimum needed to handle l.f. servo signals.

### 2.3. Processes for finding the impulse response.

Once the correlation functions have been obtained, one route to a response function for the system is by the determination of the impulse response, by the convolution process of equation (9), Chapter 1, i.e.  $C_{12}(T) = \int_0^{\infty} W(x) \cdot A_{11}(T-x) dx$ .

Since the weighting function  $W(x)$  is involved within the integral this is normally done by synthesising  $C(T)$ , by weighting successive values of  $A(T)$  with values of  $W(x)$ , and summing the results. Two quite distinct types of apparatus have been devised to do this,

(a) Delay-line synthesisers<sup>3</sup>. The scheme is shown in Fig.2. The time signal of  $A(T)$ , obtained from a curve follower, is fed into a delay line which is tapped at  $n$  points along its length. This delay line may well be a discontinuous one, as these will give better performance at low frequencies; such a line is described in a paper by Janssen<sup>16</sup>. The convolution is performed by passing the output from each tapping point through a variable attenuator,  $k_r$ , and summing the attenuator outputs. The result of this operation is

$$S(T) = \sum_{r=1}^n A(T-rd) \cdot k_r, \text{ where } \underline{d} \text{ is the delay per section.}$$

The signal  $S(T)$  is compared on a C.R.O. with the time signal  $C(T)$ , from a second curve follower, and the settings  $k_r$  are adjusted until the best fit between  $S(T)$  and  $C(T)$  is obtained. The set of values  $k_r$  by analogy with equation (9), will be a series of values of the weighting function  $W(x)$ , taken at intervals  $\underline{d}$ . Thus, provided  $W(x)$  does not



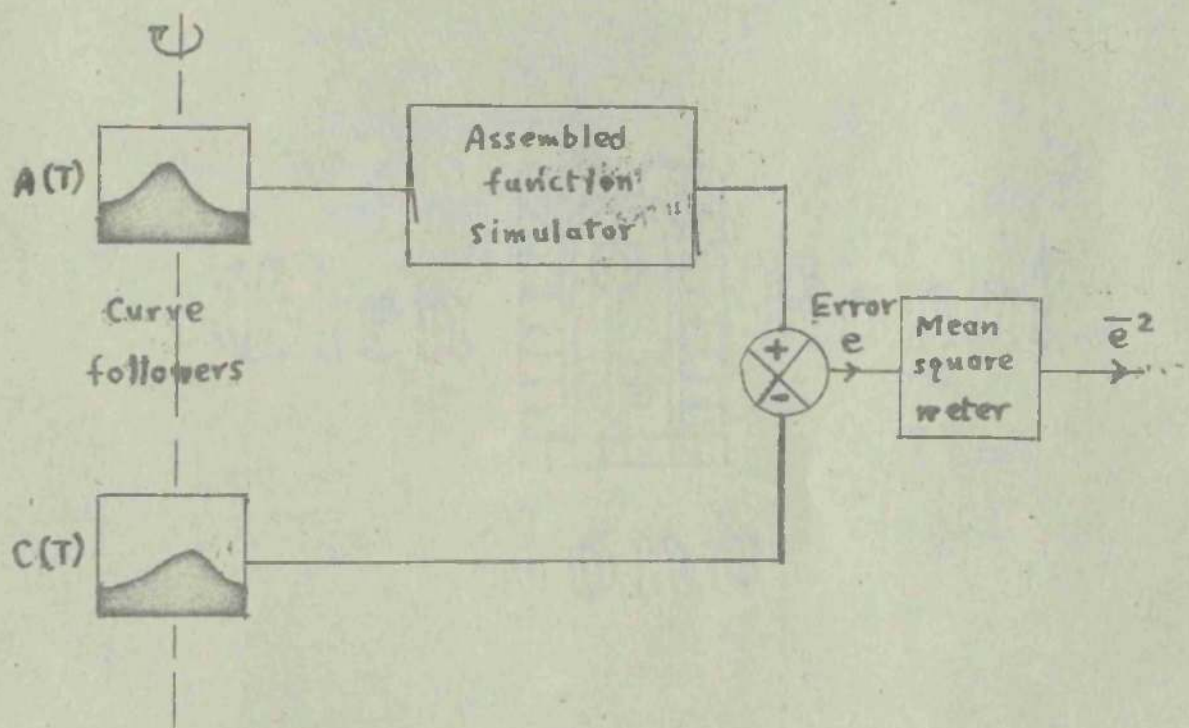


Fig.3. Schematic diagram of a linear function simulator.<sup>2</sup>



vary more rapidly than can be followed accurately by a series of samples at intervals  $\underline{d}$ , there is no restriction on the range of linear impulse responses which can be synthesised in this way.

(b) Linear function simulators. This class of devices, referred to by Henderson<sup>2</sup>, is basically a limited form of analogue computer.

Electronic units have been designed to simulate the basic factors common to many transfer functions, chiefly  $\frac{1}{p}$ ,  $\frac{1}{p+a}$ , and  $\frac{1}{p^2+ap+b}$ ,

where  $\underline{a}$  and  $\underline{b}$  can be varied. By combining these units, a range of linear transfer functions can be simulated. They are employed in the arrangement of Fig.3. The input autocorrelation function of the system under test is generated as a shaped electrical impulse by a curve follower, and this signal is applied repetitively to the input of the simulator. The output of the simulator is compared with a signal generated by a second curve follower from the cross-correlation function around the test system. The parameters of the simulator are then adjusted until the displayed error between these signals is minimised. From examination of equation (9), this condition will be seen to imply that transfer function of the simulator is now the best available approximation to that of the test system, from which the correlation functions were obtained. There can of course be a restriction placed on the range of systems tractable by this method, by the number and diversity of the factor units available. For systems which can be simulated fully in this way, the method has the merit that any desired response checks can be made on the simulator, once it has been adjusted.

Both of the methods described above demand the provision of two curve followers, to convert the graphs of the correlation functions into electrical signals for application to the convoluting apparatus.

These are generally photo-electric devices, whose construction and calibration to any degree of accuracy presents formidable problems. They also require the tedious operation of making an opaque mask for every function they are required to handle. In preference to these complex devices therefore, alternative means were sought for finding the frequency response of a system, on the basis of equation (8), Chapter 1.

#### 2.4. Equipment for finding frequency response.

The frequency response of a system can be determined from knowledge of the power spectrum of the input signal to the system, and of the cross-power spectrum between the input and output signals, by use of the relation in equation (8),

$$P_{12}(w) = P_1(w).G^*(w).$$
$$\text{i.e. } G^*(w) = \frac{P_{12}(w)}{P_1(w)}.$$

First of all, means must be found for obtaining the Fourier transforms of the correlation functions  $A_{11}(T)$  and  $C_{12}(T)$ , to give us  $P_1(w)$  and  $P_{12}(w)$ . Several analogue methods of doing this were considered.

The first of these was an optical method developed by Born.<sup>15</sup> This requires once more that the function to be transformed be produced on an opaque mask. The mask is scanned by a light beam whose intensity is modulated, in the direction of the time axis of the mask, with a sine wave whose frequency is swept over a wide range. The light passing through the mask is summed by a photocell, whose output is displayed on a C.R.O. If the time-base of the C.R.O. is synchronised to the sweep of the modulating frequency, the resulting trace will be the frequency spectrum of the input function<sup>15</sup>. The traces for  $A_{11}(T)$  and



$C_{12}(T)$  can be recorded and divided to give  $G^*(w)$ .

Tucker<sup>14</sup> describes an electrical analogue method using a similar principle. The input function is applied as a series of discrete values not as a continuous function. A delay line of many identical sections is used, whose phase shift per section must be proportional to frequency over quite a wide range of frequencies. Carrier signals, having amplitudes proportional to successive values of the input function, are applied simultaneously to successive sections of the line, and the total output of the line is measured. For one fixed carrier frequency,  $w_c$ , this output will be  $\sum_{r=1}^n f(t_r) \cdot e^{jw_c t_r}$ , where  $f(t_r)$  are the values of the input function for times  $t_r$ . If now the frequency  $w_c$  is varied with time, the output will approximate to the Fourier transform of  $f(t)$ , and can be displayed as before on a C.R.O, if the time-base is synchronised to the variation of  $w_c$ .

These two methods have the outstanding advantage that the transform is produced completely in one operation, but their apparatus is in both cases very delicate, and must be constructed with great precision. The optical method again requires the preparation of an opaque mask for each function. To provide means for obtaining the transforms with the minimum of new equipment, it was decided to use one of several numerical methods, which have been developed for use in some special applications of Fourier transformation. This is Rosenbrock's method,<sup>17</sup> applying two transparent calibrated cursors to the graphs of the time functions. The amount of graphical work involved is considerable, and in the end the spectrum is produced point by point, so the operation is quite slow, but the construction of a large quantity of delicate precision equipment is thereby avoided.



## 2.5. Final choice of equipment.

The chief consideration in deciding on the form of apparatus to be used was the ability of the equipment to produce definite evidence of the feasibility of the frequency response method of statistical analysis. There was therefore a need to develop the apparatus as quickly as possible, so that sufficient time could be spent in testing and evaluating its performance. As much use as possible was made of equipment, such as the transform cursors, which was available in a ready-made form.

While the advantages of the several fast and indeed almost automatic units described<sup>7,8,14</sup> over slower graphical methods of working are very evident, they were reluctantly set aside in face of the very extensive development work required to make them usable at low frequencies. This would require great extension in the range of variation of the controlling frequencies of the correlators<sup>7,8</sup> and also in the working frequency range of the delay line<sup>14</sup>.

It will be seen later that the mechanical and numerical methods employed, while admittedly introducing the bulk of the system error, did in fact operate well enough to demonstrate the ability of the method to produce transfer functions with the minimum of prior knowledge of the nature of the test system, and the minimum of disturbance to the working of that system.

### 3. FREQUENCY TRANSFER FUNCTION COMPUTATION

3.1. This chapter, and those which follow, describe in detail the system of computation used in this project. The system is centred round an analogue computer, a brief note on which will be found in Appendix 2. Since it was not possible to erect in the laboratory actual control systems of any size or complexity, the computer is made to serve the dual purpose of performing the required mathematical operations by analogue means, and of simulating for test purposes two different types of control systems. Two major items of auxiliary equipment were also needed, namely, a low frequency random signal generator and a time delay unit; a full account of their development will be found in Chapters 5 and 6.

#### 3.2. General sequence of operation.

The system follows the sequence of operations laid down in paragraph 2.1., sections (1) and (iii). The methods used to carry out the operations there specified are

- (i) Calculation of the autocorrelation functions of input and output, and the cross-correlation functions between them, by a time-averaging method, carried out by the analogue computer,
- (ii) Calculation of the Fourier transforms of these functions, by a numerical method involving the application of special cursors to the graphs of the correlation functions.
- (iii) Calculation of the complex transfer function and the squared amplitude response by point-by-point division of the frequency spectra obtained in (ii).

#### 3.3. Analogue computer circuit for correlation./



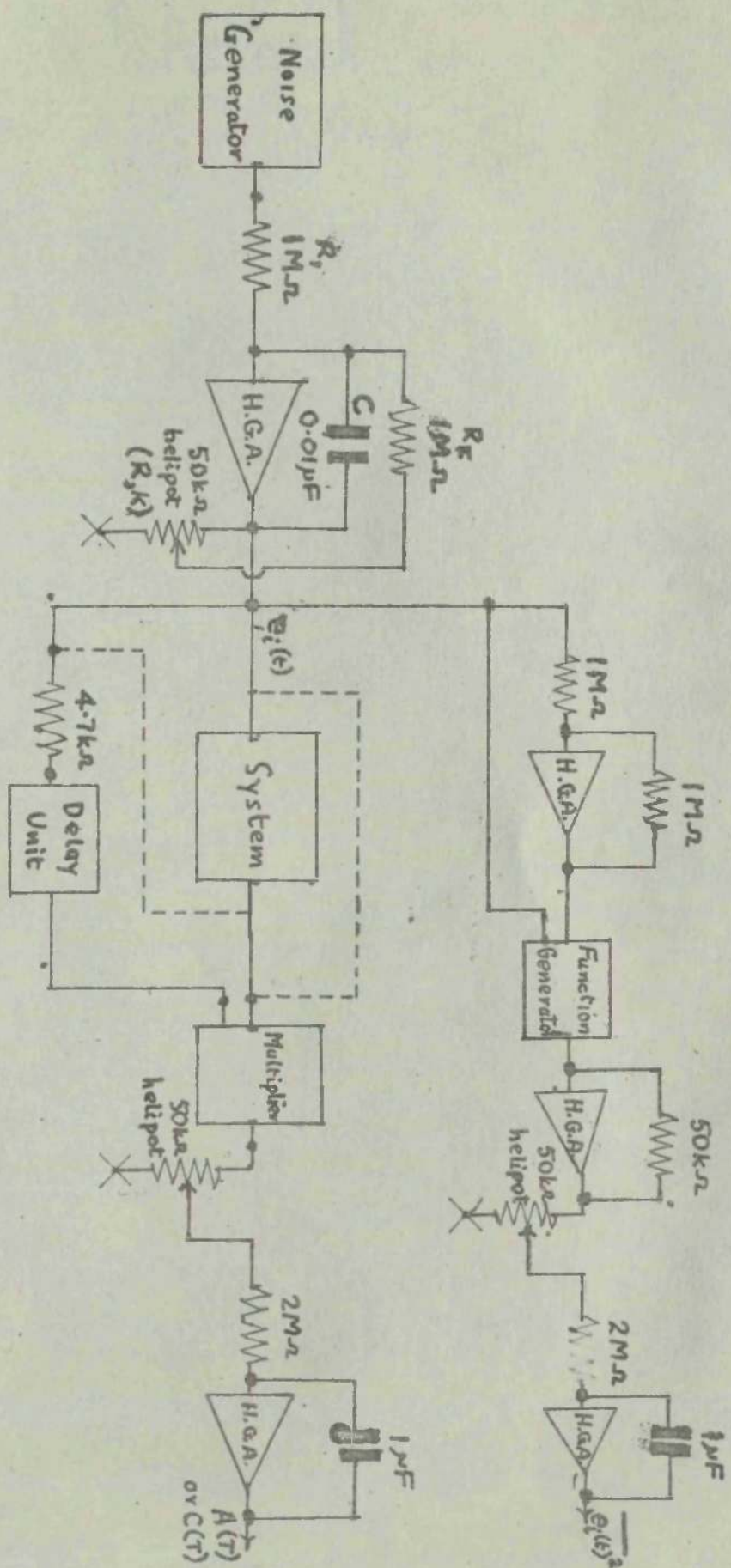


Fig. 4. Analogue Computer Circuit for Correlation.

### 3.3. Analogue computer circuit for correlation.

Fig.4. gives in full the general circuit used to compute correlation functions. The system under test, shown in Fig.4. simply as a block, is an analogue of a control system built up from various combinations of operational amplifiers. The circuit can readily be broken up into three almost independent sections, viz. the noise shaping section, the correlating section and the mean-square computer. These sections operate in the same fashion for any type of test system, so their operation can be described without reference to any particular system. Thus once the circuit has been 'patched' on to the computer, the test systems can be altered and interchanged without disturbing it.

### 3.4. Noise shaping circuit.

The development and circuitry of the noise generator is described fully in Chapter 5. It is built round a miniature thyratron as the primary source of noise. The noise output is therefore subject to occasional sharp fluctuations, and some of these bursts are severe enough to cause saturation of the amplifier stages. The clipping effect of this distorts the amplitude distribution of the low frequency output, causing it not only to depart from the desired Gaussian form, but also to become unsymmetrical, as the positive and negative clipping levels were not necessarily the same.

This clipping at low frequencies will result in the generation of harmonics of the output frequency band. One possible method of reducing the extent of the distortion is to cut down the noise



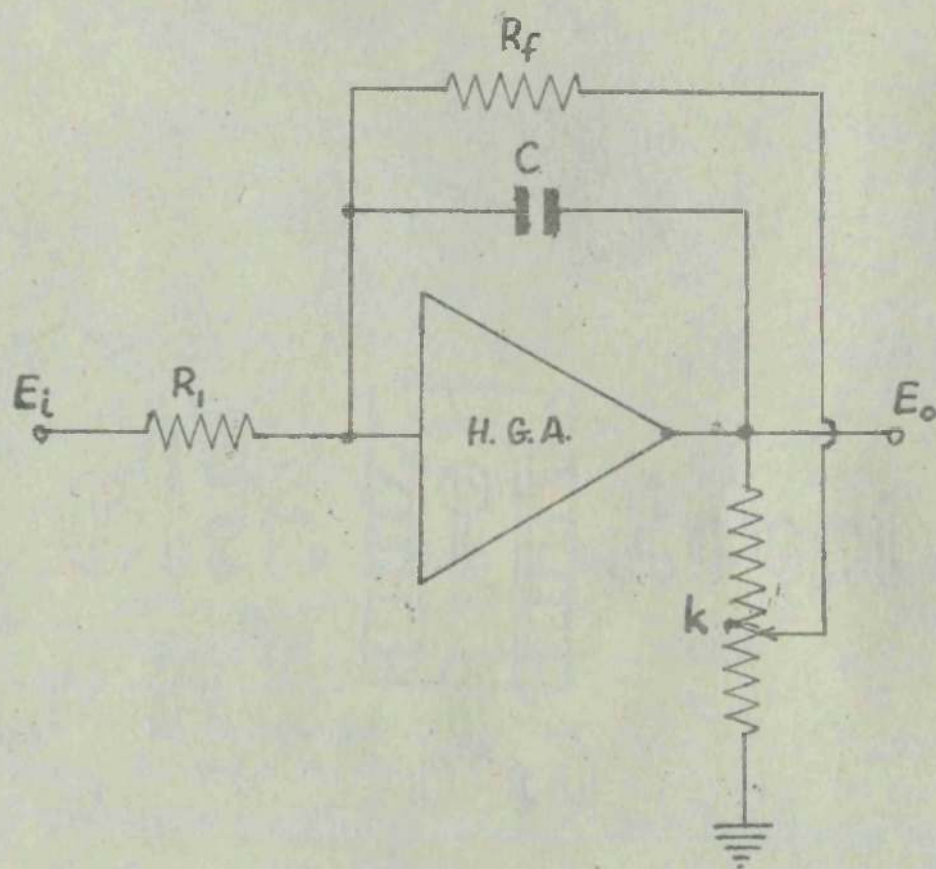


Fig.5. Circuit of variable time-constant filter.

bandwidth and filter off the harmonics before applying the noise to the test system. For this reason, the R-C filter, shown following the noise generator in Fig.4., is included for all the tests. Since the normal bandwidth of the noise generator output is about 100c/s and the output is flat to about 15c/s, this filtering has been found quite effective in improving the amplitude distribution of the noise actually applied to the test system.

The filter circuit is of interest in itself. It has been designed to give a continuous variation, simultaneously, of both gain and time constant, to allow the noise bandwidth to be easily adapted to suit the system under test. The noise bandwidth should always be wider than the system pass-band, to allow a complete response to be obtained, but if it is made too wide, say more than twice the pass-band, the autocorrelation function of it will be very narrow, and thus difficult to compute accurately, as the minimum steps in the values of delay used are of 4millisecs.

The variable feature is obtained by taking the resistive feedback from a potentiometer, instead of direct from the output of the operational amplifier. Using the virtual earth principle, in the circuit of Fig.5., the current balance equation is

$$\frac{E_i}{R_1} = -\left(pCE_o + \frac{kE_o}{R_f}\right)$$

$$\text{Thus } \frac{E_o}{E_i} = -\frac{R_f}{kR_1} \frac{1}{1 + \frac{pCR_f}{k}}$$

With the same feedback components, and direct feedback from the output, the corresponding expression would be



$$\frac{E_o}{E_i} = - \frac{R_f}{R_1} \cdot \frac{1}{1+pCR_f}$$

so it is clear that the effect of the potentiometer is to alter both the gain and the time constant of the filter by a factor of  $\frac{1}{k}$ . Thus by varying  $k$  the gain and time constant can be varied over a wide range.

### 3.5. The correlating circuit.

The lower branch of the circuit in Fig.4. is used to produce the correlation functions. The connections shown by full lines are those used to produce the input autocorrelation function. Other connections shown by broken lines are used to form the cross-correlation function of input and output, or the output autocorrelation function. The circuit performs the calculation as a simple open-loop sequence of delay, multiplication and integration. The delay unit, described in full in Chapter 6, can delay either the input or the output signal, as required, for a period variable in gradually increasing steps up to a maximum of almost 800 milliseconds. The unit must be fed through an external charging resistor, as the storage capacitors, each of 0.1 microfarad, may have to be charged on connection to the full-scale level of 100 volts; the resistor is therefore required to keep the charging current within the load limit of the operational amplifier feeding it.

The multiplier is a continuously acting one operating on the quarter-squares principle. It forms the product of two input signals by squaring their sum and difference, then forming the difference of the squares. The squaring is done by sets of biased-diode circuits;

the diodes in each set are biased to start conducting in sequence, at ten levels in the range 0-100 volts, so that their total current output variation with input voltage follows an approximately parabolic law. The addition operations are performed by further high-gain amplifiers, and other amplifiers sum the output from the diode sets, which are biased to handle either polarity of input signal. This approximation to a square law places one restriction on the operation of the circuit. At low input levels, under 10 volts, the departure from a true square law is at its greatest; some care must therefore be taken to keep the input signal level to the multiplier above this, to minimise the resulting error. The gains of the input filter and the test circuit are accordingly adjusted to keep the r.m.s. input to each channel of the multiplier in the region of 20 volts.

Once the product of, say, the input signal and a delayed value of the output signal, has been formed by the multiplier, it is integrated by a simple integrator consisting of an operational amplifier with capacitive feedback. The rate of integration can be varied by adjusting the input potentiometer. This allows the mean product to be evaluated by integrating over a long period of time, while using quite high signal levels in other parts of the circuit, and without exceeding the maximum output level of 100 volts imposed by the measuring circuits of the computer. In general, integrating time of 100-150 seconds are needed to obtain accurate correlation functions, so considerable attenuation is needed at the integrator to keep its final output below 100 volts.



### 3.6. The mean-square computer.

This section has been added in an attempt to remove some of the errors attendant on calculating the average of a random variable over a limited period of time. These errors arise from two sources in particular. Firstly, if the random function varies only slowly with time, the computing time required for the integrator to settle to the average value, within a tolerable error, becomes very long, of the order of several minutes rather than seconds. Computation using such long times could be undertaken, but the total period needed to complete a full correlation would be of so many hours that it would become a matter of some difficulty to stabilise the characteristics of the random signal for the full period. In the tests made, the integrating time was fixed normally at 150 seconds. The results obtained from direct correlation over this period showed a considerable spread, even when the mean of two or three runs at each delay value was taken. The spread in such short-term tests will also be due in part to small fluctuations in supply levels to the noise generator, etc., which are not smoothed out sufficiently by short-term integration.

In the second place, compatibility of results in these tests depends on ensuring that each result is obtained by integrating over the same length of time, to within very close limits. Since the timing of the computer is controlled manually, by operating push-buttons in synchronism with a stop-watch, the timing is liable to errors of up to about half a second. This too tends to scatter

the results. In the attempt, therefore, to reduce these effects, the mean-square loop was introduced.

The basis of its operation is this. If the mean square value of the input signal to the test system is computed simultaneously with the correlation function, its value will exhibit a scatter due to the same causes. If the correlation function obtained is 'normalised' in a particular way, by dividing it by the mean-square input over the period of its computation, it is to be expected that the scatter of the normalised values will show an improvement over the direct method. Such an improvement has indeed been obtained in practice; a direct test was made at one point to establish this, and showed a reduction in spread, measured as a variance.

$$X^2 = \frac{\overline{|x_i - \bar{x}|^2}}{\bar{x}^2}$$

from  $12 \times 10^{-4}$  to  $2 \times 10^{-4}$ , where the signal level was high (40 volts) and from  $32 \times 10^{-4}$  to  $4 \times 10^{-4}$ , at low level (10 volts). Thus the improvement gained justifies the increase in circuit complexity needed to achieve it.

The circuit itself, shown as the upper branch in Fig.4., comprises a function generator, which performs the squaring, and an integrator of the same type as that in the correlator. The function generator has biased-diode circuits similar to those in the multiplier. For squaring, two sets of five circuits are used, and their break-points are set, as in the multiplier, to give a current out-put approximately proportional to the square of the input voltage.



Both sets are biased to conduct only for positive inputs; one set is fed directly with the system input signal, the other with the same signal passed through a sign-reversing amplifier, and the outputs of the two sets combined. The incoming signal is thus squared continuously regardless of its polarity.

### 3.7. The cursor system of Fourier transformation.

Once the correlation functions have been computed as described above, the next step is the taking of Fourier transforms to convert them to frequency spectra. The numerical process used to do this was developed by Rosenbrock.<sup>17,18</sup> The process was originally developed for transforming transient responses to frequency responses, and vice versa, so certain modifications to the technique are necessary before it will suit the present purpose.

Before the method can be applied, special graphs must be prepared for it. These must be produced on a particular type of paper, having three logarithmic decades on a 25-centimetre base. This must be done for the scale to fit a set of two calibrated transparent cursors, one to produce the sine and the other the cosine transform. The basis of the calibration of the cursors is given in Rosenbrock's paper.<sup>17</sup> When a graph of the function to be transformed has been prepared in the correct fashion, the cursors are placed over it, and the sum of the intercepts of the curve on the vertical scale lines of the cursor is read. This sum can be represented mathematically as follows;- for the cosine cursor, the sum  $S_c$  of the intercepts is

$$S_c = \frac{200}{\pi} \int_0^{\infty} \frac{f(x)}{x} \cos wx \, dx. \text{-----}(10)$$

and for the sine cursor, the sum  $S_s$  is given by

$$S_s = \frac{200}{\pi} \int_0^{\infty} \frac{f(x)}{x} \sin wx \, dx. \text{-----} (11)$$

where  $f(x)$  is the function whose transform is required.

There are two modifications required to fit this relation to the present requirements. We require in each case the transform

$$S = \int_0^{\infty} F(T) \frac{\cos}{\sin} wT \, dT.$$

Hence the functions  $f(x)$  in (10) is not equivalent to  $F(T)$ , but to  $T.F.(T)$ . So the curves to be plotted logarithmically for use with the cursors are  $T.A(T)$  and  $T.C(T)$  respectively. Also it will be noted that the sums in equations (10) and (11) represent only the positive half-range of the transform integral in each case. To obtain the power spectrum from the correlation function, the full range integral is required. For the transformation of autocorrelation functions, which are even functions of  $T$ , the sum read from the cursor will therefore simply be doubled. With the cross-correlation function, however, more care must be exercised. This is an irregular function of  $T$ , and can be divided into two sections, for positive and negative values of  $T$ . In general,  $C(T)$  will be positive over most of both sections;  $T.C(T)$  will therefore change sign with  $T$ . Over the positive range of  $T$ , the positive section of  $T.C(T)$  can be transformed normally for both sine and cosine transforms. The weighting applied by the cursors to  $T.C(T)$  is  $\frac{\cos wT}{T}$  or  $\frac{\sin wT}{T}$ , where  $T$  is always positive. The weighting required in the negative range of  $T$ . to complete the transform is  $\frac{\cos w(-|T|)}{-|T|}$  and  $\frac{\sin w(-|T|)}{-|T|}$ . If then the negative section of  $T.C(T)$  is transformed using the cursors,



this is equivalent to weighting it with  $\frac{\cos w|T|}{|T|}$  or  $\frac{\sin w|T|}{|T|}$ ; the sum obtained from applying the cosine cursor to this section of  $T.C(T)$  thus requires its sign reversed before it is added to the sum obtained from the positive section, while the sum obtained from the application of the sine cursor to the negative section can be added directly. This arises because the weighting

$$\text{applied, } \frac{\cos w|T|}{|T|} = - \frac{\cos w(-|T|)}{-|T|}$$

$$\text{while } \frac{\sin w|T|}{|T|} = \frac{\sin w(-|T|)}{-|T|}$$

Provided these two modifications are observed, the cursor system performs the required transformations quite effectively. It is, however, rather slow and cumbersome, so a development along the lines of some of the more automatic methods outlined in Chapter 2, by suitable for low frequency applications, would seem to be called for if the system is to be applied on a larger scale.

### 3.8. Evaluation of the transfer functions.

When the operations detailed above are complete, we are in possession of three spectral density curves, viz. input and output power spectra,  $P_1(w)$  and  $P_2(w)$ , and their cross-spectral density,  $P_{12}(w)$ . The final stage in the procedure consists simply of dividing the corresponding ordinates of these curves, in accordance with equation (8) in Chapter 1. From the three spectral densities we can obtain two forms of the frequency response, the complex function  $G(w)$  and the squared-amplitude response,  $P_t(w)$ , which will be a real function of  $w$ . The final step in the evaluation is thus

$$G^*(w) = \frac{P_{10}(w)}{P_1(w)} ; \quad P_t(w) = \frac{P_2(w)}{P_1(w)}$$

#### 4. TESTING AND ASSESSMENT OF SYSTEM.

##### 4.1. General test schedule.

This section deals with the tests carried out on the complete apparatus, in assessing its performance when carrying out its primary purpose of system analysis. Other tests which were carried out on individual units of the apparatus to determine their operating limitations are described, with their development, in the two chapters which follow this.

As a preliminary to full-scale tests on actual control systems, a number of tests were made of the correlating circuits alone, first using a sinusoidal input, whose correlation function could readily be checked, then with a noise input. These were followed by full tests on two specific systems, one a simple single-stage filter, the other a closed-loop control system of third order. The data obtained from these tests was processed completely to obtain the transfer functions of the systems, and direct comparison was made with functions plotted from the theoretical equations of the systems.

In the case of the filter, after making certain simplifying assumptions, evaluation was also made of the theoretical correlation functions, for comparison with those obtained in practice. The development of these functions is carried out in Appendix 1.

##### 4.2. Preliminary testing of correlating circuits.

The first test carried out was to determine the autocorrelation function of a sine wave. To simplify operation of the delay unit, the range of delay used was restricted to 100 milliseconds; accordingly, the frequency of the sine wave was chosen at 10 c/s, to allow a full cycle of the autocorrelation function to be computed.



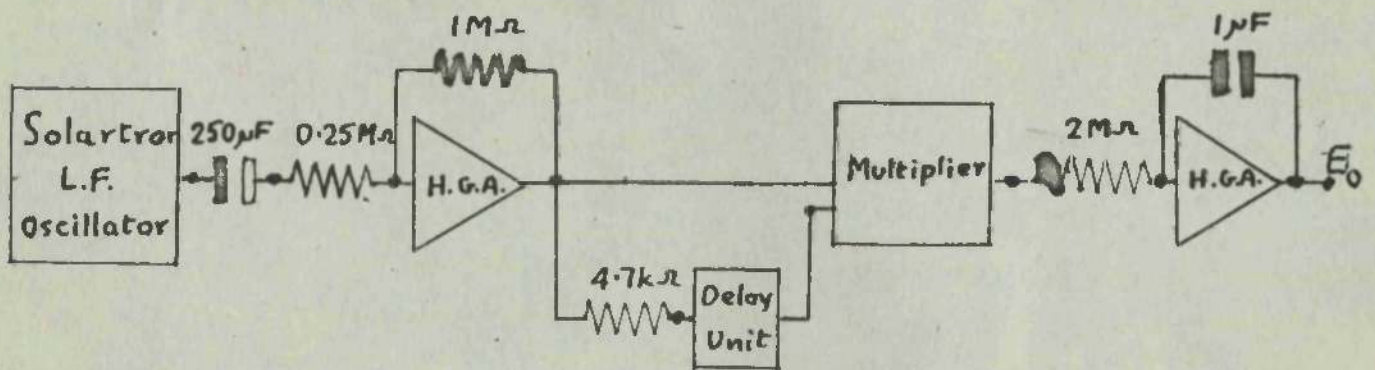


Fig.6. Circuit used for autocorrelation of sine wave.

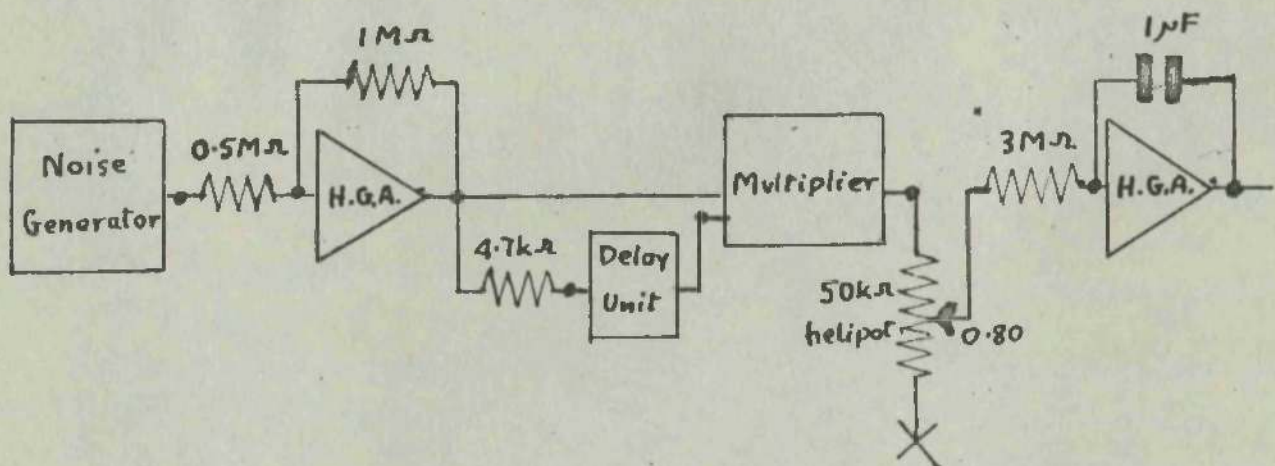


Fig.7. Circuit used for autocorrelation of noise.

The circuits used in the preliminary tests did not include the mean-square loop, which was introduced at a later stage. The circuit for the sine-wave test is shown in Fig. 6. A stage of amplification before the correlator was found necessary to raise the signal level at the multiplier, as the output available from the signal generator used was only 12 volts peak. A test at this level gave very scattered results; the multiplier signal at this low level was almost swamped by the quite small amount of 'hum' present. Operation at about 48 volts peak successfully cured this. The desired autocorrelation function for a sine input, say  $E = E_i \cos wt$ , is

$$\begin{aligned} A_{ii}(T) &= \lim_{x \rightarrow \infty} \frac{1}{2x} \int_{-x}^x E_i \cos wt \cdot E_i \cos w(t+T) dt. \\ &= \lim_{x \rightarrow \infty} \frac{1}{2x} \int_{-x}^x \frac{E_i^2}{2} (\cos wT + \cos 2wt + wT) dt. \\ &= \lim_{x \rightarrow \infty} \frac{1}{2x} \left[ \frac{E_i^2}{2} \cdot t \cos wT \right]_{-x}^x + \lim_{x \rightarrow \infty} \frac{1}{2x} \left[ \frac{E_i^2}{2} \sin \frac{(2wt + wT)}{2w} \right]_{-x}^x \\ &= \frac{E_i^2}{2} \cos wT. \text{ ----- (12)} \end{aligned}$$

The results obtained, after correction for switching losses as set out in Chapter 6, are plotted on Graph 1. From Fig. 6., it can be seen that the actual output voltage of the correlator is related to the correlation function as follows:

$$\text{Output voltage, } E_o = \frac{8}{100} \int_0^x E_i(t) \cdot E_i(t+T) dt., \quad x = \text{integrating time.}$$

$$\text{Thus } A_{ii}(T) = \frac{1}{x} \int_0^x E_i(t) \cdot E_i(t+T) dt. = \frac{100}{8x} E_o.$$

In the test, the integrating time used was 15 seconds, or 150 cycles of the input sine wave. Hence  $A_{ii}(T) = 0.833 E_o$ . Using this figure the output amplitude can be checked, for from equation (12) above,



$$A_{ii}(0) = \frac{E^2}{2} = \frac{11.7^2}{2} = 68.5.$$

Hence the output voltage after 15 secs.,  $E = \frac{68.5}{0.833} = 82.2$  V.

The practical value achieved at  $T = 0$  was 79.5 V.; a sufficiently close estimate to allow the unit to be used in its existing form; results at other values of  $T$ , after correction, were also acceptable.

Following this test, as soon as the noise generator was complete, an evaluation was made of the autocorrelation function of the noise it produced. This was done partly to test the full scheme of analysis including the Fourier transforms, and partly to help investigate the frequency spectrum of the noise. Earlier attempts to do this, using conventional waveform analysers with tuned amplifiers, had not succeeded in producing conclusive results, as the time constants of the measuring circuits used were not long enough to damp out the random fluctuations in amplitude of the components selected by the amplifiers.

The slightly different circuit used for this test appears in Fig.7. Again the noise is amplified before being passed to the correlator. Further attenuation is required before the integrator on this occasion, as the integrating time was increased to 100 secs. to cope with the very low frequencies present in the noise. The noise does not in fact extend down to d.c., as there is a further low-cut filter at the generator output; this cuts off at 0.01 to 0.02 c/s, depending on the load impedance on the generator. The autocorrelation function obtained is given in Graph 2, and the frequency spectrum resulting from Fourier transformation of it is given as Graph 3. It will be evident from the latter that the actual spectrum obtained is by no means as flat as would be desirable if

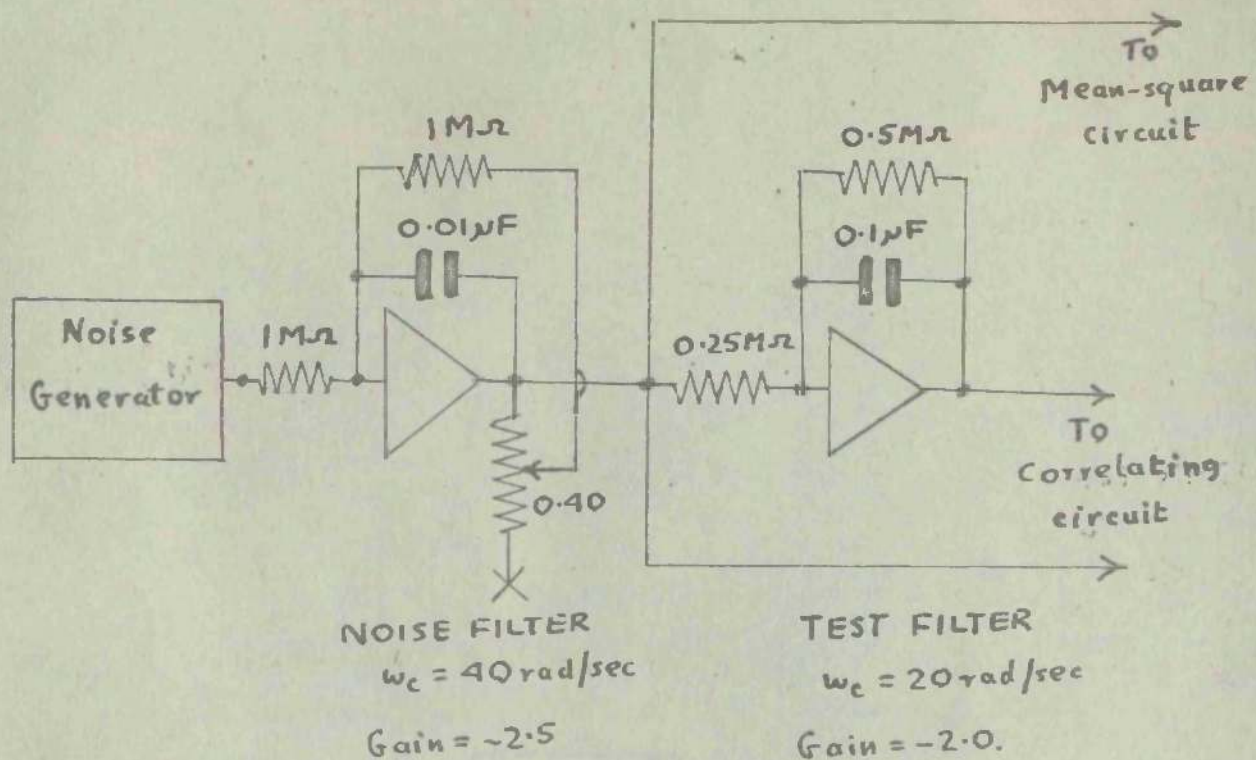


Fig.8(a). Circuits used for filter test.

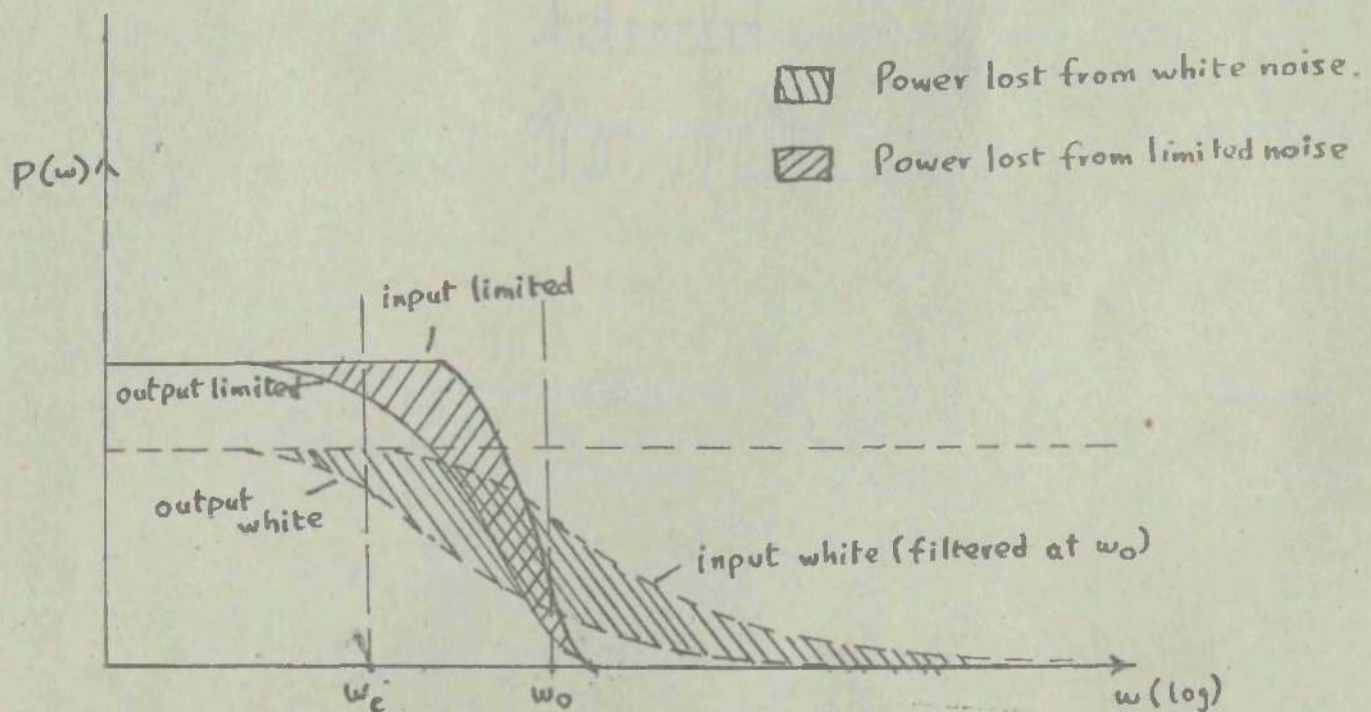


Fig.8(b). Comparison of power lost in an R-C filter (cutoff  $\omega_c$ ) from prefiltered white noise (broken lines) and from band-limited noise (full lines), of similar mean level.



wide-band systems were to be analysed. Since the main purpose is to investigate servo systems operating at frequencies generally below 10 c/s, the noise obtained will in fact be adequate, and this will still be true when further filtering is added to improve the amplitude distribution of the noise.

#### 4.3. Test of full method - single-stage R-C filter.

In this test, and the one following, the complete analysing circuit was used to produce both complex and squared-amplitude responses for the system. The full circuit is that discussed in Chapter 3, and illustrated in Fig.4. The test system in this instance consisted of another single-stage R-C filter, built on an analogue amplifier in a similar manner to the one shown following the noise generator in Fig.4. The test stage has a fixed cutoff frequency of 3.18 c/s. The cutoff of the first stage was adjusted accordingly to be exactly twice, i.e. 6.36 c/s, using the variable time-constant facility mentioned in Chapter 3. The final settings to achieve this are shown in Fig.8. The later parts of the correlating circuit have been omitted from this figure for clarity; apart from adjustment of the attenuation at the integrator, to allow for the variation in output levels of the correlator during the several different computations, the remainder of the circuit is exactly as in Fig.4.

A set of three correlation functions was computed, and Fourier transforms obtained for all three. Graph 4 shows the input and output power spectra so obtained; the power spectrum to be expected at the output of the first stage on application of pure white noise is also given for the same power level. Comparison of this with the

input power spectrum to the test system demonstrates that, over the pass-band of the first stage, the noise applied from the generator quite closely approximates to white noise. The latter spectrum falls off rather more rapidly beyond the filter cutoff frequency, indicating a deficiency in higher frequency components, which is in agreement with the spectrum obtained earlier (graph 3) by direct correlation of the noise. The mean-square loop was in use for this test, so all the correlation functions produced are 'normalised' by division by the mean-square value, computed simultaneously, of the input signal to the test system. The effect of this is simply to reduce the spread in results, giving a smoother curve; it does not alter the basic shape of the curve. Since the set of functions are all divided by the mean square signal at the same point, no alteration is needed in the preparation of curves for the transformation process, and the calculation of the transfer functions is likewise unaltered.

The normalised correlation functions obtained in this test are shown on Graphs 5,6 and 7. With them are shown for comparison the corresponding functions obtained analytically, on the assumption that the input noise is completely white, from the equations developed in Appendix 1. Two major differences are noteworthy. First, in  $A_{22}(T)$ , the theoretical function makes a steeper departure from the vertical axis than the rounded practical function. This emphasises the presence of deficiencies, at both low and high frequencies, in the noise generator output. Further, the peak values of  $A_{33}(T)$  and  $C_{23}(T)$  in theory are markedly less than in practice. Reference to Fig.8(b) may explain this. The normalised function in Graph 7 is  $\frac{A_{33}(T)}{\bar{E}_2^2} = \frac{A_{33}(T)}{A_{22}(0)}$ ; so, at  $T=0$  the



peak value is  $\frac{A_{33}(0)}{A_{22}(0)} = \frac{\text{mean o/p power}}{\text{mean i/p power}}$  for the second filter. The spect

curves of Fig.8(b), for white noise and h.f.deficient noise, suggest that the output power, as a fraction of the input power, will be less for the pure white noise, as its greater h.f. content will suffer heavy attenuation. This supports the results of Graphs 6 and 7, as a similar finding will be made for  $C_{23}(T)$ , when allowance is made in both cases for the filter gain.

#### 4.4. Design of the third-order servo system.

The servo used in this example was designed as a third order system with a pair of complex poles and one real pole. Its response when designed initially was quite heavily damped (damping ratio = 0.3), but it was thought that a more interesting and useful test of the method would be to employ a more lightly-damped system, to test the effect on the correlation functions of the oscillatory nature of the impulsive response, to which they are of course related. Alterations were made accordingly, and the ultimate specification of the system was

$$K(p) = \frac{4640}{p^3 + 12p^2 + 1090p + 4640} .$$

This was considered as an open-loop system, with unity negative feedback applied round it, and the open-loop transfer function required for this arrangement was found,  $G(p) = \frac{K(p)}{1-K(p)} = \frac{4640}{p(p^2 + 12p + 1090)} .$

This in turn was synthesised on the computer by setting up the two factors,  $\frac{1}{p}$  and  $\frac{1}{p^2 + 12p + 1090}$ , in cascade, sharing the open-loop gain of 4640 between them, and applying unity negative feedback





round the open-loop system. The final analogue circuit resulting from this computation is given in Fig.9.

An approximate guide to the performance of the system may be gained by factorising the closed-loop transfer function. Since the system was designed to have a pair of complex poles and a real pole, this factorisation is readily done, and yields

$$K(p) = \frac{4640}{(p + 4.36) (p^2 + 7.64p + 1057)} .$$

This is equivalent to an open-loop system, having a second-order section and a low-pass filter in cascade. The filter has a very low cutoff (4.36 rad/sec.), while the second-order section has a natural frequency of 32.5 rad/sec. and is quite lightly damped ( $\zeta = 0.118$ ). The factorisation also gives the poles of the closed loop transfer function, and these are plotted in Fig.10, while Fig. 11 shows an approximate plot of the system step response obtained in practice.

#### 4.5. Random signal analysis of the third-order servo.

The system as set up above has a bandwidth less than that of the noise filter used in the previous test, so this filter was used unchanged to filter the noise before application to the system. This gave a very low output signal level indeed, far too low to give an accurate response from the multiplier. The output signal was therefore amplified before application to the correlating circuits at all, as shown in Fig.9., and allowance made for this change when the correlation functions were evaluated.

A set of three correlation functions was computed as before. In preliminary scanning to determine the extent of the functions, it was

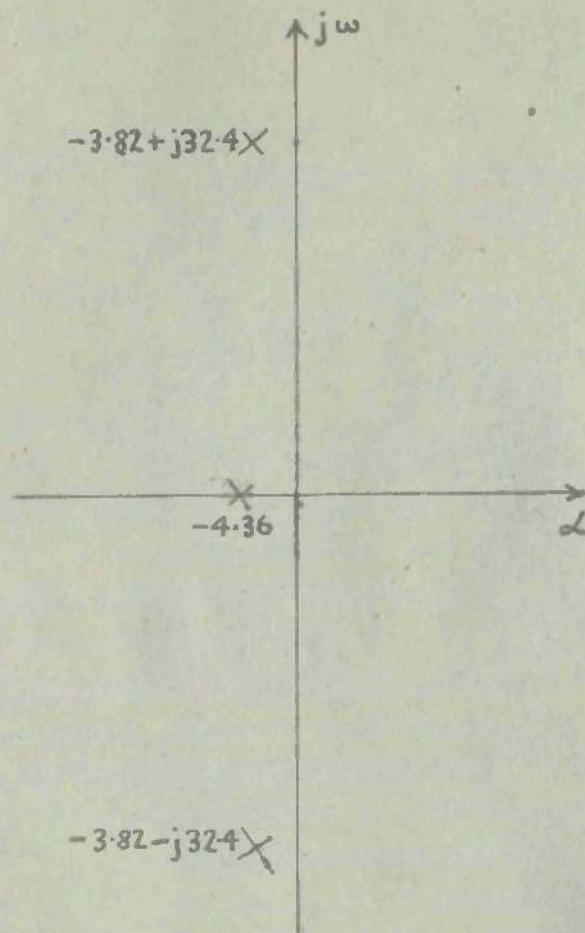


Fig.10. Poles of third-order servo system.

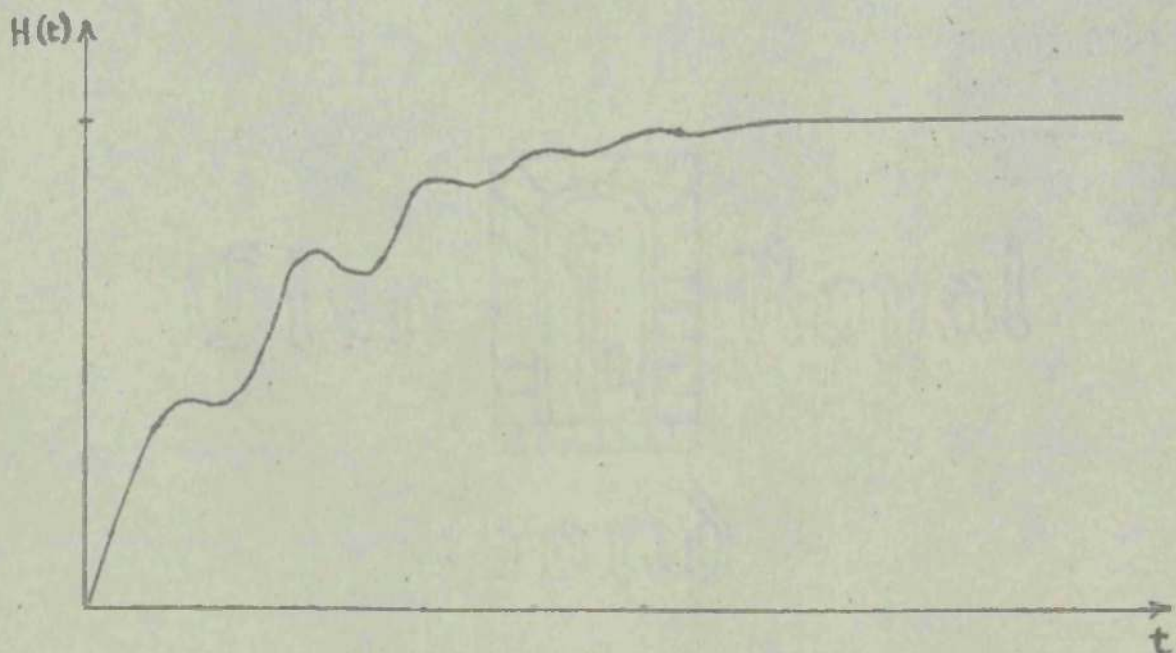


Fig.11. Approximate transient response of third-order servo.



soon evident that they extended significantly beyond the maximum delay of 400 milliseconds then available. Changes were made in the speed of rotation of the delay unit, to increase the maximum delay, so that the final curves could be extended to 800 milliseconds. As a result, the interval between successive points also increases, so the shape of the curve at these long delays becomes difficult to determine; this greater error is to be expected in the final transfer function when so great a range of delay is needed.

This is further aggravated by the necessity, when using the transform cursors, to transform the function  $T.A(T)$ , instead of simply  $A(T)$ , for this means that, even though  $A(T)$  is quite small, when  $T$  is large, the product  $T.A(T)$  remains large. It is therefore necessary to terminate the curve  $A(T)$  at a finite value of  $T$ , by bringing it to zero at this point, in order that the curve  $T.A(T)$  may be terminated within the computed range of  $T$ . This difficulty would seem to indicate that in general the use of the cursors for a purpose other than that for which they were designed distorts the process of transformation, and increases the likelihood of error in it; for this application to  $T.A(T)$  extracts, from the long tail of the correlation function, a contribution to the transform which is disproportionately important, when compared with the contribution from the major part of the function at low values of  $T$ . A method of transformation operating directly on the correlation function itself would probably produce a much smaller error due to this cause. It is suggested that other methods, referred to earlier in paragraph 2.4., to which the correlation functions could be applied directly, might

meet with more success on this point.

Once the full range of delays up to 800 milliseconds was available, a set of three correlation functions was computed for the servo also. The integrating time in use for this test, as on previous occasions, was two minutes; since the servo output is a very slowly varying time function, even an integrating time as long as this produced quite a considerable spread in the results, so three readings were taken at each delay value, and their average value used. Transformation of the correlation curves obtained presented no particular difficulty, as the whole functions could still be contained in the same three decades of  $T$  as before. It was not in fact found necessary to transform the input autocorrelation function again, as when compared point by point with that obtained in the filter test, using the same noise filter, very close correspondence was found. This, in a test conducted several days after the filter test, was a promising indication of stable output from the noise generator.

#### 4.6. Preparation and examination of transfer functions.

The power spectra produced above, from the 'normalised' correlation functions, were then ready to be divided to obtain the two transfer functions of the systems. In both cases, since the transfer functions were known in theory, the theoretical functions were computed and plotted first, for comparison. The pairs of functions obtained, theoretical and practical, are shown in Graphs 9 and 10 (complex transfer functions) and Graph 11 (squared-amplitude responses). The output power spectrum of the servo appears in Graph 12, together with the power spectrum of the input, while Graph 8 gives the correlation functions for the servo.



Examination of these graphs will show that, while the essential features of the responses of both systems have been preserved, there is present in all of the practical results a substantial degree of error. Analysis of the type and occurrence of the error gives very little definite information on its probable causes, as the errors in the results for the two systems, when plotted versus frequency, vary almost randomly in amplitude and in phase. In short, it seems very unlikely that the error is due to any one principal cause, but rather that it is an accumulation of errors occurring at different stages in the process of computation, none of which are regularly of great importance by themselves, or even very systematic, but which, when combined in the final result, produce an error of substantial size and of near random distribution.

A critical examination of the details of the process of computation does, however, reveal some portions of the process which appear more likely to give rise to rather unpredictable errors than others. A brief inspection of these may be expected to give a lead to the most satisfactory approach to the problem of improving the accuracy of the method. In an attempt to distinguish errors occurring in one particular part of the process, the errors found have been plotted and analysed in a great variety of ways, as amplitude error, phase error, and as error in the two separate parts of the complex response, but no definite relation has yet been found between any two of these. It is therefore felt to be more constructive to examine each stage of the process in turn, and estimate the possible sources of error at each stage; these individual errors will not necessarily

be of a systematic nature, so when combined in the final result, the total error will have a random character.

#### 4.7.Sources of error in the correlation process.

Two restrictions are placed on the computation of the correlation function which are liable to cause error, Firstly, the time of computation of the function is strictly limited, usually to about 150 seconds. For simple mathematical time functions, the error due to this limitation can readily be estimated (Solodovnikov<sup>6</sup>,p.114), e.g., for a sine wave of angular frequency  $w_0$ , the error involved in restricting computation to C seconds is approximately

$$e = \frac{1}{w_0 C}$$

If then the random signals used in the tests are represented by an assembly of sine waves, we can estimate the error due to, say, the lowest frequency component; this can be defined, since there is a lower limit to the noise spectrum, due to the output filter on the noise generator, of  $w_0 = \frac{1}{8}$  rad/sec. For a computing time of 150 seconds, the error in the contribution of the lowest frequency component is

$$e = \frac{1}{\frac{1}{8} \cdot 150} \text{ or } 5.33\%$$

while at the upper frequency limit of interest, about  $w_0 = 40$  rad/s. the error would be  $e = \frac{1}{40 \cdot 150}$  or 0.016%. So for any frequency above say 1 rad/sec., the error in that component of the correlation function will be less than 1%.

More serious, and less easily predicted, is the error due to the finite steps by which the delay is varied. As is described in Chapter 6, the delay is variable in four ranges, 0-100,0-200,0-400 and 0-800 milliseconds. Each range has 25 equal steps, so the steps



themselves increase in the higher ranges, and are of approximately 4,8,16 and 32 milliseconds respectively. When the two highest ranges are in use, the difficulty of plotting an accurate curve through the widely spaced points produced by it is great, and a substantial error is almost inevitable here. As was mentioned above, the occurrence of an error of this kind in the correlation function will be aggravated by the form of the transformation process used, which deals more severely with errors at large delays, due to the multiplication by the delay time  $T$ .

There is also some loss due to discharge of the delay storage capacitors on read-out, but, as is shown in Chapter 6, this loss is very nearly constant over the range of input frequencies used, so can be compensated by multiplying all the results by a constant factor, and this has been done in all the tests.

#### 4.8. Errors occurring in the transformation process.

The basic weighting function used in the calibration of the cursors (Rosenbrock<sup>17</sup>) is the graph of  $\frac{\cos}{\sin} wT$  against  $\log w$  (or  $\log T$ .) The oscillations in sign of this function will thus become very closely crowded together as  $w$  increases, so that in the last quadrant of  $w$  only one value of the weighting function per cycle is available. At the same time, slow fluctuations in the correlation function are also crowded by the logarithmic scale; in some cases, these become so narrow that they fall between two weighting scales and are eliminated from the transform sum altogether. The error arising from these omissions is not easy to estimate, as it is dependent on the exact position of the cursor, but it can be said that some error is almost certain to occur due to this cause at all

frequencies. Additionally, the distorting effect involved by the use of cursors making an indirect transformation, as here, of  $T.A(T)$ , rather than a direct transform of  $A(T)$ , will place undue emphasis on the region of the correlation function where  $T$  is high, and where consequently the accuracy of the function is poorer (para.4.7.). Once again, errors due to these causes are not of a nature which is readily tractable mathematically, so prediction of their size and occurrence is not really possible without recourse to assumptions about the mechanism of their production which cause too great a departure from the practical situation.

#### 4.9. Conclusions on the accuracy and possible development of the method

Since the sources of error are so diverse, and individual errors due to each source cannot readily be separated from the general error, numerical estimates of the accuracy of the computation process in any one particular case are of little value. The r.m.s. error in the case of the third order servo is 10.7%, yet the mean error for the same system is under 4% of the theoretical value. There is no reason to believe, however, that these figures would apply equally to any type of test system, as the errors do depend to a considerable extent on the exact pass-band of the system. It should be stressed that the qualitative performance of the method, in determining the salient features of the system response function, such as resonant and cutoff frequencies, and the relative gain values at these frequencies, has been shown in both tests to be quite satisfactory.

The foregoing analysis of the most probable sources of error in the existing apparatus does serve to indicate a number of particular



points in the sequence of computation at which attention could be given to improvements. These can be summarised as follows:

(i) Correlator. Improvements are required in the construction of the delay switch to allow the delay time to be varied in equal steps over the entire available range of delays, so that the correlation functions can be plotted with uniform accuracy throughout.

(ii) Transformation. The adoption of a system of transformation which is capable of handling the correlation function directly, and whose accuracy of transformation is as nearly as possible independent of the particular values of the transform variables in use, is to be recommended. One or two such systems are outlined in Chapter 2.

In general, the computing components used to simulate the test control systems and to assist in performing the necessary mathematical operations gave no trouble whatever; indeed, the main problem requiring attention is that of developing the remainder of the equipment to a standard of accuracy comparable with that of the operational units. In these, all the fixed components are highly stable, and have been adjusted to an individual accuracy of better than 0.1%, while the potentiometers are multi-turn helical types built to a high standard of resolution and linearity. The low-frequency performance of all these has been above reproach.

## 5. THE RANDOM SIGNAL GENERATOR.

### 5.1. Specification.

The random signal generator described here was required as an auxiliary to the analogue computer, which has a working range of  $\pm 100V$ . Its output requirements were therefore to produce a random signal of at least 10V r.m.s. amplitude, including peaks to at least three times this value, and having a flat frequency spectrum from just above d.c. to about 10 c/s. The signal was to have zero mean value.

### 5.2. Review of generation techniques for random signals.

The generation of low frequency random signals must almost always be done indirectly by derivation from random signals of higher frequency, as the l.f. power produced by the normal primary sources of noise is very low. If this low-power signal were amplified in normal valve amplifier circuits, it would become heavily contaminated with hum and bursts of flicker noise from the valves, with consequent damage to its frequency spectrum. The bulk of techniques therefore extract noise in the a.f. range, amplify it and process it to produce a low-frequency signal either by beating or by envelope detection.

The most popular and convenient source of a.f. random noise is the miniature thyratron. This produces noise almost uniformly over a band extending from about 60 c/s to some tens of kilocycles; some increase in power can also be obtained by running it in the field of a permanent magnet. The next step, common to the majority of systems, is to extract a narrow, fairly flat band of noise from the a.f. band by use of a tuned amplifier.<sup>10,11,12,19</sup> From this point onwards, several different treatments are employed, so they will be given separately.



The most direct technique is that used by West and Roberts,<sup>12</sup> in which two narrow bands are selected, at about 5 and 8kc/s, and passed through a simple peak rectifier to obtain the l.f. envelope. The envelopes of the two signals are subtracted to give a l.f. output of nearly Gaussian distribution. A slightly different approach is made by Douce and Shackleton,<sup>11</sup> also using a non-linear element. This time the noise is severely clipped; a following low-pass filter removes the fundamental band and the harmonics, leaving only the l.f. modulation products of these. These are shown by West<sup>1</sup> to give a signal with an almost flat spectrum.

Another popular technique, which forms the basis of the generator built for this project, uses a modulating circuit, from which only the lower sideband is extracted. The main difficulty with this type of circuit is that of achieving adequate stability in the carrier frequency, and in the frequency response of the tuned amplifier. This circuit is described fully by Bennett and Fulton<sup>10</sup>, while Bell and Rosie<sup>19</sup> employ a similar circuit with a more stable type of amplifier and a built-in local oscillator.

One further rather novel technique has been developed, and described recently by Rainal,<sup>13</sup> which represents quite a departure from all those already described. This involved the production of a random signal from an assembly of samples of higher-frequency noise. The sampling process also operates randomly, and is said to produce samples with a distribution closely approximating to Gaussian.

### 5.3. Description of the actual circuit used.

The general layout of the generator is given as a block diagram in Fig. 12. The generator as a whole runs as a simple on-off device,

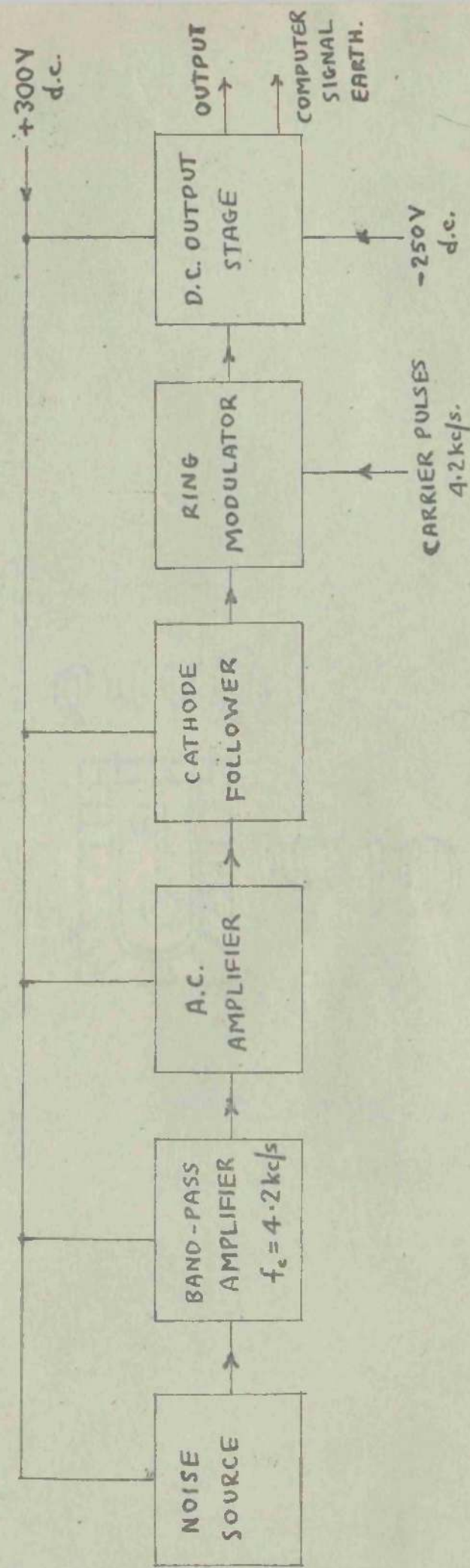


Fig.12. Block diagram of random signal generator.



controlled by switching on the supply to the thyatron. Fig.13. is a diagram of the complete circuit details. All the power supplies (+ 300 and - 250V d.c. and heaters) are obtained from external units, as also is the carrier supply for the modulator.

The noise source is a type 2D21 miniature thyatron, run at a fixed grid potential, and carrying a mean current of 16mA. Under these conditions, the output current shows vigorous plasma oscillations at 35-45kc/s, together with a wide band of background noise. The band selected was a compromise, as higher noise power is available at around 10kc/s, but increasing frequency complicates the design of a really narrow-band band-pass amplifier. Within the chosen band, around 4.2kc/s, the power available varies considerably with the mean current, so extensive tests were needed to determine the best operating current.

The thyatron output is passed through a band-pass amplifier, having two identical L-C tuned circuits, coupled by a small air capacitor. The frequency response of this amplifier is given on Graph 13, where it will be seen that the bandwidth at the minimum value of coupling capacitance is about 90c/s and with maximum capacitance about 110c/s. The narrow band of noise is amplified by an R-C coupled stage, and thence through a cathode-follower to the modulator.

The modulator is a ring circuit, employing four germanium diodes. It is coupled to the cathode follower by a centre-tapped matching transformer, at the centre tap of which is applied a carrier square wave at 4.2kc/s, generated by an external instrument. This wave is of 50V peak-to-peak amplitude, much in excess of the expected input, and so controls the state of conduction of the diodes, to produce at

the output a 4.2kc/s carrier wave modulated by the input a.f. noise. This signal will therefore contain the fundamental frequencies in the input band, together with their odd harmonics, and their sum and difference with the carrier. A large capacitor across the output of this stage eliminates all the a.f. components, leaving only the low difference frequencies. The output signal is push-pull, unsuitable for use in the computer, so the output stage used, which now has to be direct coupled, is a balanced 'long-tailed pair' circuit. This enables single-sided output to be taken from one anode. The d.c. level is then removed by a low-cut filter (cutoff 0.01c/s). The final output is thus a low-frequency random signal, of zero mean level, and suitable for direct injection into the analogue computer.

#### 5.4. Performance testing of the generator.

Once the generator was completed in its final form, a series of tests were carried out on it to determine the salient features of its output. These tests took several different forms, viz., calculation of the output mean level, r.m.s. level, and power spectrum, and a check on the long-term stability of the output levels, as it was anticipated that the work for which it would be used would involve test runs of long duration.

(i) Output mean and r.m.s. levels. The mean level of the noise was measured by integrating the output, using an operational amplifier and integrating for 150 seconds. The resulting mean value was 0.577V. This value fluctuated considerably on repeated tests, and is thought to arise chiefly through d.c. leakage through the electrolytic capacitor used in the final filter. Assuming that this mean level was maintained during a correlation test, which on the evidence available



seems unlikely, the effect of it on the output voltage of the circuit of Fig.8, after 150 seconds integration, would be a drift of about 2.5 or about 3% of output.

The r.m.s. noise level was determined both by computation (by squaring in the multiplier and integrating) and by direct measurement using a dynamometer voltmeter. The result in each case was of the order of 14V, a level quite sufficient for direct use in the computer.

(ii) Measurement of output power spectrum. An attempt was made to evaluate the output power spectrum by the use of a Muirhead-Pametr wave analyser. This instrument employs very narrow-band tuned amplifier circuits to select a narrow band of frequencies, and displays the r.m.s. signal in that band on a meter. Unfortunately the time constant of the meter circuit was much too short to average the fluctuations of this r.m.s. level, so the attempt with this method had to be abandoned. The spectrum was finally obtained by performing an autocorrelation on the noise output, as described in Section 4.2. The transform of this is Graph 3, and shown clearly the higher frequency deficiencies of the output. The flat band up to 40 rad/sec. has however proved to be adequate for testing the low bandwidth circuits used to simulate control systems.

(iii) Tests of output long-term stability. The stability of the output over a period of several hours is of considerable importance to the success of correlation tests at low frequencies, as on average the computation of one correlation function took some two and a half hours to complete. In the design of the generator, a number of precautions were taken to try to ensure this; for example, the d.c. power is obtained from high quality stabilised supply units, and the a.c.

supplies for valve heaters, and for the pulse generator which provides the carrier pulses, were derived from the mains through a 1000VA capacity electronic stabiliser. To check the effectiveness of these measures, a test of some three hours duration was carried out, in which the output of the generator was rectified, filtered and recorded by a pen recorder. The filtering circuit comprised a silicon diode, followed by an R-C filter stage with a time constant of 3.3. seconds, and was fed from the generator through a cathode follower. The result of this test, after analysis of the pen record (some 14 feet long) was that, in 2 hours 47 minutes recording, only two small departures from a steady mean output were recorded, neither of which lasted for more than about fifteen seconds. The output stability would therefore appear to be quite reliable for the two or three hour tests on which the generator was later employed.

5.5. Conclusion. The generator produced fits the specification set out for this type of work nearly enough for useful work to be done with it. Improvements are certainly possible, particularly in respect of the amplitude distribution, which on visual examination appears to be somewhat distorted as a result of a degree of clipping within the generator. If the use of a modulation technique for derivation of l.f. noise is to be continued, the incorporation of an internal carrier oscillator<sup>19</sup> appears to improve stability of operation, and would certainly remove the complication of tuning the external unit before operating the generator, as the internal unit could be tuned once for all. More reliable and controllable outputs could best be achieved, however, by the use of a form of the passive non-linear techniques already described.<sup>11,12</sup>



## 6. THE TIME DELAY UNIT.

### 6.1. Specification.

The computation of correlation functions requires the provision of facilities for delaying a time signal, with the minimum of loss in amplitude and minimum distortion, for a period of time which is clearly defined, but which can readily be varied over quite a wide range. The device used must have a low output impedance, suitable for coupling to other computing units, and must maintain reliable performance over several hours continuous operation.

The device described here was designed initially to give delays up to 100 milliseconds, at intervals of 4 milliseconds, but this was later found in practice to be inadequate for complete determination of some correlation functions. The range was accordingly increased to almost 800 milliseconds, but with the restriction that at the upper values the interval between available delay values was also increased to 32 milliseconds.

A further requirement was that the frequency response of the device should be as flat as possible up to at least 20c/s, to simplify any compensation which might prove necessary for losses in the device.

### 6.2. General note on storage techniques.

Several techniques have been developed for delaying a signal, some for delaying the complete continuous signal, others producing it as a series of discrete values. The first-mentioned manner of storage will of course include storage on magnetic tape, involving the use of a fairly complex modulation system to prepare the l.f. signal for application to the tape. This type of storage could be used for delaying data continuously, by using a loop of tape which would be re-used

once the first set of data recorded on it had been played back, but it would work more conveniently recording a sample of the data, which could then be played back with different values of time delay. In this system, the time delay is achieved by having separate recording and playback heads, which are spaced to operate on portions of tape some distance apart. Provided the two heads can be located accurately and one is capable of calibrated movement relative to the other, this system could be very efficient, but the amount of auxiliary apparatus needed is considerable.

An alternative, which normally will use discrete values of the input signal, is to store sampled values of the input on a series of isolated capacitors, whence the stored voltage can be read out at a later time, in sequence, to reconstitute the original signal. This system does not produce any permanent record of the signal passed through it, so the source of the input signal must be in operation during the whole time that the delayed signal is required. This is in contrast to the tape system, where a sample of data may be recorded once and a complete range of delayed signals suitable for correlation may be obtained from that one sample, without further reference to the source of the data for further information. One device operating on the capacitive storage principle is described by Janssen<sup>16</sup>. In it, the signal is passed, step by step, down a chain of capacitors, until it is finally read out. The passing-on of the sampled signal from one stage to the next is controlled by the operation of relays, and the total delay time taken to pass down the length of the chain is varied by altering the frequency of operation of the relays. The capacitors are separated by buffer stages to minimise losses in transit, so good



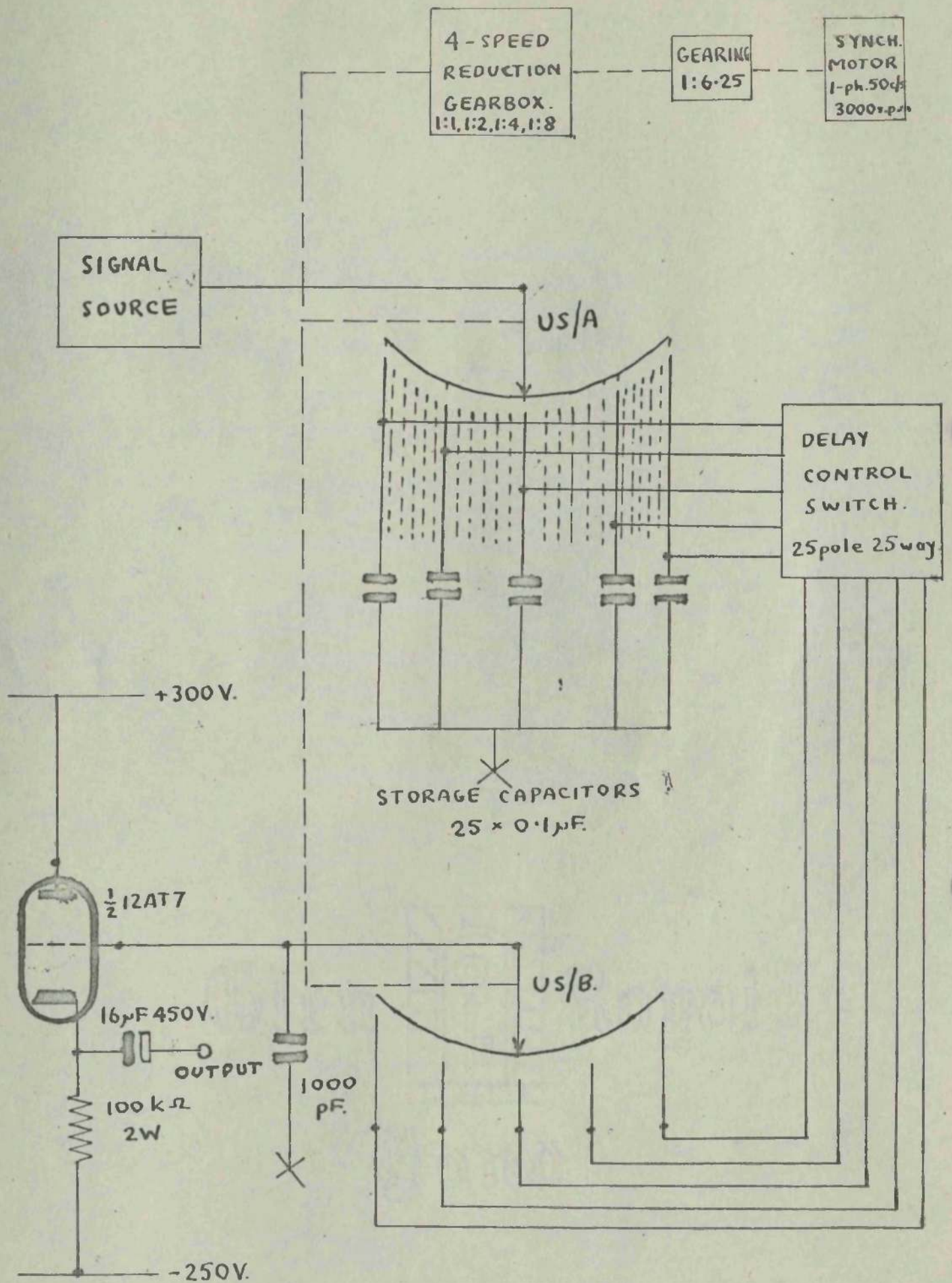


Fig.14. Circuit layout of complete delay unit.

reproduction of the input is to be expected, and the means of controlling the delay time is simple and accurate.

The system actually developed for use with the computer is a simpler form of this, in which the capacitors are quite separate, and are charged in sequence to successive sampled values of the input. The stored values are read out, in the same sequence, at a later time. The exact delay time is varied by altering the connections to and from the capacitors.

### 6.3. Construction of the delay unit.

The layout of the delay unit as a whole is shown on Fig.14. The incoming signal is fed to one moving arm of a standard Post Office Uniselect, the shaft of which is fitted with a large 150-tooth gear, and is driven as shown by a single-phase synchronous motor, through several stages of reduction gearing. The input arm, sweeping across the set of contacts US/A, charges in turn each of a bank of twenty-five storage capacitors. Simultaneously, a second arm is sweeping across an identical set of contacts US/B; the storage capacitors are connected to contacts US/B through the delay control switch. The position of this switch (described below) determines the amount of 'stagger' between the positions of the contacts on US/A and US/B which are connected to the same capacitor. Hence the 'stagger' determines the time delay between the charging of any one capacitor through US/A and the reading out of its stored potential through US/B, this is therefore the time delay applied to the whole signal in its passage through the unit.

The signal forms produced by this delaying process are shown on Fig.15. The upper waveform is a typical random input signal. At the



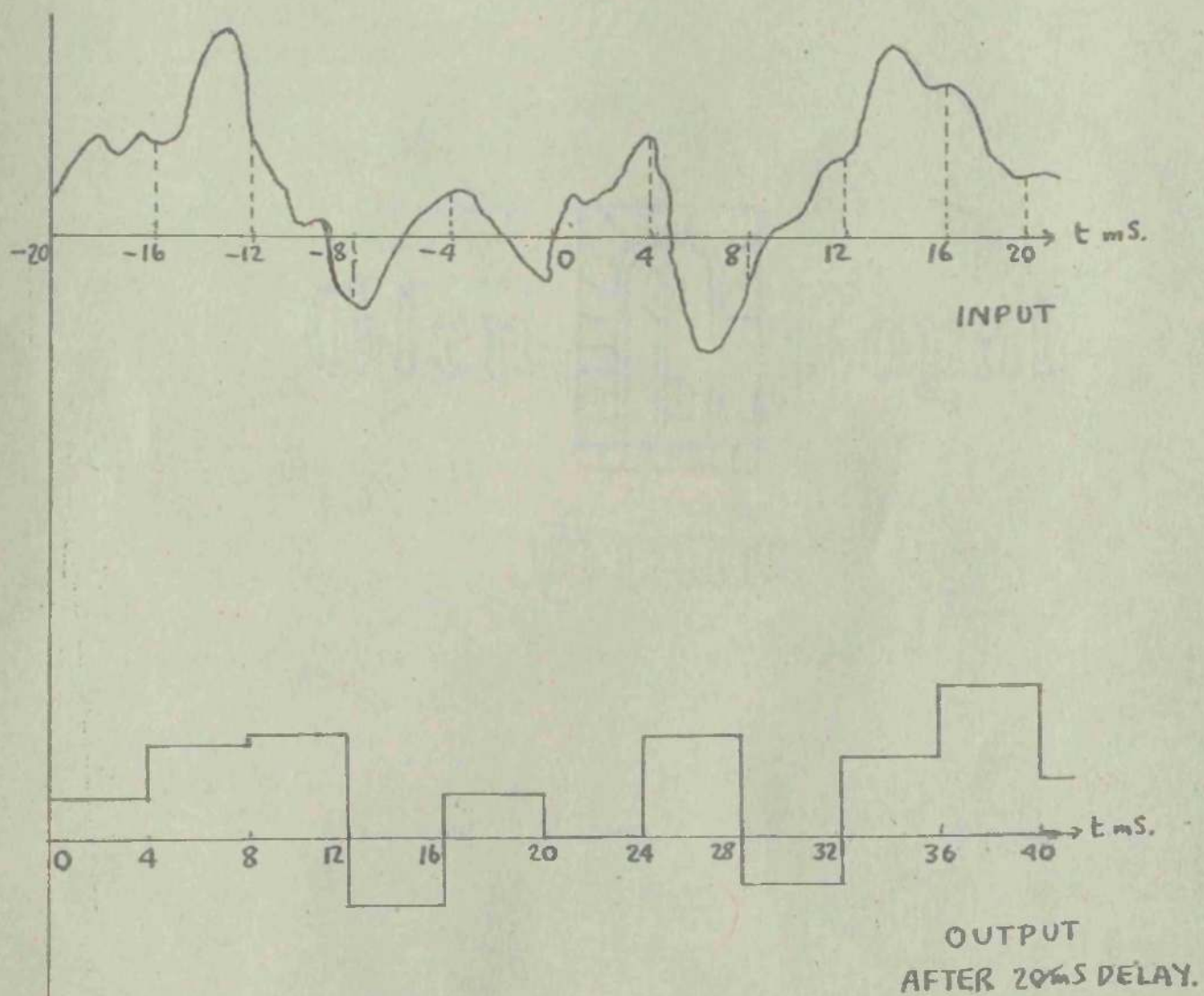


Fig.15. Typical input and output waveforms of delay unit.

highest rotational speed of the unit, this waveform would be sampled at intervals of 4 milliseconds, as shown by the broken lines, and the sampled levels stored. The lower waveform is the output which would be obtained after a delay of 20 milliseconds, the time origin being placed at the beginning of the output wave. The output thus consists of a series of discrete voltage steps, corresponding to the discrete values of the input.

This stepped output waveform is passed directly to the grid of the cathode follower valve, to offer a high impedance to discharge of the storage capacitors. A small 1000pF. capacitor is also placed in shunt with the main storage capacitor during readout. This is needed to maintain the output level during the 'break' period in the operation of the break-before-make contacts on the Uniselector. With these precautions taken in the circuit, the loss due to discharge in the readout circuit had been found to be barely detectable on inspection of the output waveform. Some loss is incurred, however, through bouncing of the moving contacts, which were not of course designed for continuous rotation. This effectively reduces the time available for charging the capacitors, which thus do not attain the full sample voltage.

As in the noise generator, there is a large capacitor at the output of this unit to remove the d.c. level arising in the cathode follower.

#### 6.4. Construction and operation of the delay control switch.

A special type of switch had to be constructed to perform the switching function required in changing the 'stagger' of the capacitor connections. The requirement is that the connections of all twenty-five



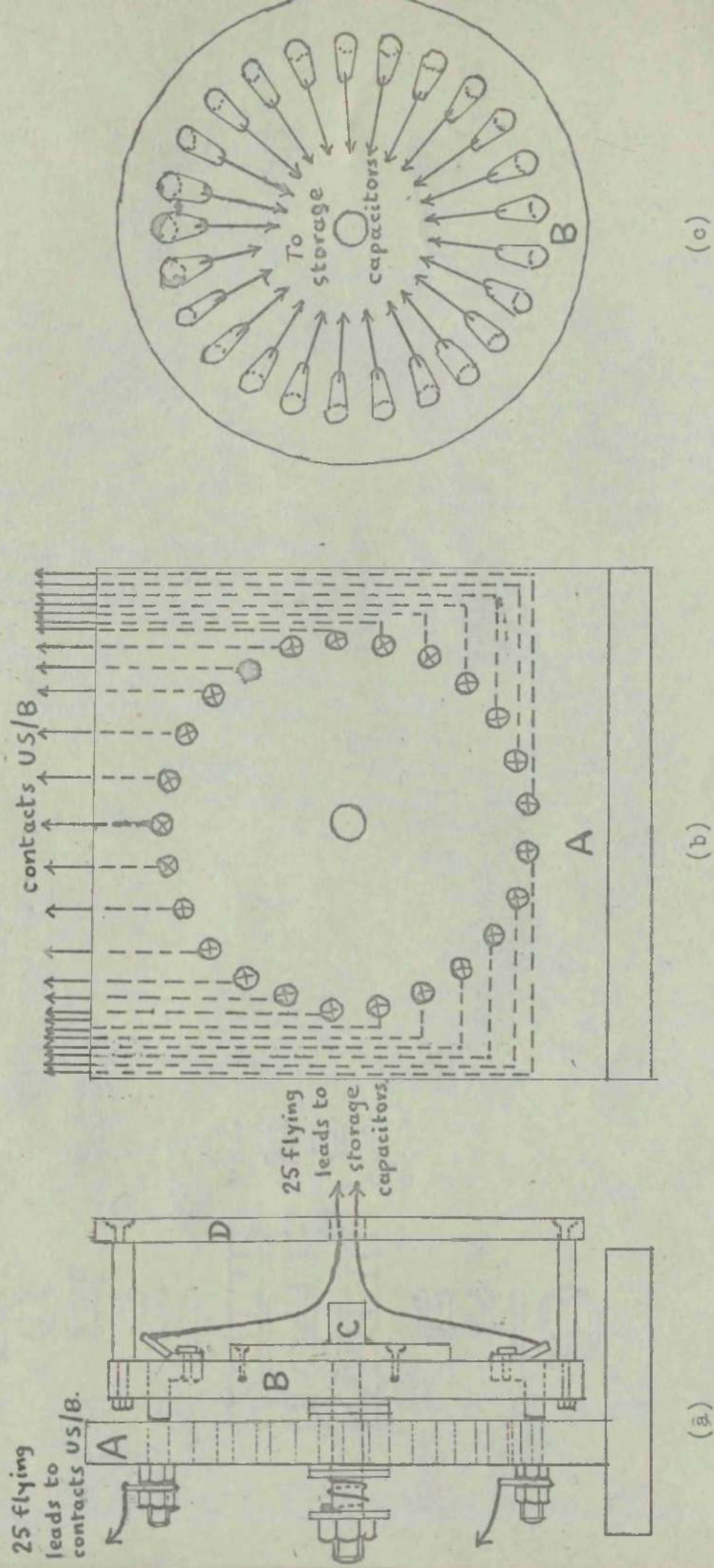


Fig.16. Construction and assembly of delay control switch.

capacitors be transferred, simultaneously, between any two of the twenty-five contacts on the Uniselector, while ensuring that the capacitors will still be scanned, by the moving arm, in the same order in time.

The construction of the switch to do this is shown in Fig.16. Fig.16(a) shows the assembled unit, edge on, while Figs.16(b) and (c) show the construction of the fixed backplate A and the movable disc B respectively. Plate A carries 25 stud contacts, arranged in a ring and connected in cyclic order to the set of Uniselector contacts US/B. The moving disc B carries 25 sprung plunger contacts, set in a ring concentric with that on A and connected in order to the 25 storage capacitors. When assembled it can be rotated relative to A by handle D. The spindle assembly C serves to align the two sets of contacts and maintain pressure between them. It will be seen that rotation of disc B relative to A will transfer the capacitor connections simultaneously in the manner prescribed. The edge of the disc B is indexed to show the number of steps through which it has been moved relative to a fixed mark on A, thus indicating the exact stagger of the connections. On test, the mean contact resistance at each of the 25 points after several full-circle rotations, was found to be only 0.4 ohm.

#### 6.5. Evaluation of exact time delay due to the unit.

It is essential to know to a high degree of accuracy the exact delay applied to the signal in transmission through the delay unit. This is readily calculable from the details of the drive mechanism used to turn the Uniselector. The driving motor is a single-phase, two-pole, 50c/s synchronous machine; the prime mover speed is thus 3000 r.p.m. The drive is then taken through a fixed reduction gear of 6.25:1 ratio, then through a four-speed reduction gearbox giving



a reduction of 1:1, 2:1, 4:1 or 8:1. The final drive to the Uniselecto gives a further reduction of 150:96. Hence the highest final shaft speed is  $N_1 = 3000 \cdot \frac{1}{6.25} \cdot \frac{96}{150} = 307.5$  r.p.m. The time of one revolution is thus 195.3 milliseconds. In this time, each of the 25 contacts has been swept twice, so the time of passage of the arm over one contact is  $\frac{195.3}{50}$  or 3.906 milliseconds. This time is the delay gained by staggering the input and output contacts one step, so this may be regarded as a unit delay. Hence at top speed the delay is variable by steps of one unit up to 24 units, or 93.74 milliseconds. The three lower speeds will evidently produce delays which are multiples of the unit defined above, so the range of delay available may be summarised thus:-

Top speed of 307.5 r.p.m.	-	"	"	"187.5 mS "	"	"	7.
Second speed of 153.75r.p.m.	-	"	"	"187.5 mS "	"	"	7.
Third speed of 76.88r.p.m.	-	"	"	"375.0 mS "	"	"	15.
Bottom speed of 38.44r.p.m.	-	"	"	"750.0 mS "	"	"	31.

It is evident therefore that the increasing interval between available delay values will cause the accuracy of plotting of correlation curves to deteriorate as the delay increases. These curves must of course be plotted exactly, taking full account of the rather awkward values of exact delay, since they are used for transformation. The graphs of correlation functions included with this thesis, for convenience in plotting, are plotted to a base line calibrated in delay units, the unit being that defined above of 3.906 mS.

#### 6.6. Performance testing of the delay unit.

It was expected that some degree of loss was inevitable in the passage of a signal through a device of this type. Some tests were

therefore devised to estimate the extent of the loss and its variation over the frequency range likely to be encountered in the noise signals. The sources of loss have been outlined in Section 6.3.; the most serious, and the most difficult to cure, is that due to suspected 'bouncing' of the tips of the moving arms in passing over the fixed contacts of the Uniselect. As could be expected, this caused the loss to increase at higher speed, and also increased with wear on the tips after a lengthy period of operation. A small loss in amplitude, of about 1%, will also occur when the 1000pF 'carry-over' capacitor is placed in parallel with the main storage capacitor of 0.1 $\mu$ F during the read-out period. Loss due to discharge of the main capacitor on read-out is almost completely eliminated by the presence of the direct-coupled cathode follower.

The tests were carried out by measuring the mean-square signal at the output of the unit, set to a delay of 20 mS (approx.), and comparing this with the mean-square input signal. The input signal used was a sine wave varied in frequency from 0.1c/s to 20c/s. The test was carried out at the three upper speeds, and the results are shown in Graph 14, where the ratio  $\frac{\text{mean square o/p}}{\text{mean square i/p}}$  is plotted as a function of frequency. Also shown on that graph is the corresponding result at the top speed without the use of the cathode follower, to demonstrate its efficiency in reducing losses. It will be noted that the loss for all speeds is nearly independent of frequency; this enabled correction to be made for it by multiplying the subsequent results obtained with the unit by a simple constant factor. This is found on the basis that, since in correlation only one of the two signals whose product is averaged has been delayed, the amplitude error



resulting from the delay is related to the mean square loss found above as follows:-

Let the mean-square loss be a fraction  $E$  of the input mean square

Then the mean-square output of the delay unit is

$$\bar{E}_o^2 = \bar{E}_i^2 (1-E)$$

Hence  $E_{or} = E_{ir} (1-E)^{\frac{1}{2}}$ , where  $E_{or}$  and  $E_{ir}$  are r.m.s. of  $E_o, E_i$

If the undelayed component in the correlation product is  $E_s$

the correlation product will be

$$\phi = \overline{E_i(t) \cdot E_s(t+T)}$$

$$\text{For } T = 0, \phi_o = \overline{E_i(t) \cdot E_s(t)} = E_{ir} \cdot E_{sr}$$

If then the error in  $\phi_o$  due to delay loss is  $e$ , we have

$$\phi_o(1-e) = E_{ir} \cdot E_{sr} (1-E)^{\frac{1}{2}}$$

$$\text{i.e. } 1-e = (1-E)^{\frac{1}{2}}$$

so approximately,  $e = \frac{1}{2}E$ .

Since it has been found that the loss is nearly constant for all values of  $T$ , including zero, this result can be applied uniformly to all the correlation products obtained.

From the loss curves of Graph 14, the mean value of the mean-square loss  $E$  is found to be 0.09, so the error  $e$  in the correlation products will be 0.045. Accordingly all products so obtained have been corrected by multiplication by a factor of  $\frac{1}{0.955}$ .

Graph 14 shows a slight increase in the loss at the highest speed of 307.5 r.p.m. In fact, as the wear on the contacts of the Uniselector became rather severe after some 50 hours operation, a later test at this speed showed a marked increase in loss. Since the lower speeds were not similarly affected, the use of the highest speed was thereafter restricted to the minimum needed to complete the early parts of

the correlation functions.

#### 6.7. Conclusion.

The delay unit produced as described above has fulfilled the requirements of this application sufficiently well to enable useful work to be done with it. It has, however, some intrinsic limitations which require to be carefully observed if substantial errors are to be avoided. Principally these are due to mechanical characteristics of the equipment used, which have a more severe effect when the equipment is used in conditions far removed from those for which it was designed. This change of use has resulted in a very high rate of wear of the principal contact surfaces, with consequent aggravation of losses. The discontinuous type of delay has been shown to be well suited to this servo application, so a development of the principle, using preferably static switching techniques instead of mechanical devices, would seem to offer attractive possibilities in this field.



## 7. CONCLUSIONS.

A system has been developed for determination of the complex frequency transfer function of a control system, by the use of the correlation functions of signals directly associated with that system. It has been demonstrated in principle that signals derived from normally-operating equipment can be used for this purpose, with the minimum of disturbance to the system. Special equipment and circuits have been developed to form correlation functions, including the construction of a low-frequency variable delay device, but as yet it had not been possible to perform the second stage of the computation, i.e., the Fourier transformation of these functions, automatically. Attention to this point would seem to be the next logical step in the development of the method.

Testing of this equipment on its own, and later as a complete computation system, has revealed several basic points to which further attention is required in improving the accuracy and versatility of the method. In particular, in the delay unit, it is hoped that a future step would be the replacement of the existing mechanical switching apparatus by a static device, as the rate of wear on the contact surfaces of the mechanical equipment has proved to be very high, with consequent loss of accuracy of reproduction of the delayed signal. This development would also make possible the automation of the correlation process, so that the whole function could be produced, for a preset range of delay, in one continuous operation. A further step in the construction of an automatic Fourier transformer, capable of handling the output of the correlator, would then render the whole

process of system analysis almost completely automatic.

Trials have been made of the existing correlating equipment, using a numerical method of Fourier transformation, on two control circuits, which were simulated for the test by an analogue computer. The results obtained from these trials, for linear systems, suggest an accuracy of about 5% in the final complex transfer function. Qualitatively, all principal features of the system frequency responses, e.g., resonant frequencies, have been clearly defined by the practical results. The major drawback of the method in its present form of execution is the long time required to perform the correlation process; this in turn requires that the signals from the test system remain available for a considerable time, which in many applications would not be possible. The method is, however, readily capable of adaptation to work with recorded data if required, if the delay section were changed to a magnetic tape system. This would further enhance the versatility of the method.

For laboratory purposes, these tests require the provision of a random signal source. One such generator has been built, and has operated successfully throughout the tests, but it is felt that much would be gained by the provision of a more readily controllable source, in which the mean amplitude and bandwidth of the random signal would be more precisely controlled.

The results so far obtained have served to demonstrate the effectiveness of this approach to system analysis in principle. If further development is carried out on the lines indicated, in improving the speed and accuracy of the operation, the resulting equipment should provide an attractive and versatile method of analysis.



REFERENCES.

1. WEST, J.C., DOUCE, J.L. and LEARY, B.G.:-'Frequency Spectrum Distortion of Random Signals in Non-Linear Feedback Systems':-Proceedings I.E.E., Monograph No.419M, March 1961 (108C, p.259).
2. HENDERSON, J.G. and PENGILLEY, C.J.:-'The Experimental Determination of System Transfer Functions from Normal Operating Data':- Paper CV/2, Brit.I.R.E. Convention on 'Electronics in Automation' Cambridge, June 1957.
3. GOODMAN, T.P. and RESWICK, J.B.:-'Determination of System Characteristics from Normal Operating Data':- Trans.Amer.Soc.Mech.Engrs., Vol.78, p.259, 1956.
4. MURPHY, G.J.:-'Control Engineering', (Van Nostrand, 1959).
5. JAMES, H.M., NICHOLS, N.B., and PHILLIPS, R.S.:-'Theory of Servomechanisms', M.I.T. Radiation Lab. Series, Vol.25 (McGraw-Hill, 1947).
6. SOLODOVNIKOV, V.V.:-'Introduction to the Statistical Dynamics of Automatic Control Systems', (Dover, 1960).
7. LEE, CHEATHAM, and WIESNER:-'Application of Correlation Analysis to the Detection of Periodic Signals in Noise':-Proc.I.R.E., Vol.38, pp.1165-71, 1950.
8. SINGLETON:-'A Digital Electronic Correlator':-Proc.I.R.E., Vol.38, pp.1422-28, 1950.
9. BELL, D.A.:-'Electrical Noise', (Van Nostrand, 1960)
10. BENNETT, R.R. and FULTON, A.S.:-'Generation and Measurement of Random Noise':-Journal of Applied Physics, Vol.22, p.1187, 1951.
11. DOUCE, J.L. and SHACKLETON, J.M.:-'L.F. Random Signal Generator':- Electronic and Radio Engineer, Vol.35 p.295, 1958.

REFERENCES. (Continued).

12. WEST, J.C. and ROBERTS, G.T.: - 'Low Frequency Random Signal Generator'  
Journal of Scientific Instruments, Vol. 34, p. 447, 1957.
13. RAINAL, A.J.: - 'Sampling Technique for Generating Gaussian Noise': -  
Review of Scientific Instruments, Vol. 32, p. 332, March, 1961.
14. TUCKER, D.G.: - 'An Analogue Computer for Fourier Transforms': -  
Journal Brit. I.R.E., Vol. 18, p. 233, 1958.
15. BORN, FURTH and PRINGLE: - 'A Photoelectric Fourier Transformer': -  
Philosophical Magazine, Vol. 37, pp. 1-13, 1946.
16. JANSSEN, J.M.L.: - 'Discontinuous Low Frequency Delay Line with  
Continuously Variable Delay': - Nature, Vol. 169, p. 148, 1956.
17. ROSENBROCK, H.H.: - 'An Approximate Method of Determination of  
Transient Response from Frequency Response': - Proceedings I.E.E.  
Paper No. 1907M, November 1955 (102 B, p. 744).
18. ROSENBROCK, H.H.: - Instructions for Use of Transform Cursors,  
Costain-John Brown Ltd., para. 16.
19. BELL, D.A. and ROSIE, A.M.: - 'Low Frequency Noise Generator': -  
Electronic Technology, Vol. 37, No. 6. pp. 241-5, June 1960.
20. MURPHY, G.J.: - 'Basic Automatic Control Theory', (Van Nostrand, 1957)
21. MYLES, J.S.: - 'An Electronic Multiplier': - A.R.C.S.T. Thesis, 1959.
22. GRANT, I.: - 'Control Panel for an Analogue Computer': - A.R.C.S.T.  
Thesis, 1960.



# APPENDIX L.

## Analytical Derivation of Correlation Functions.

It is of interest to evaluate the several correlation functions used in the above analysis, for a number of types of control systems, and in particular to compare them with the functions obtained in practice from the apparatus. To do this, it will be assumed that the input to the system consists of noise which is 'white' over a band of frequencies considerably wider than the pass-band of the system; its power spectrum can therefore be represented by a constant power per unit bandwidth, and for convenience this constant will be taken as unity.

### A1.1. General Theory.

The fundamental functions used have already been defined above, and may be summarised as follows:- Time delay between function values

Autocorrelation function, of signal at point m,  $A_{mm}(T) = \int_{-\infty}^{\infty} f_m(t) f_m(t+T) dt$

Cross-correlation function, between signals at points m and n,

$$C_{mn}(T) = \int_{-\infty}^{\infty} f_m(t) f_n(t+T) dt$$

Transfer function of system,  $G(w)$

Power spectrum of signal at point m,  $P_m(w) = \int_{-\infty}^{\infty} A_{mm}(T) \cdot e^{-jwT} dT$  ----- (1)

$$A_{mm}(T) = \frac{1}{2\pi} \int_{-\infty}^{\infty} P_m(w) \cdot e^{jwT} dw$$
 ----- (2)

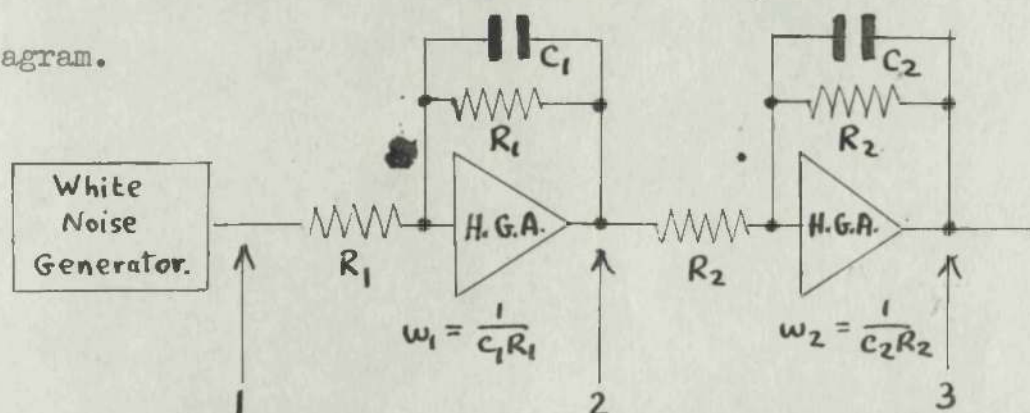
Also the following relation between auto- and cross-correlation functions;

$$C_{mn}(T) = \int_0^{\infty} W(x) \cdot A_{mm}(T-x) dx$$
 ----- (3)

where  $W(x)$  is the impulse response of the system between the points  $m$  and  $n$ .

### A1.2. Application to Filter Circuits used experimentally.

In the test circuits used above, the signal from the noise generator is passed through a single-stage low-pass R-C filter before being applied to the system under test. The cutoff frequency of this filter is at least twice that of the system. A similar filter of lower cutoff is also used as one of the test systems. Analysis will now be made of these two filters in cascade. The arrangement is shown in the block diagram.



#### (a) Autocorrelation of system input (point 2)

The input noise power spectrum,  $P_1(\omega) = 1$ .

Transfer function of first stage,  $G_1(j\omega) = \frac{1}{1 + j\frac{\omega}{\omega_1}}$

So the output power spectrum,  $P_2(\omega) = P_1(\omega) \cdot |G(\omega)|^2$

$$= \frac{\omega_1^2}{\omega^2 + \omega_1^2}$$

Autocorrelation function of system input,  $A_{22}(T) = \frac{1}{2\pi} \int_{-\infty}^{\infty} P_2(\omega) e^{j\omega T} d\omega$

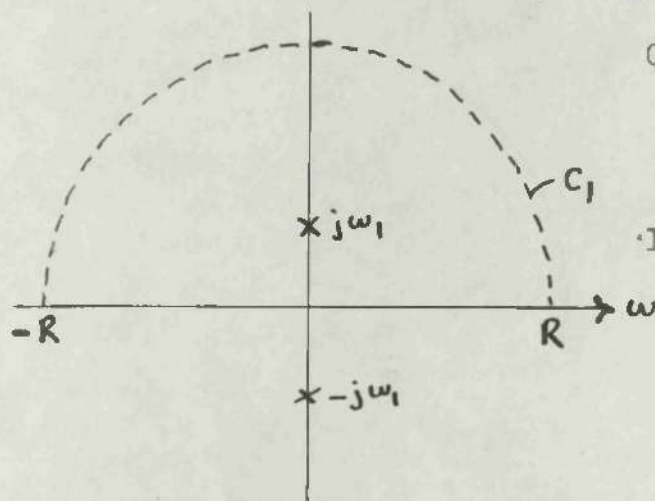
$$= \frac{1}{2\pi} \int_{-\infty}^{\infty} \frac{\omega_1^2 e^{j\omega T}}{\omega^2 + \omega_1^2} d\omega$$



This integral can be evaluated using Cauchy's residue theorem, and treating it as a contour integral.

This theorem states that, if a function  $f(z)$ , of the complex variable  $z$ , has a singularity at  $z = z_0$ , the integral  $I = \oint_C f(z) dz$  is given by  $I = 2\pi j \times$  residue of  $f(z)$  at  $z_0$ . The residue of  $f(z)$  at  $z_0$  is defined as  $R(z_0) = \lim_{z \rightarrow z_0} (z - z_0) f(z)$ .

Applying this to the integral above, we must first define the contour in the  $w$ -plane over which integration is to be effected. A suitable contour is the very large semi-circle shown in the sketch.



On this contour,

$$\int_{-\infty}^{\infty} F(w) dw = \int_{-R}^R F(w) dw + \int_{C_1} F(w) dw.$$

It can be shown that, as  $R$  tends to infinity, the second term tends to zero. In our case, the function  $F(w)$  has poles at  $w = \pm jw_1$ , as shown; only the

pole at  $w = jw_1$  lies within the contour of integration, so only the residue at this pole contributes to the value of the integral.

$$\begin{aligned} \text{Hence, we have } A_{22}(T) &= \frac{w_1^2}{2\pi} \cdot 2\pi j \cdot \lim_{w \rightarrow jw_1} (w - jw_1) \frac{e^{jwT}}{w^2 + w_1^2} \\ &= jw_1^2 \frac{e^{-w_1 T}}{2jw_1} \\ &= \frac{w_1}{2} e^{-w_1 T} \end{aligned}$$

However,  $A_{22}(T)$  is an even function of  $T$ , so we must replace  $T$  in the above expression by  $|T|$ . Thus finally  $A_{22}(T) = \frac{w_1}{2} e^{-w_1 |T|}$  ----- (4)

(b) Autocorrelation of system output (point 3)

The transfer function of the second stage is  $G_2(j\omega) = \frac{1}{1 + \frac{j\omega}{\omega_2}}$

So we have  $P_3(\omega) = P_2(\omega) |G_2(\omega)|^2 = \frac{\omega_1^2 \omega_2^2}{(\omega^2 + \omega_1^2)(\omega^2 + \omega_2^2)}$

Thus the output autocorrelation function is

$$A_{33}(T) = \frac{1}{2\pi} \int_{-\infty}^{\infty} P_3(\omega) \cdot e^{j\omega T} d\omega.$$

$$= \frac{\omega_1^2 \omega_2^2}{2\pi(\omega_1^2 - \omega_2^2)} \int_{-\infty}^{\infty} \frac{e^{j\omega T}}{\omega^2 + \omega_2^2} \frac{e^{j\omega T}}{\omega^2 + \omega_1^2} d\omega.$$

This integral may be evaluated by the method of residues also, using the same contour of integration as before; in this case, each part of the integral has two poles, but only one pole of each lies within the contour and so contributes to the value of the integral. The application of the method of residues yields the following:-

$$A_{33}(T) = \frac{\omega_1^2 \omega_2^2}{2\pi(\omega_1^2 - \omega_2^2)} \cdot 2\pi j \cdot \left[ \lim_{\omega \rightarrow j\omega_2} \frac{e^{j\omega T} \cdot (\omega - j\omega_2)}{2(\omega^2 + \omega_2^2)} - \lim_{\omega \rightarrow j\omega_1} \frac{e^{j\omega T} \cdot (\omega - j\omega_1)}{\omega_1(\omega^2 + \omega_1^2)} \right]$$

$$= \frac{\omega_1^2 \omega_2^2}{2(\omega_1^2 - \omega_2^2)} \left[ \frac{e^{-\omega_2 T}}{\omega_2} - \frac{e^{-\omega_1 T}}{\omega_1} \right] \text{-----(5)}$$

(c) Cross-correlation function around the filter.

The cross-correlation function around the filter can be evaluated with the same assumptions as before by use of the convolution integral of equation (3), paragraph A1.1., thus:-

$$C_{23}(T) = \int_0^{\infty} W(x) \cdot A_{22}(T-x) dx.$$

Bearing in mind that the cross-correlation function is an irregular function of T, which must be evaluated over the full positive and



negative ranges of  $T$ , care must be taken to observe the limits of validity of analytical representations of the functions involved.

These limits are, for the impulse response,  $W(x)$ ,

$$\left. \begin{aligned} W(x) &= w_2 e^{-w_2 x}, \text{ for } x > 0, \\ W(x) &= 0, \text{ for } x < 0. \end{aligned} \right\}$$

and for the input autocorrelation function ( from eqn.(4) above),

$$\begin{aligned} A_{22}(T-x) &= \frac{w_1}{2} e^{-w_1 |T-x|} \\ &= \frac{w_1}{2} e^{-w_1 (T-x)}, \text{ for } 0 < x < T \\ &= \frac{w_1}{2} e^{-w_1 (T-x)}, \text{ for } x > T. \end{aligned} \quad \left. \begin{aligned} & \\ & \\ & \end{aligned} \right\}$$

In order to observe these limits, the operation of convolution must be divided into two parts, that over the positive range of  $T$  and that over the negative range.

For positive  $T$ , the appropriate expression is

$$\begin{aligned} C_{23}(T) &= \int_0^T w_2 e^{-w_2 x} \cdot \frac{w_1}{2} e^{-w_1 (T-x)} dx + \int_T^\infty w_2 e^{-w_2 x} \cdot \frac{w_1}{2} e^{-w_1 (T-x)} dx \\ &= \frac{w_1 w_2}{2} \left[ \frac{e^{-w_2 T} - e^{-w_1 T}}{w_1 - w_2} + \frac{e^{-w_2 T}}{w_1 + w_2} \right] \\ &= \frac{w_1^2 w_2}{w_1^2 - w_2^2} \cdot e^{-w_2 T} - \frac{w_1 w_2}{2(w_1 - w_2)} \cdot e^{-w_1 T} \quad \text{---(6)} \end{aligned}$$

For negative  $T$ , we have, since  $x$  is always greater than  $T$ ,

$$\begin{aligned} C_{23}(T) &= \int_0^\infty w_2 e^{-w_2 x} \cdot \frac{w_1}{2} e^{-w_1 (T-x)} dx \\ &= \frac{w_1 w_2}{2(w_1 + w_2)} \cdot e^{-w_1 T} \quad \text{---(7)} \end{aligned}$$

### A1.3. Application to a circuit having complex poles.

Another type of circuit frequently encountered in an analysis of this sort is the quadratic resonant circuit, having two complex conjugate poles. It is therefore useful to derive the autocorrelation function of white noise (as defined above) after application to one such circuit.

Let the transfer function of the circuit be

$$G(jw) = \frac{1}{b^2 + 2j a w - w^2}$$

If the input noise as before has a spectral density of unity, the output spectral density will be

$$\begin{aligned} P(w) &= |G(jw)|^2 \\ &= \frac{1}{(b^2 - w^2)^2 + (2aw)^2} \\ &= \frac{1}{(w+k+ja)(w+k-ja)(w-k+ja)(w-k-ja)} \quad \text{where } k = \sqrt{b^2 - a^2} \\ &\quad \text{and } k > 0 \\ &= \frac{V}{w+k+ja} + \frac{W}{w+k-ja} + \frac{X}{w-k+ja} + \frac{Z}{w-k-ja} ; \text{-----(8)} \end{aligned}$$

The coefficients of the partial fractions are

$$V = \frac{1}{8jak(-k-ja)}; \quad W = \frac{-1}{8jak(-k+ja)}; \quad X = \frac{-1}{8jak(k-ja)}; \quad Z = \frac{1}{8jak(k+ja)}$$

The autocorrelation function of the output noise can then be obtained by Fourier transformation of equation (8), and is

$$\begin{aligned} A(T) &= \frac{1}{2\pi} \int_{-\infty}^{\infty} P(w) e^{jwT} dw. \\ &= \frac{V}{2\pi} \int_{-\infty}^{\infty} \frac{e^{jwT}}{w+k+ja} dw. + \frac{W}{2\pi} \int_{-\infty}^{\infty} \frac{e^{jwT}}{w+k-ja} dw. + \frac{X}{2\pi} \int_{-\infty}^{\infty} \frac{e^{jwT}}{w-k+ja} dw + \frac{Z}{2\pi} \int_{-\infty}^{\infty} \frac{e^{jwT}}{w-k-ja} dw \end{aligned}$$



These integrals can be evaluated as before by the method of residues. The same semi-circular contour of integration is used, so only two of the four complex poles of  $A(T)$  will be included by it. There will therefore be no contribution to the integral from the first or the third term above; only the second and fourth terms, from the poles at  $w = \pm k + ja$ , will have non-zero residues. The result of this operation is

$$\begin{aligned} A(T) &= jW e^{j(-k+ja)T} + jZ e^{j(k+ja)T} \\ &= jW \cdot e^{-aT} \cdot e^{-jkT} + jZ \cdot e^{-aT} \cdot e^{jkT} \\ &= \frac{-e^{-aT} \cdot e^{-jkT}}{8ak(-k+ja)} + \frac{e^{-aT} \cdot e^{jkT}}{8ak(k+ja)} \\ &= \frac{-e^{-aT}}{a^2 + k^2} \left[ -(k+ja)(\cos kT - j \sin kT) + (-k+ja)(\cos kT + j \sin kT) \right] \\ &= \frac{e^{-aT} (k \cos kT - a \sin kT)}{4ak(a^2 + k^2)} \end{aligned}$$

Once again, since  $A(T)$  must be an even function of  $T$ , we replace  $T$  by  $|T|$ , to give

$$A(T) = \frac{e^{-a|T|} (k \cos k|T| - a \sin k|T|)}{4ak(a^2 + k^2)} \quad \text{------(9)}$$

#### Al.4. Application to a general polynomial network.

As a final example, the results of applying white noise to a general network, whose transfer function can be represented as a polynomial fraction of degree  $n$ , can be evaluated. Let us suppose that the network transfer function is

$$G(p) = \frac{(p-z_1)(p-z_2) \dots (p-z_m)}{(p-p_1)(p-p_2) \dots (p-p_n)} \quad \text{where } m \leq n$$

After application of white noise, defined as usual to have unity power per unit bandwidth, the output power spectrum will be

$$P(w) = 1. |G(p)|^2$$

$$= \frac{\prod_{r=1}^m |jw - z_r|^2}{\prod_{r=1}^n |jw - p_r|^2} = \frac{\prod_{r=1}^m (jw - z_r)(jw - z_r^*)}{\prod_{r=1}^n (jw - p_r)(jw - p_r^*)}$$

Since  $m \geq n$ , this function can be separated into a series of partial fractions of the form

$$P(w) = \sum_{r=1}^n \frac{k_r}{(jw - p_r)} + \frac{l_r}{(jw - p_r)^*}$$

$$= \sum_{r=1}^n \frac{k_r}{(jw - p_r)} - \frac{l_r}{(jw + p_r^*)}$$

The coefficients  $k_r, l_r$  of the partial fractions are determined from the complex poles and zeros  $p_r$  and  $z_r$  in the usual manner, namely

$$k_r = \lim_{w \rightarrow -jp_r} (jw - p_r).P(w),$$

$$\text{and } l_r = \lim_{w \rightarrow -jp_r^*} (jw + p_r^*).P(w) \quad (\text{Murphy}^4, \text{ p.32}).$$

Hence the output autocorrelation function, by Fourier transformation is

$$A(T) = \frac{1}{2\pi} \int_{-\infty}^{\infty} P(w) e^{jwT} dw.$$

$$= \frac{1}{2\pi} \sum_{r=1}^n \left[ \int_{-\infty}^{\infty} \frac{k_r \cdot e^{jwT}}{(jw - p_r)} dw - \int_{-\infty}^{\infty} \frac{l_r \cdot e^{jwT}}{(jw + p_r^*)} dw \right]$$

This integral can be evaluated term by term, by the methods described above, If the same contour of integration is employed, it will be no



that only the upper half of the w-plane is enclosed by it. It follows that only poles lying in the upper half of the plane, i.e. poles with positive imaginary parts, will contribute to the final integral. Examination of the form of  $A(T)$  shows that it has poles at  $jw = p_r$  and at  $jw = -p_r^*$ , or at  $w = -jp_r$  and  $w = jp_r^*$ . Hence if the system examined is stable, i.e. if all the  $p_r$  have negative real parts, all the poles  $w = -jp_r$  will have positive imaginary parts, and so will be included in the integral, while all the poles  $w = jp_r^*$  will be excluded.

For a stable system, therefore, the result of integration is

$$A(T) = j \sum_{r=1}^n k_r \cdot e^{p_r T}, \text{ which for stable } p_r \text{ is convergent.}$$

Should the system have an unstable pole, however, say at  $p_k$ , the pole at  $w = -jp_k^*$  will be included by the contour. On integration, this pole will contribute a term  $l_k \cdot e^{-p_k T}$ , which for an unstable  $p_k$  is also convergent. No direct indication of instability is thus to be obtained from inspection of the autocorrelation function of the system output under noise conditions. From the convolution integral of equation (3), it would appear that an unstable system, for which  $W(x)$  will diverge as  $x$  increases, will also have a bounded cross-correlation function. This implies that it may be possible to determine a full set of correlation functions for such a system, and so obtain its frequency response in the usual way, and so establish its stability.

#### Al.5. Effect of 'normalisation' on the above calculations.

As has been stated in paragraph 4.3., the correlation functions obtained in practice were 'normalised', by division by the simultaneously computed mean-square value of the input noise. The intended effect of this device was to remove the distortion caused by small

fluctuations in the input power level, and in this it succeeded. The resulting function is thus independent of the actual power level in use, so if the theoretical functions calculated from the formulae determined above are 'normalised' in the same way, direct comparison will be possible, without knowledge of the power level used in the tests.

To normalise the functions, we need to know analytically the mean-square input to the test circuit. An evaluation will be made of the theoretical correlation functions for the R-C filter test circuit, so it is useful to compute the mean-square input to that. From the definition of an autocorrelation function, it is evident that the mean square value of the signal to which it applies is related to it as follows:-

$$\overline{E}_{ii}^2 = A_{ii}(0)$$

For the case of the filter circuit, with white noise input as defined above, and preceded by a noise filter (R-C stage, cutoff  $w_1$  rad/sec), as in section 4.3., the autocorrelation function of the input signal is, from equation (4) above,

$$A_{22}(T) = \frac{w_1}{2} e^{-w_1 |T|}$$

Hence the mean square input to the circuit is

$$\overline{E}_2^2 = A_{22}(0) = \frac{w_1}{2}.$$

Therefore all three correlation functions obtained analytically from equations (4), (5), (6) and (7) above are normalised by dividing each by  $\frac{w_1}{2}$ . The results of this normalisation are plotted beside the corresponding experimental functions on Graphs 5, 6 and 7.



### Al.6. Evaluation of the correlation function for the practical filter.

Numerical evaluation will now be made of the correlation functions for the actual filter circuit shown in Fig.8. In this process, in addition to the definition of noise, etc. used above, account must also be taken of the d.c. gain of the filter, which in this case is 2. The cross-correlation function will accordingly be multiplied by 2, and the output autocorrelation function by 4.

#### (a) Normalised input autocorrelation function.

Normalisation as defined in section Al.5 implies division by the input mean-square value, so this is required first, and is

$$\overline{E}_2^2 = A_{22}(0) = \frac{w_1}{2}$$

The input autocorrelation function is given by equation (4),

$$A_{22}(T) = \frac{w_1}{2} e^{-w_1|T|}$$

$$\text{Hence the normalised form is } \frac{A_{22}(T)}{\overline{E}_2^2} = e^{-w_1|T|} = \underline{e^{-40|T|}}$$

since from Fig.8. the cutoff frequency  $w_1$  of the first stage is 40 rad/sec.

This function is plotted on Graph 5.

#### (b) Normalised output autocorrelation function.

From equation (5) above, this function is, with d.c. gain K,

$$A_{33}(T) = \frac{K^2 w_1^2 w_2^2}{2(w_1^2 - w_2^2)} \left[ \frac{e^{-w_2|T|}}{w_2} - \frac{e^{-w_1|T|}}{w_1} \right]$$

From Fig.8., the circuit constants are  $w_1 = 40$  rad/sec  
 $w_2 = 20$  rad/sec  
 $K = 2$

Hence the normalised value is

$$\begin{aligned}\frac{A_{33}(T)}{A_{22}(0)} &= \frac{K^2 w_1 w_2}{(w_1^2 - w_2^2)} e^{-w_2 |T|} - \frac{K^2 w_2^2}{(w_1^2 - w_2^2)} e^{-w_1 |T|} \\ &= \frac{4.800}{1200} e^{-20|T|} - \frac{4.400}{1200} e^{-40|T|} \\ &= \underline{2.667e^{-20T} - 1.333e^{-40T}}, \text{ plotted on Graph 7.}\end{aligned}$$

(c) Normalised cross-correlation function.

The normalised forms of this function, again with d.c. gain K, can be derived from equations (6) and (7), and are

$$\begin{aligned}\text{For } T > 0, \quad \frac{C_{23}(T)}{A_{22}(0)} &= \frac{2Kw_1 w_2}{(w_1^2 - w_2^2)} e^{-w_2 T} - \frac{Kw_2}{w_1 - w_2} e^{-w_1 T} \\ &= \frac{4.800}{1200} e^{-20T} - \frac{2.20}{20} e^{-40T} \\ &= \underline{2.667e^{-20T} - 2.000e^{-40T}}.\end{aligned}$$

$$\text{For } T < 0, \quad \frac{C_{23}(T)}{A_{22}(0)} = \frac{Kw_2}{w_1 + w_2} e^{w_1 T} = \frac{2.20}{60} e^{40T} = \underline{0.667e^{40T}}.$$

These functions are plotted on Graph 6.



L.H. SIDE

R.H. SIDE

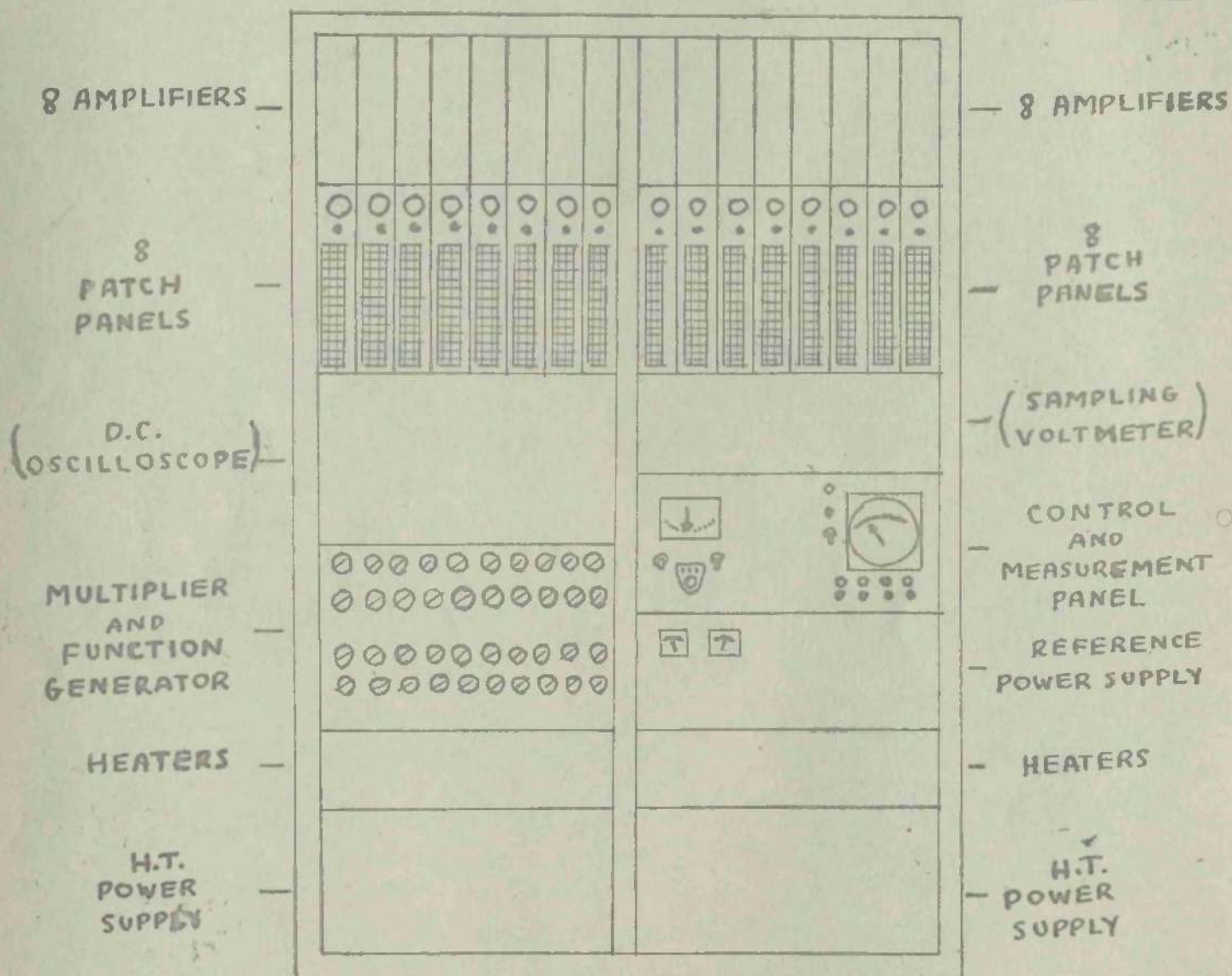


Fig.17. Lay out of component parts of analogue computer.

## APPENDIX 2.

### The Analogue Computer

#### A2.1. General Layout.

The computer used in the work described in the main body of this thesis was designed and built in the laboratory, as a general purpose computer suitable for a wide variety of classes of work. Its immediate application was to servo problems, so it was made capable of simulating quite slow systems. As a simulator, it is quite self-contained, but provision is made for simple coupling of any external auxiliary apparatus that may be required. All power supplies are built into the main chassis, as also is a highly sensitive measuring circuit. The operation of the computer can be controlled in three ways; it may be run manually, controlled by push-buttons, it may be triggered from an external source, or it may run on a continuous cycle of computation, controlled by a set of multivibrators.

A brief survey will now be made of the various component parts of the machine, outlining their performance features. A diagram of the layout of the machine is given in Fig.17, on which the location of all the principal units is shown.

#### A2.2. Computer components.

The disposition of the main components in the computer is shown in Fig.17. The layout is governed principally by considerations of weight and heat distribution among the components. Hence the heavy power supplies are placed at the bottom of the frame, while the sets of operational amplifiers are kept to the top to give maximum ventilation. The power supplies are force-cooled by fans mounted at



the rear of the chassis. All the units are mounted in a rack, built from steel angle, and fitted with castors to enable the complete machine to be moved about the laboratory if required; units can thus be readily removed for adjustment or repair if necessary.

(a) H.T. Power Supplies. Two main power supplies, one for each half of the machine, provide H.T. d.c. power for the amplifiers and some control circuits. Three supplies are available, of +300V, -200V and -300V, all of which are electronically stabilised by conventional techniques based on a neon reference tube.

(b) Heater Supplies. Heater power is obtained from sets of transformers mounted on separate trays above the H.T. supplies. The total load is carefully distributed among the transformers to keep them within rating and maintain stability of voltage level. The transformers themselves are high quality types having two separate secondary windings each giving a 250:6 ratio. To provide the amplifier valves with exactly 6.3V, the primaries are 'boosted' as shown in Fig.18 using another identical transformer, to give an on-load output of exactly 6.3V.

(c) Operational Amplifiers. The computer has as its core a set of sixteen identical operational amplifiers, which in combination with their patch panels perform the mathematical functions needed for simulation and computation. Each amplifier is a multistage direct-coupled type, carefully balanced and stabilised by an auxiliary chopper stage. It has a forward gain of several thousand, and is very free from d.c. drift; as an independent unit, the amplifier has very high input impedance, and a negligibly low output impedance.

(d) Patch Panels. The patch panels are sub-units, mounted below the amplifier which they serve, which contain high-precision resistors and capacitors which may be connected to the amplifier input and output in a variety of ways to produce summing junctions, integrators, filters and other operational units. They also contain a three-turn helical potentiometer, and two high-speed relays which control the working of the amplifier.

The necessary connections to the components and the amplifier are made by linking some of a pattern of small sockets on the face of the panel. These sockets are distinctively coloured according to their function, and provide access to the amplifier input and output, to the relay contacts, the ends of the precision components, and to the reference voltage lines, mention of which will be made later. The relays on the panel perform the 'hold' and 'zero-set' functions under the control of circuits in the control panel, more details of which are given below.

The precision components provided are as follows:

Resistors :- 9 in all (4 @  $1M\Omega$ , 2 @  $250k\Omega$ , 3 @  $100k\Omega$ ). Each is a metal film resistor with a nominal accuracy of 1%, 'padded' with wire-wound resistors in shunt to a final accuracy of better than 0.1%.

Capacitors :- 3 in all, one each of  $0.01\mu F$ ,  $0.1\mu F$ , and  $1\mu F$ . All are precision units with polystyrene dielectric, accurate to 0.1%.

(e) Reference voltage supply.

For making accurate measurements from simulated circuits, and for setting up the initial conditions for testing such circuits, it is necessary to have available a source of highly stable voltage for



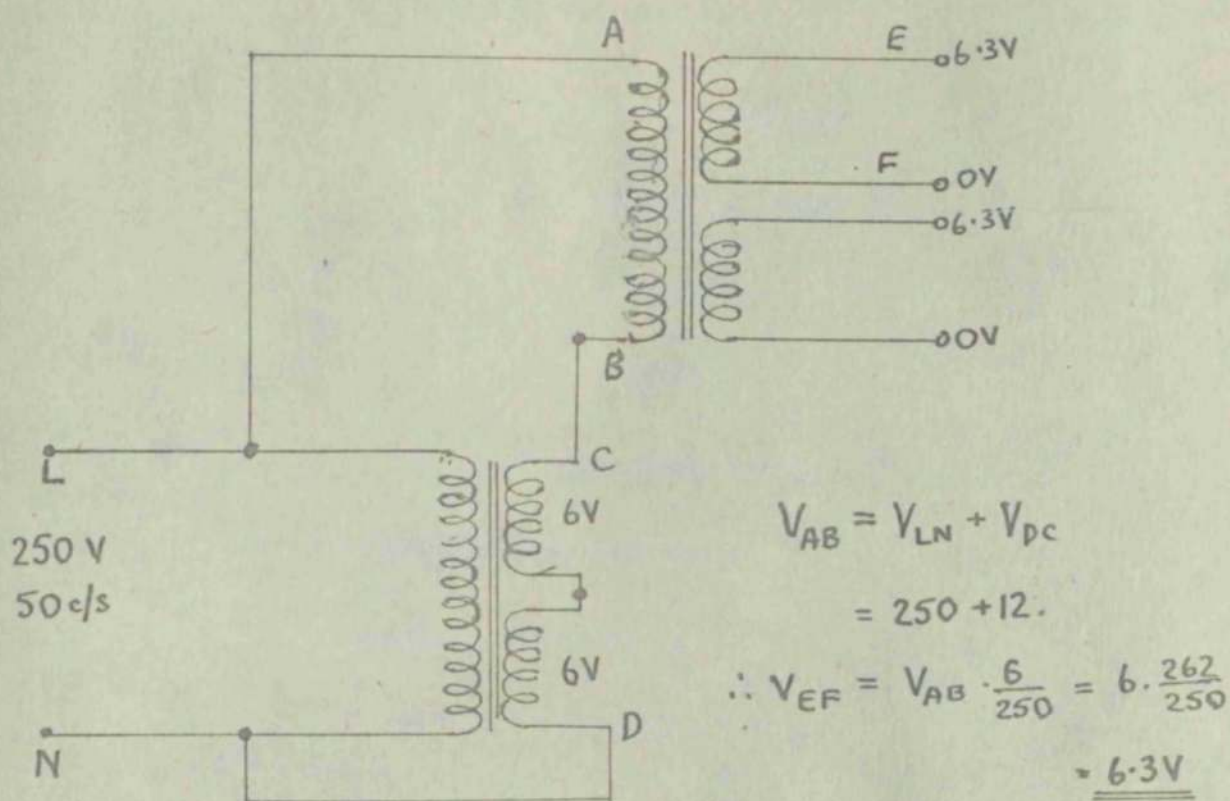


Fig.18. Booster transformer circuit for heaters.

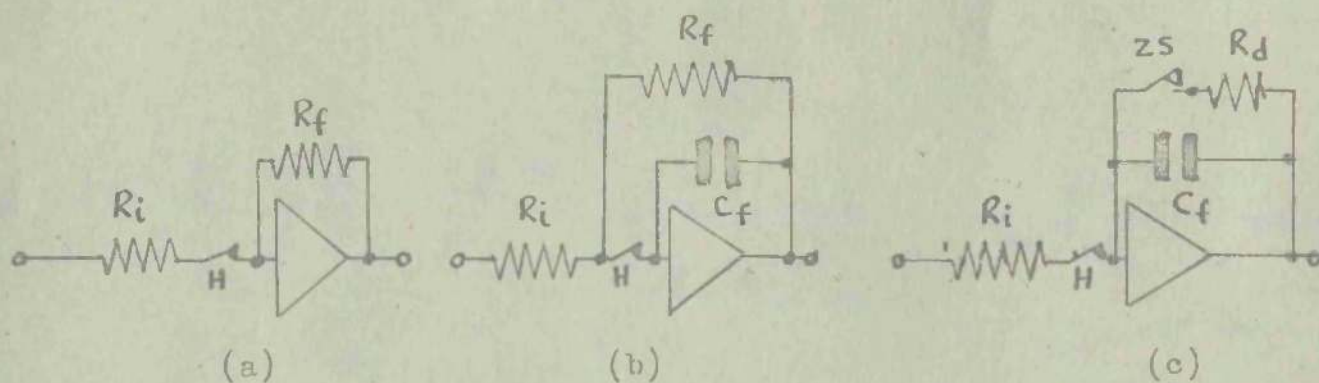


Fig.19. Connections of patch panel relays.

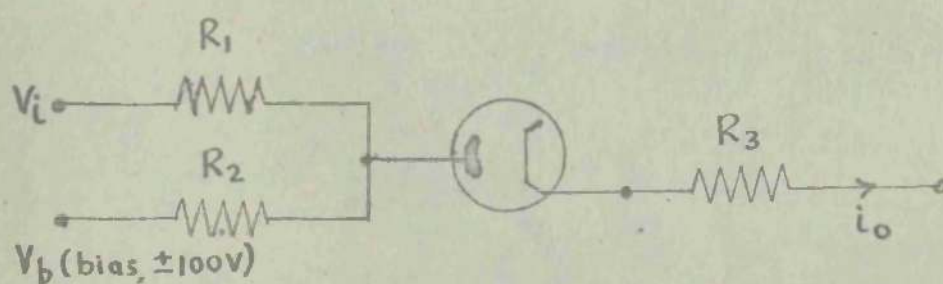


Fig.20. Standard biased-diode circuit for function generation.

reference and comparison purposes. This is provided as a separate supply at  $\pm 100\text{V d.c.}$  The supply unit for this has its own rectifying circuits and is stabilised by a comparison circuit which employs as an error amplifier two of the standard operational amplifiers in cascade, giving a very high stability factor indeed.

Supply lines are taken from this unit to the patch panels (for initial conditions), to the measurement circuit in the control panel, and to the multiplier and function generator (to bias the diode circuits). The unit is capable of supplying a load of 100mA from each half.

#### (f) Control and Measurement Panel.

This is the 'nerve centre' of the whole machine. It contains two parts performing quite separate functions, so these will be treated separately.

Control circuits. :- The control section of the panel consists of a set of multivibrator circuits controlling the operation of the 'hold' and 'zeroset' relays on the patch panels, and associated higher-powered circuits providing the current for the relays. The multivibrators are arranged to trigger either from an internal control waveform (for continuous cycling), from an external waveform, or by step signals initiated by push-buttons. The function of the two relays is as follows:-

Hold This relay is connected in series with the input to an amplifier, in one of the two ways shown in Fig.19. Connection (a) is used for summing amplifiers or integrators, connection (b) for lag filters.

When opened, the relay disconnects the input from the amplifier. The modified layout (b) is necessary to prevent discharge of a filter capacitor, in this condition, through its parallel feedback resistor.

Zeroset. This relay is connected between input and output of the amp-



lifier, when capacitive feedback is in use. Normally it is open, but on closure it discharges the feedback capacitor through a 330-ohm resistor permanently placed in series with the relay. This connection is shown for an integrator in Fig,19(c).

In the light of this knowledge of the operative effect of the relays, the control of the computer can briefly be summarised. There are five principal states, set up by four separate push-buttons, viz:  
Start :- HOLD relay closes, ZEROSET relay opens; computation begins.  
Stop and Reset :- HOLD relay opens, ZEROSET relay closes; computation stops and all capacitors are discharged, resetting all amplifier outputs to zero.

Hold :- HOLD relay opens, ZEROSET relay remains open; computation is suspended, and all amplifier output levels at the instant of operation are clamped for inspection and/or measurement.

Cancel Hold :- Hold relay recloses; computation proceeds from where it was stopped by the 'hold' operation.

Stop and Hold :- achieved by sequential operation of the 'stop' and  
or Set-up 'cancel hold' buttons; HOLD and ZEROSET relays are both closed; used for long-term drift correction. Mainly used to set up patch panel potentiometers. These are set by applying - 100V from the reference supply and balancing output against a preset level from the measuring circuit. This position enables the potentiometer to be normally loaded during set-up, without transmitting its d.c. output during the operation to any other amplifiers.

These operations take place simultaneously on the relays controlling

all sixteen amplifiers.

Measuring circuits :- Two methods of measuring amplifier output voltages are provided. A multirange voltmeter may be connected, by a switch, to any of the 16 outputs, or for precise measurements the galvanometer circuit may be used. This consists of a high-sensitivity (100  $\mu$ A f.s.d.) moving coil galvanometer, fully protected against over-voltages, which balances the amplifier output voltage against one derived through a ten-turn precision helical potentiometer from the reference supply. It may also be used in setting up the patch panel potentiometers to any desired attenuation.

(g) Multiplier and Function Generator.

The machine contains a quarter-squares multiplier and function generator, both of which work on the same principle. The basic circuit employed appears in Fig.20.  $R_2$  is a fixed resistor,  $R_1$  and  $R_3$  are variable over a range. By adjusting  $R_1$ , the value of  $V_i$  at which the diode begins to conduct may be varied, while, by altering  $R_3$ , the ratio  $V_i:i_o$  is adjusted. When a set of similar circuits are placed in parallel, after suitable adjustment the overall input voltage -output current relationship can be made to approximate to any given curve.

The multiplier consists of four sets of circuits, each following a square law, two squaring positive voltages and two negative. These square the sum and difference of two input voltages; subtraction of their outputs then gives the required product.

The function generator has twenty single circuits, which may be combined in a variety of ways to follow a specified law for positive and/or negative inputs. A switching arrangement feeding up to ten of



the circuits with a phase-inverted version of the input enables non-monotonic laws to be set up, by causing these circuits, on conduction, to contribute currents of opposite polarity to the total output, so producing an inflection in the overall characteristic.

#### A2.3. Further References.

A much fuller treatment of the detailed design principles and circuitry of the computer than could competently be provided here will be found in a series of theses, by the designers of individual components, upon the design basis of each of these components.<sup>21,22.</sup>

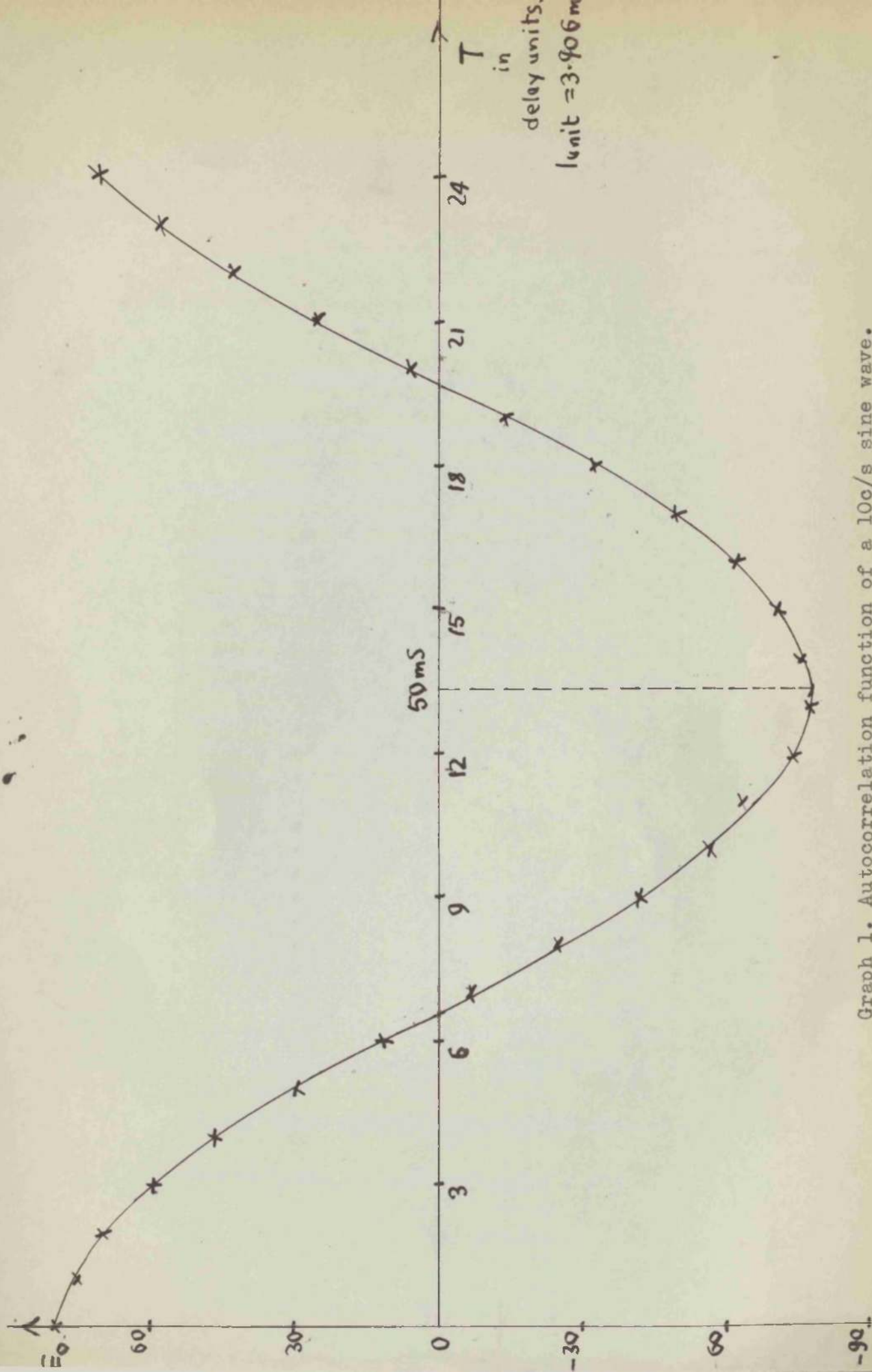
RESPONSE OF SINGLE-STAGE R - C FILTER.

Frequency $\omega$ rad/sec	Squared-amplitude response, $P_t(\omega)$		Transfer function $G(\omega)$	
	Theory	Practice	Theory	Practice
1	3.99	3.50	1.995-j0.100	2.155-j0.166
2	3.96	3.50	1.980-j0.198	2.065-j0.190
3	3.91	3.50	1.955-j0.293	2.005-j0.315
4	3.85	3.50	1.925-j0.385	1.950-j0.429
5	3.76	3.43	1.880-j0.470	1.890-j0.555
6	3.67	3.34	1.836-j0.550	1.810-j0.580
7	3.56	3.34	1.780-j0.624	1.790-j0.655
8	3.45	3.32	1.725-j0.690	1.725-j0.680
9	3.33	3.20	1.665-j0.748	1.640-j0.710
10	3.20	3.16	1.600-j0.800	1.585-j0.795
15	2.56	2.70	1.281-j0.960	1.240-j0.885
20	2.00	2.04	1.000-j1.000	0.955-j0.920
25	1.56	1.59	0.780-j0.976	0.705-j0.900
30	1.23	1.26	0.615-j0.923	0.735-j0.855
40	0.80	0.62	0.400-j0.800	0.398-j0.790
50	0.55	0.42	0.276-j0.690	0.372-j0.800



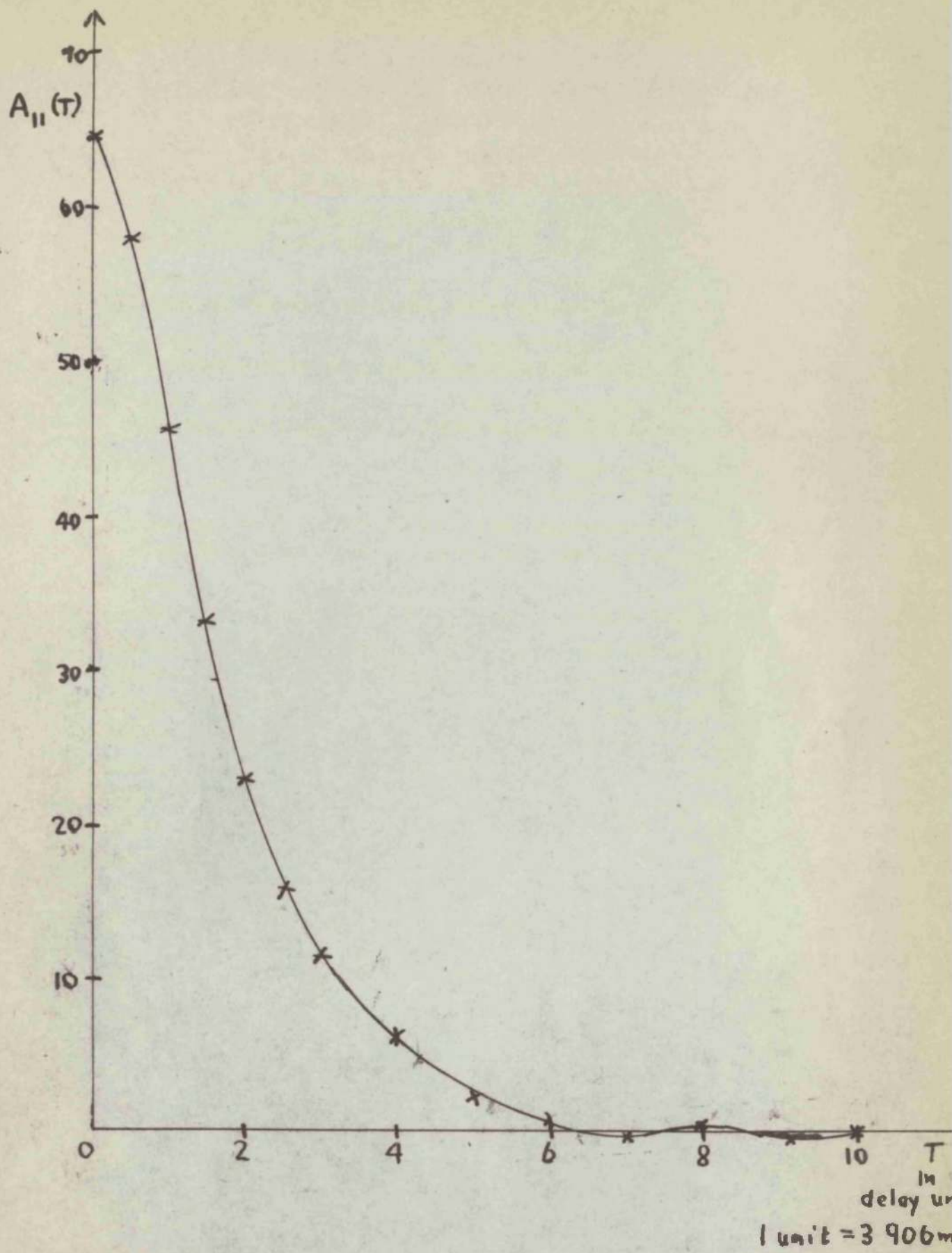
RESPONSE OF THIRD ORDER SERVO SYSTEM

Frequency $\omega$ rad/sec	Squared-amplitude response $P_t(\omega)$		Transfer function $G(\omega)$	
	Theory	Practice	Theory	Practice
1	0.238	0.214	0.475-j0.112	0.474-j0.117
1.5	-----	-----	0.447-j0.158	0.448-j0.167
2	0.208	0.192	0.412-j0.195	0.403-j0.213
2.5	-----	-----	0.376-j0.224	0.367-j0.248
3	0.173	0.161	0.338-j0.242	0.322-j0.279
4	0.141	0.123	0.270-j0.260	0.225-j0.286
5	0.114	0.100	0.213-j0.262	0.150-j0.285
6	0.093	0.071	0.169-j0.254	0.105-j0.248
7	-----	-----	0.135-j0.242	0.087-j0.216
8	0.065	0.053	0.109-j0.232	0.068-j0.188
9	-----	-----	0.089-j0.220	0.062-j0.182
10	0.049	0.044	0.073-j0.209	0.072-j0.182
12	0.039	0.036	0.049-j0.191	0.032-j0.190
15	0.031	0.014	0.026-j0.175	0.005-j0.149
17	-----	-----	0.015-j0.169	0.006-j0.163
20	0.028	0.031	-0.002-j0.168	-0.022-j0.158
22	-----	-----	-0.015-j0.173	-0.046-j0.163
25	0.038	0.018	-0.046-j0.188	-0.046-j0.188
27	0.048	0.048	-0.086-j0.202	-0.102-j0.239
29	0.066	0.069	-0.155-j0.205	-0.206-j0.211
30	0.074	0.076	-0.198-j0.183	-0.257-j0.143
31	0.085	0.0765	-0.252-j0.146	-0.269-j0.094
33	0.075	0.052	-0.274-j0.001	-0.243+j0.006
35	0.044	0.011	-0.189+j0.089	-0.174+j0.072
37	0.022	0.0009	-0.111+j0.098	-0.083+j0.071
39	-----	-----	-0.067+j0.083	-0.071+j0.058
40	-----	-----	-0.054+j0.075	-0.022+j0.052

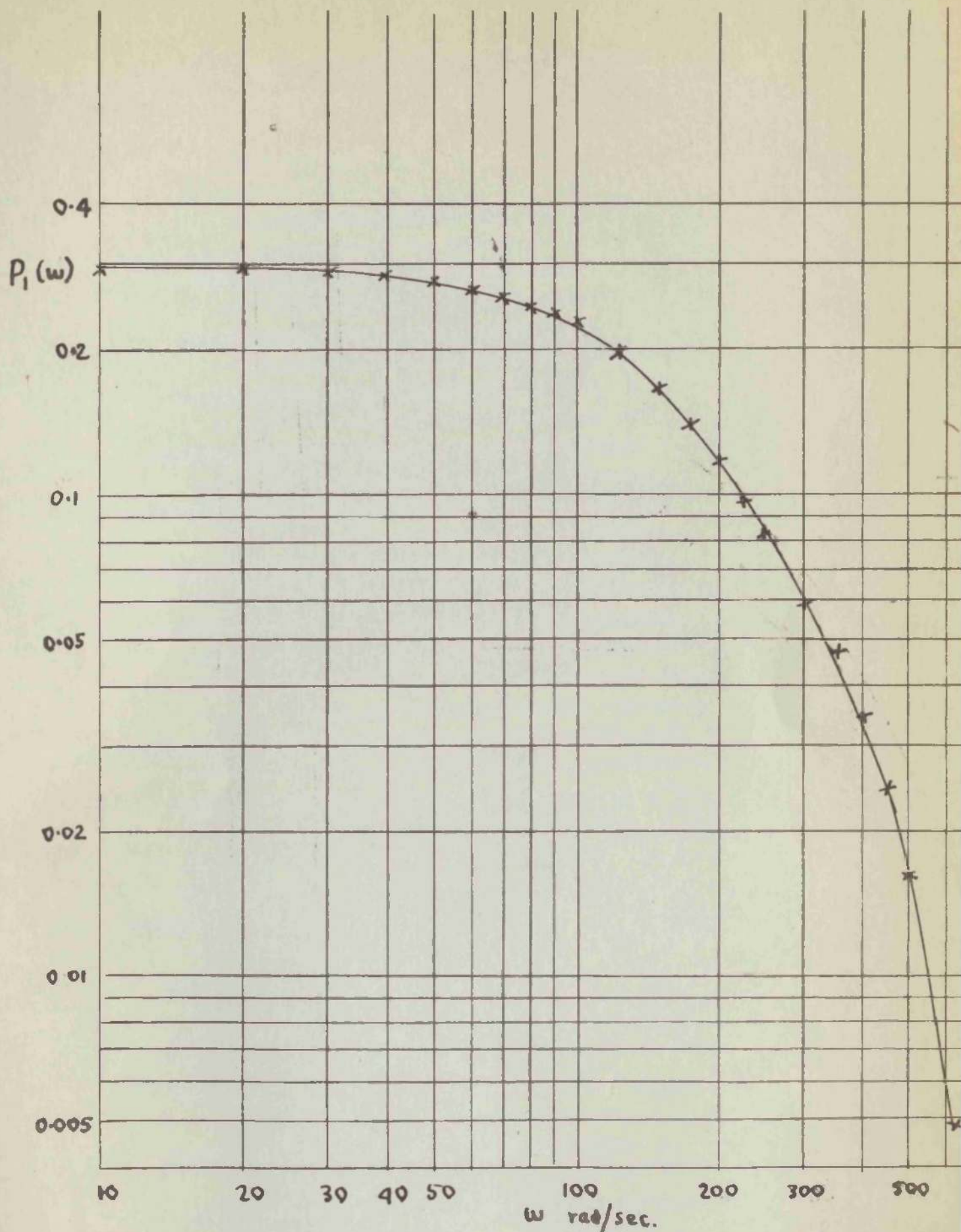


Graph 1. Autocorrelation function of a 100/s sine wave.



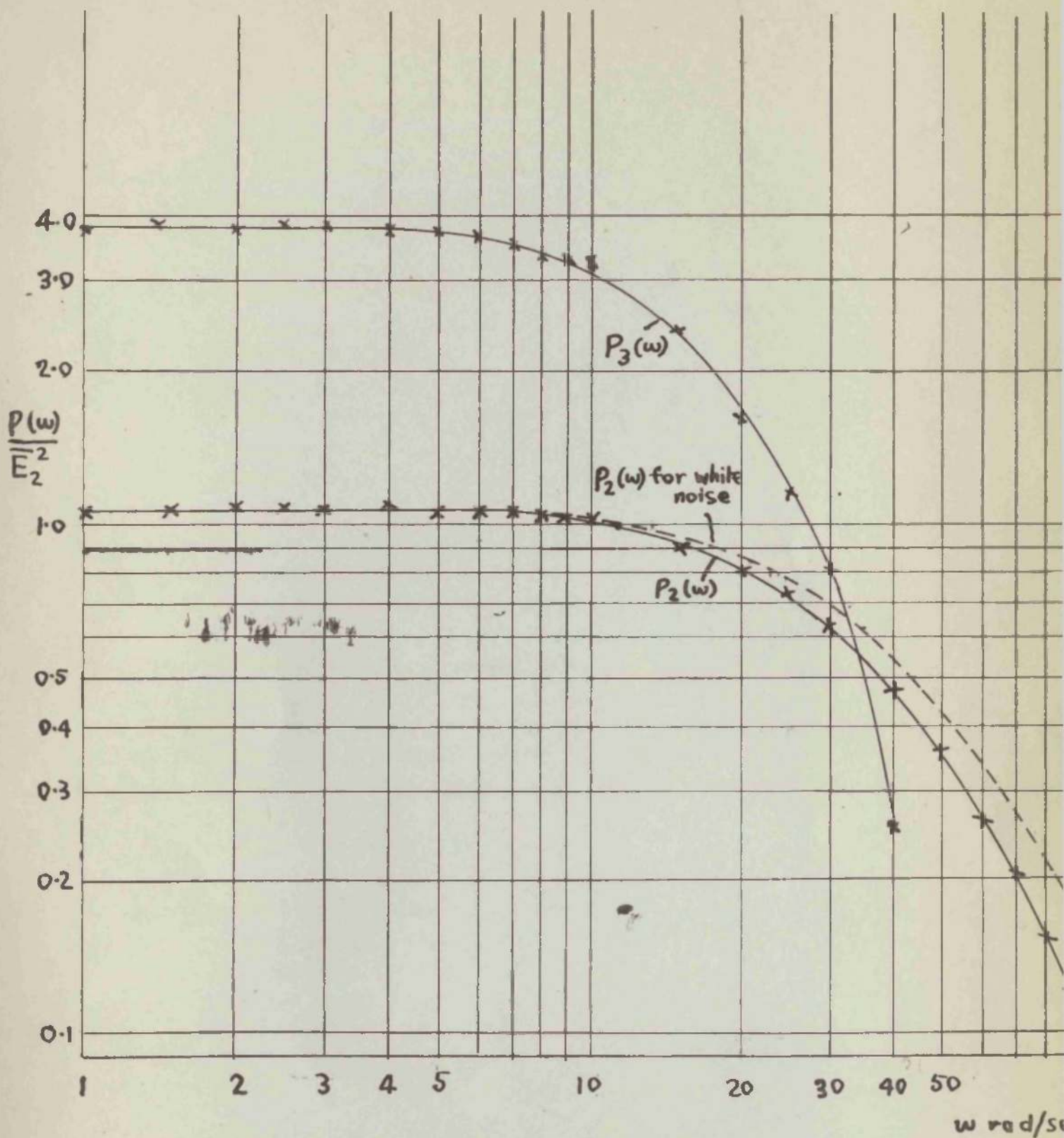


Graph 2. Autocorrelation function of the output of the random signal generator (R.S.G.).



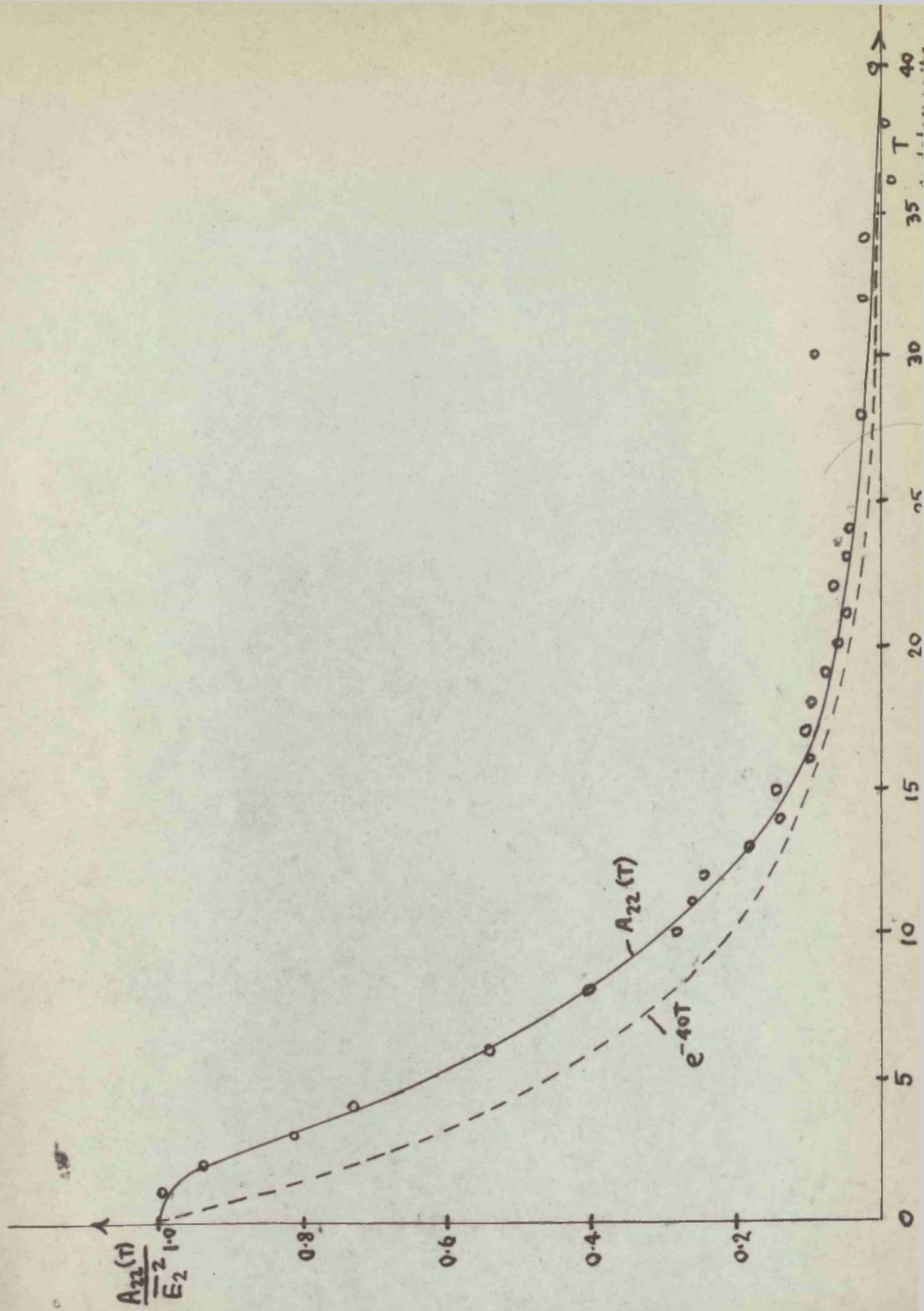
Graph 3. Power spectrum of the output of the R.S.G.  
(Fourier transform of Graph 2).



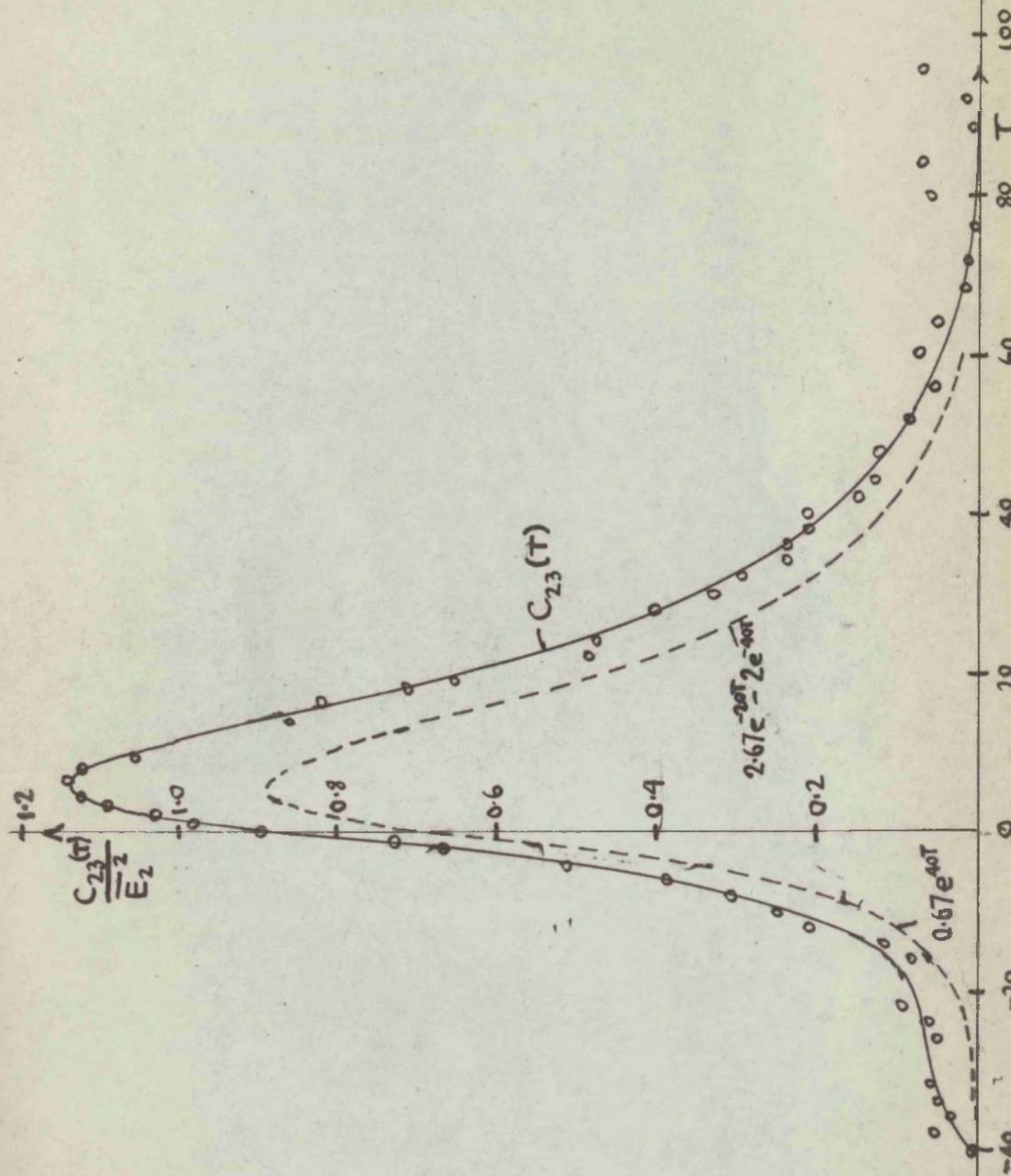


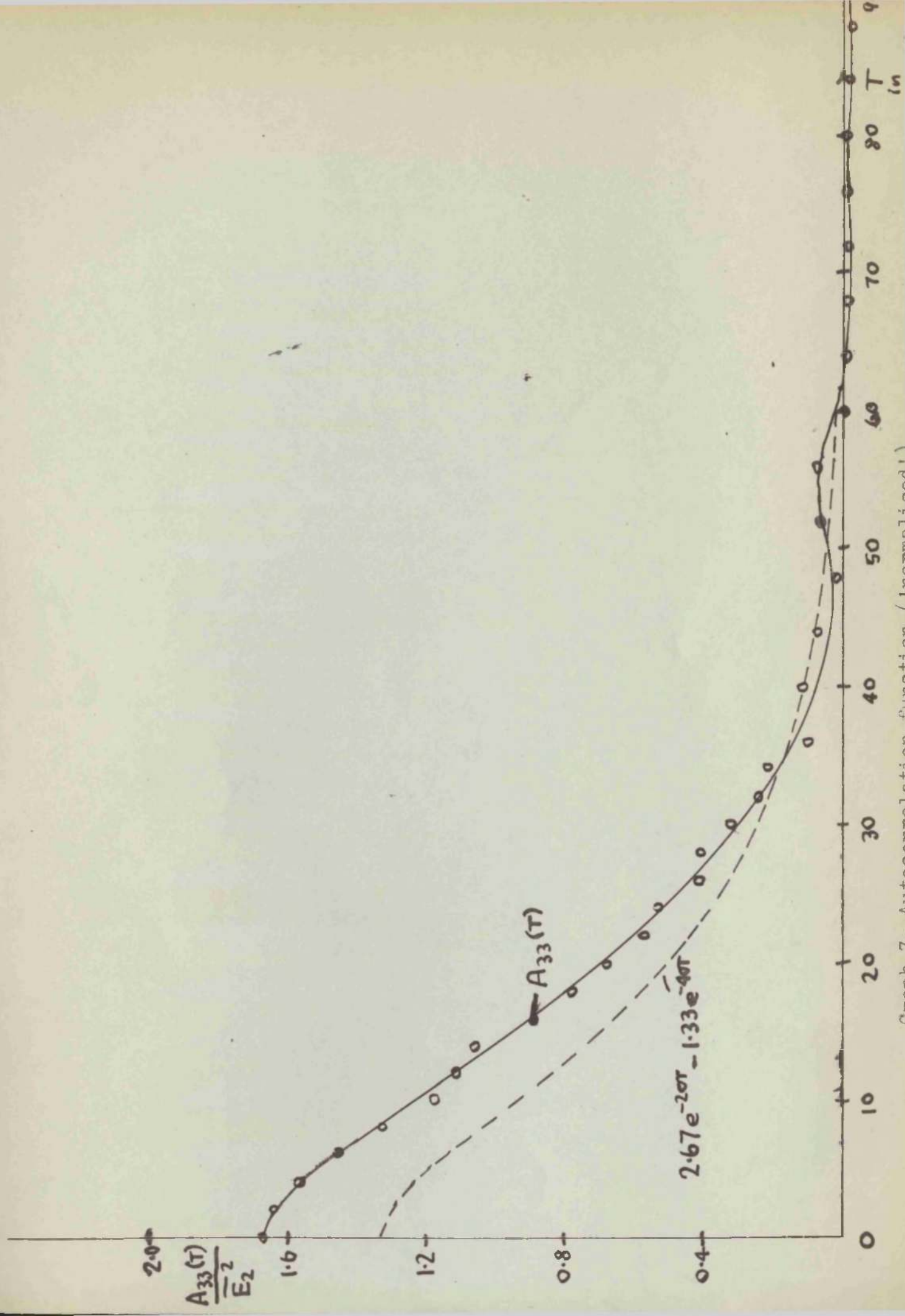
Graph 4. 'Normalised' power spectra of the input,  $P_2(w)$ , and output,  $P_3(w)$ , of the R-C test filter, with  $P_2(w)$  for a 'white' noise source for comparison.

(Fourier transforms of Graphs 5 and 7).



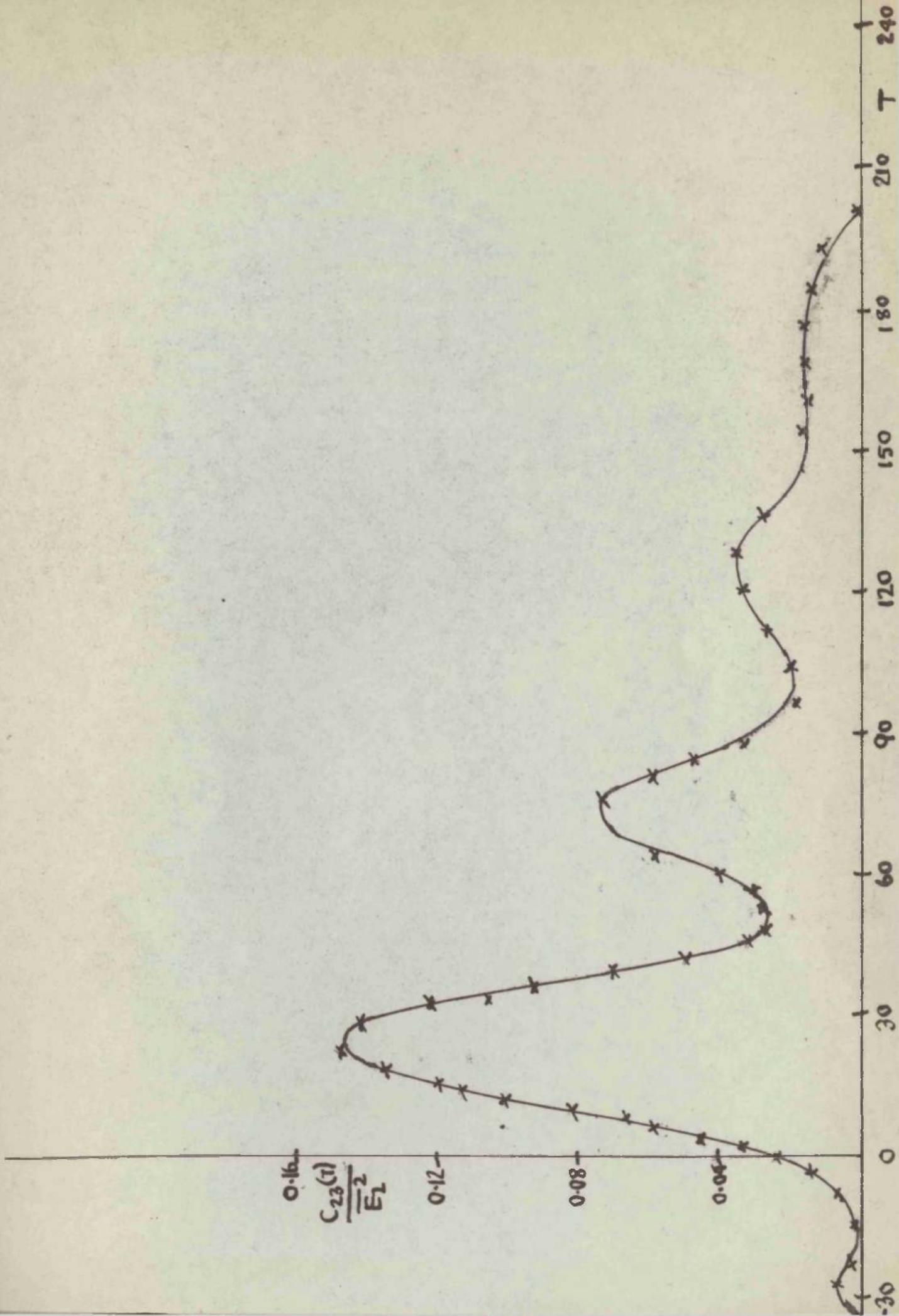


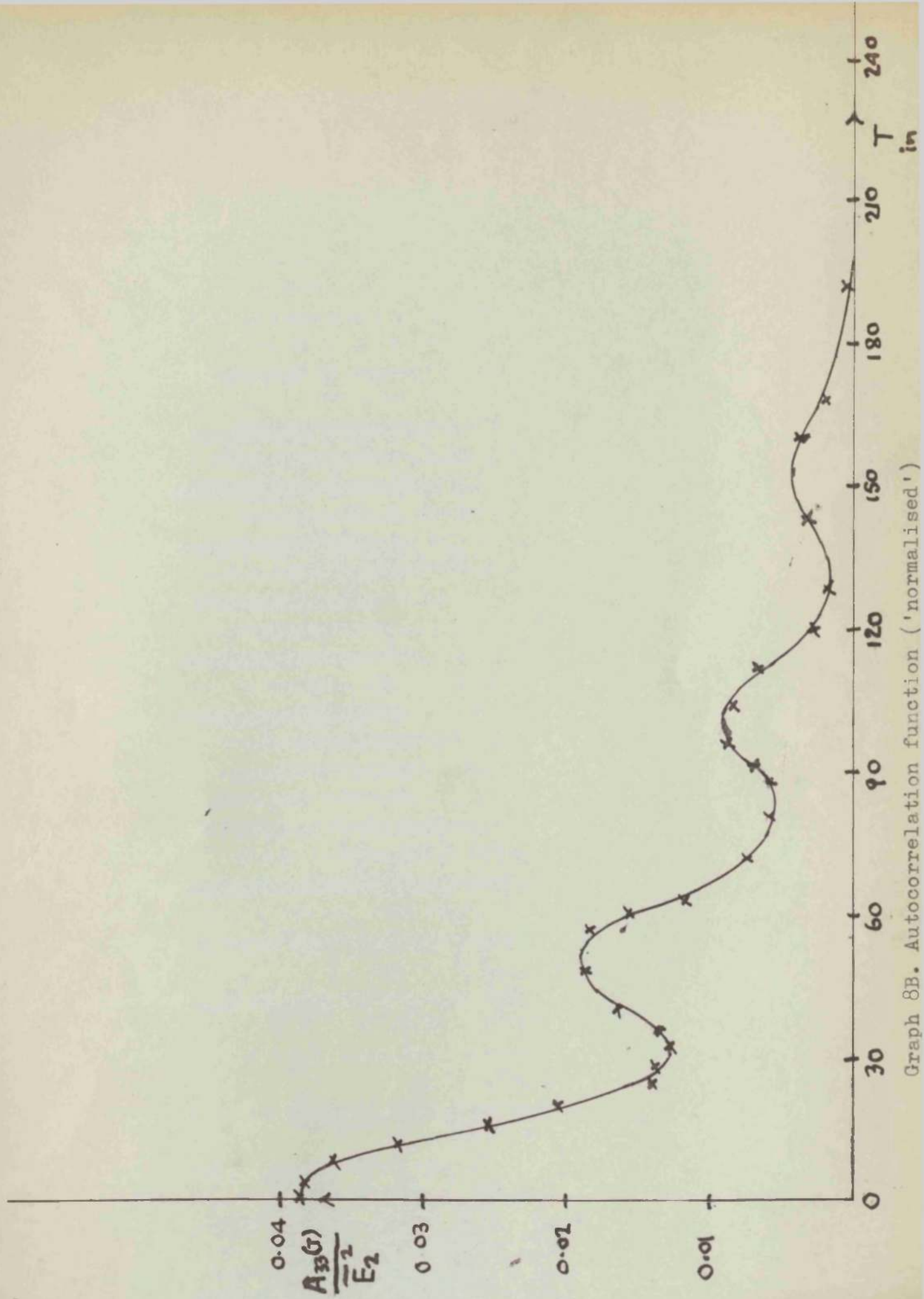




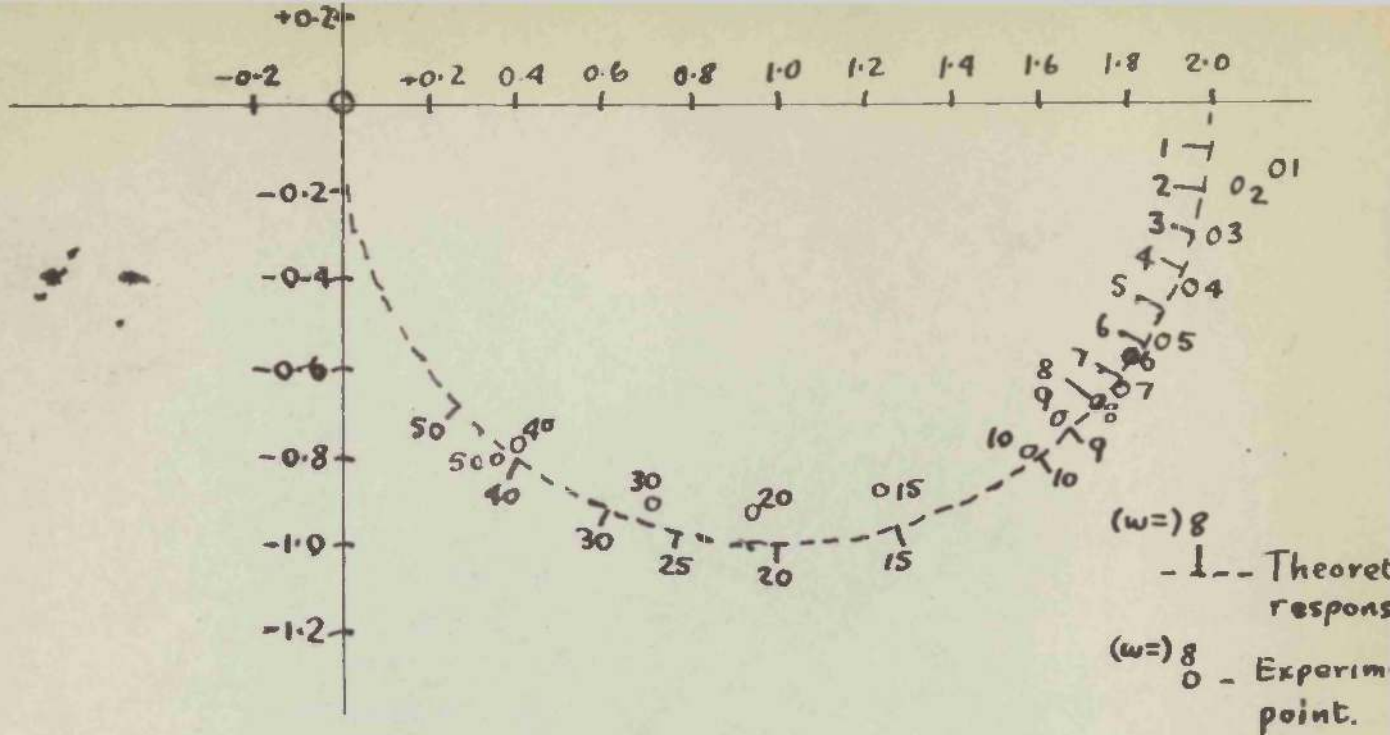
Graph 7. Autocorrelation function (normalised)



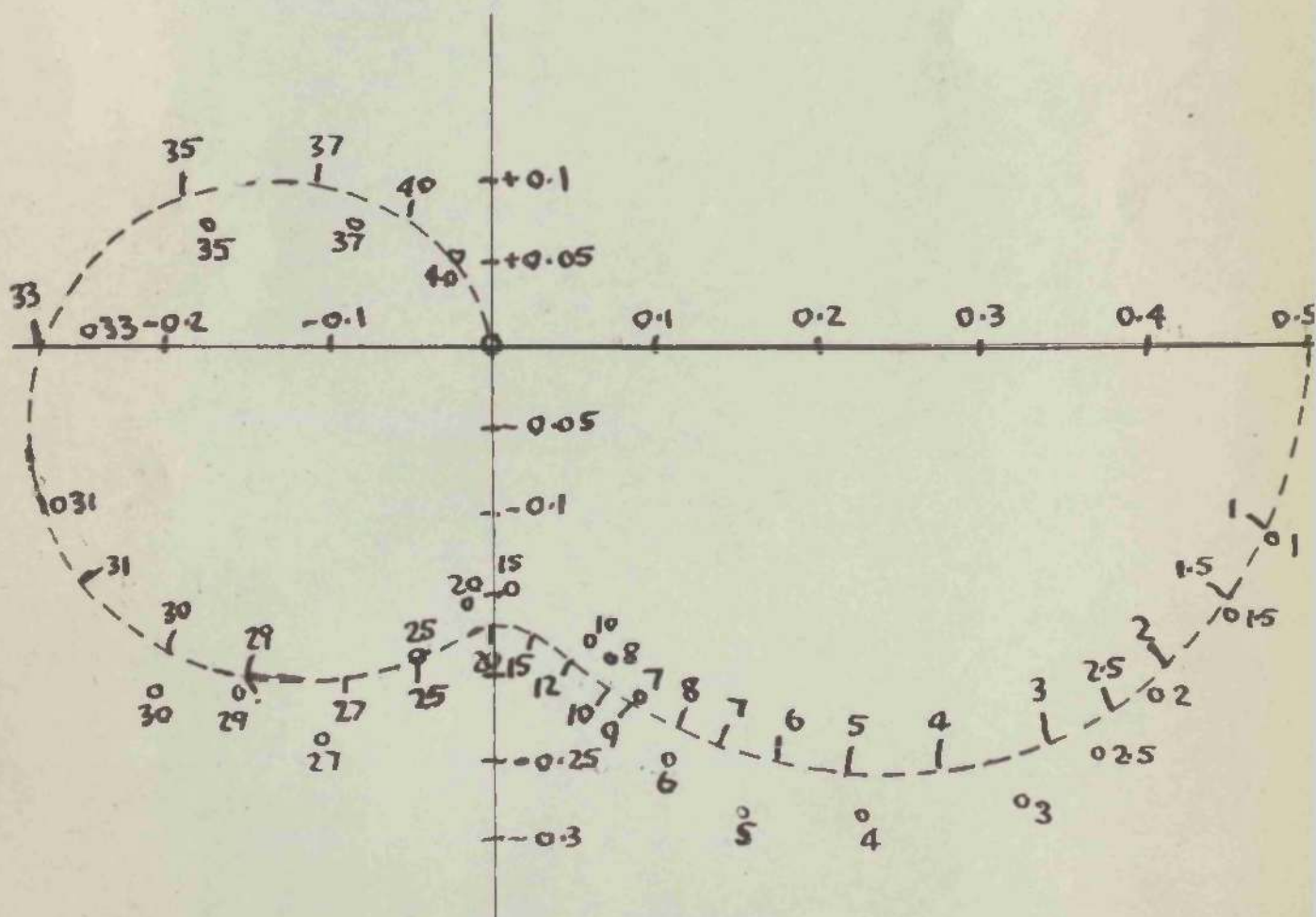




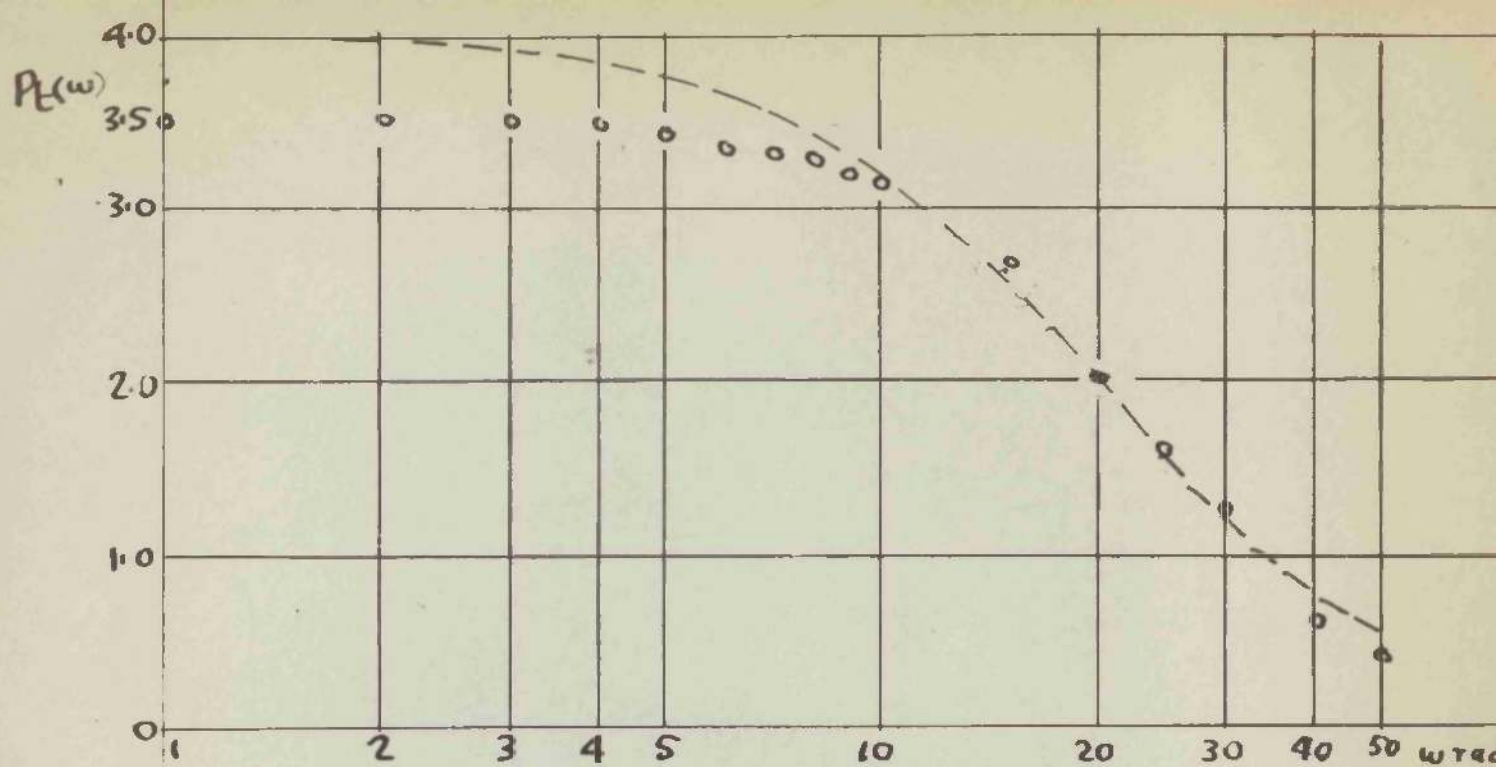




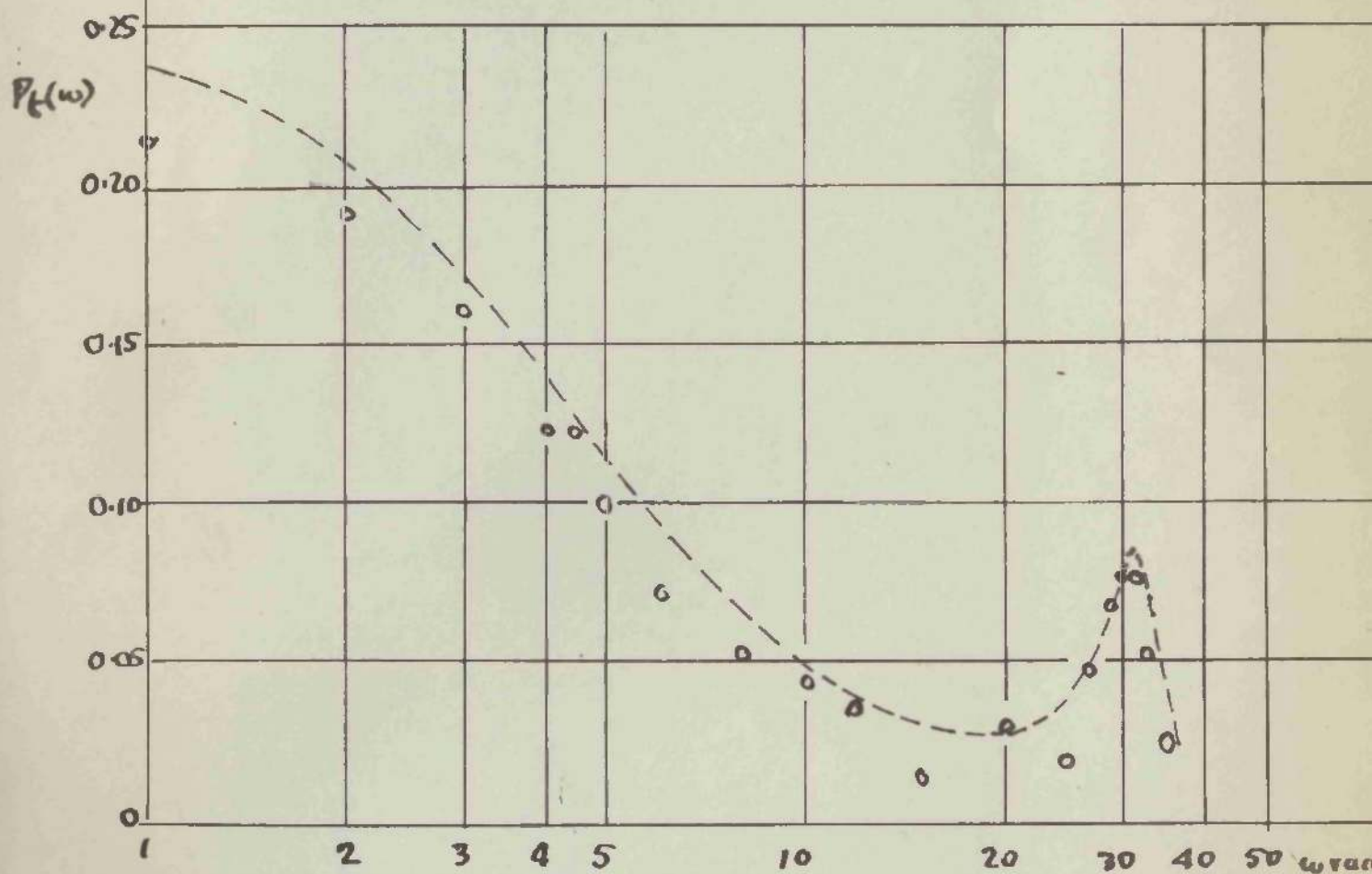
Graph 9. Complex response of the R-C filter.



Graph 10. Complex response of the third order servo system.



(a) R-C Filter.

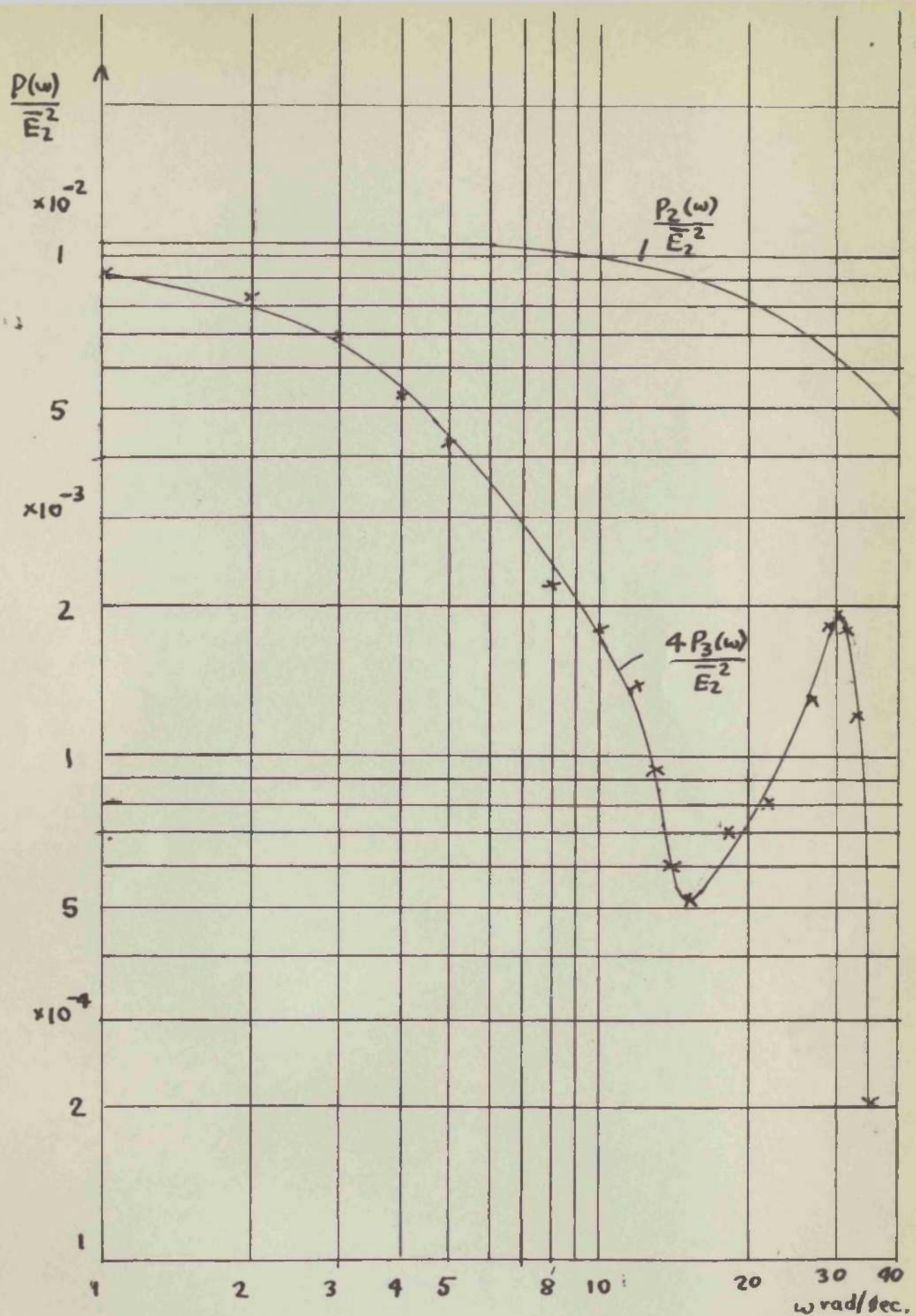


(b) Third Order Servo.

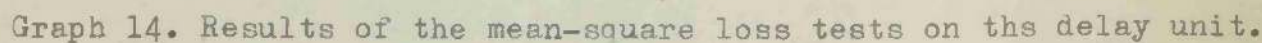
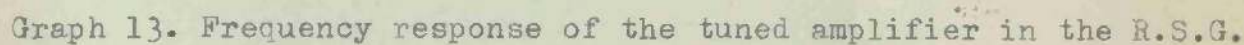
---- Theoretical response.    o - Experimental points.

Graph 11. Theoretical and actual squared-amplitude responses of (a) the R-C filter, and (b) the servo system.





Graph 12. 'Normalised' power spectra of the input,  $P_2(\omega)$  and output,  $P_3(\omega)$  of the servo system. (Fourier transforms of Graphs 5 and 8B).





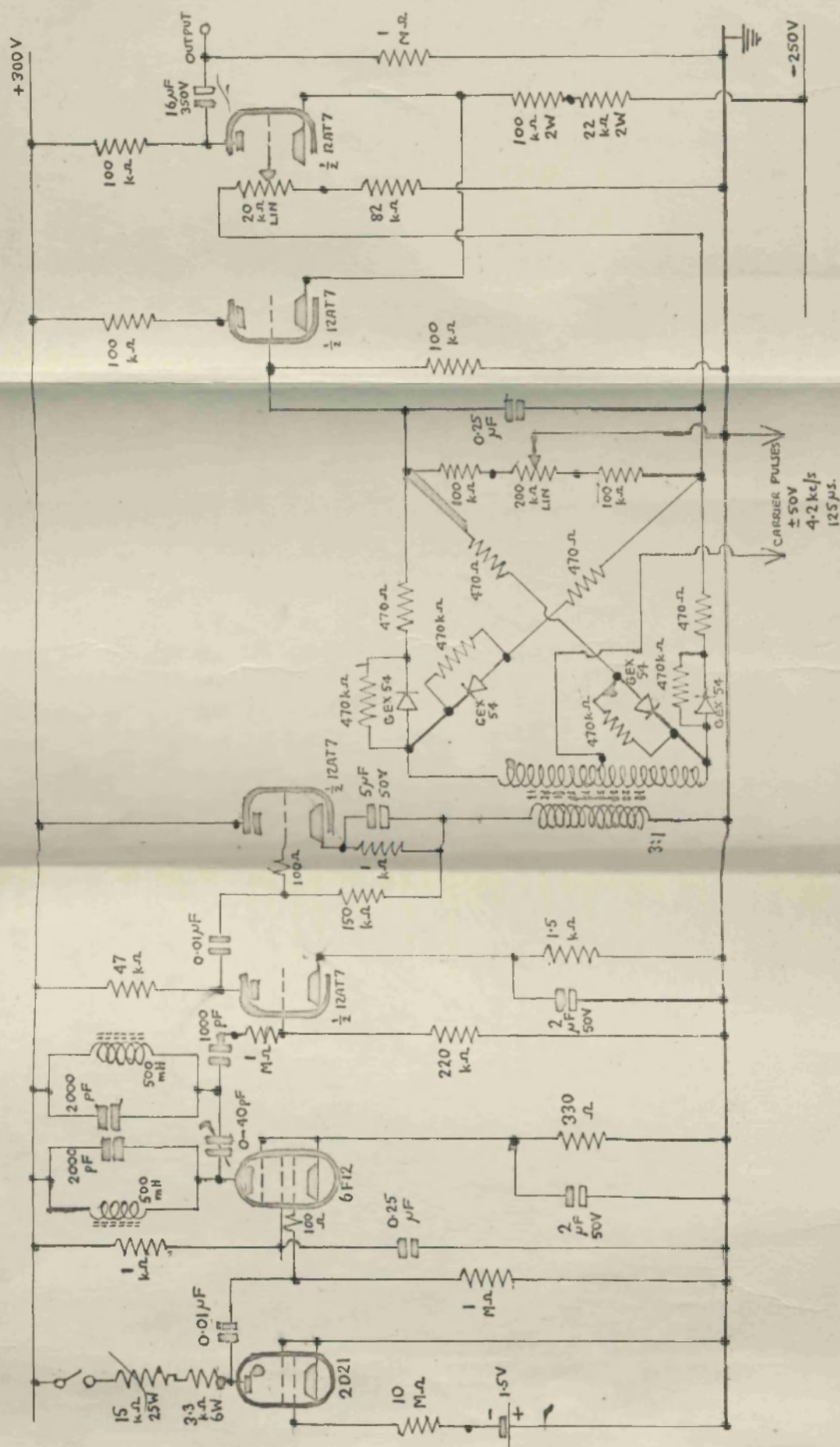


FIG. 13. CIRCUIT DIAGRAM OF L.F. NOISE GENERATOR.